

Characterization of TRAPP interacting proteins

FLJ13611 and SPATA4

Débora Teixeira Duarte

A Thesis in The Department of Biology

Presented in partial fulfillment of the requirements for the Degree of Master of Science
(Biology) at Concordia University, Montreal, Quebec, Canada

June 2012

© Debora Duarte, 2012

CONCORDIA UNIVERSITY

School of Graduate Studies

This is to certify that the thesis prepared by: Debora Teixeira Duarte

Entitled: Characterization of TRAPP interacting proteins FLJ13611 and SPATA4

and submitted in partial fulfillment of the requirements for the degree of

Master of Science (Biology)

complies with the regulations of the University and meets the accepted standards with respect to originality and quality.

Signed by the final Examining Committee:

_____ Selvadurai Dayanandan, PhD (Chair)

_____ Catherine Bachewich, PhD (Examiner)

_____ Christopher Brett, PhD (Examiner)

_____ Alisa Piekny, PhD (Examiner)

_____ Michael Sacher, PhD (Supervisor)

Approved by _____

Selvadurai Dayanandan, PhD (Graduate Program Director)

June 2012 _____

Dean of Faculty

ABSTRACT

Characterization of TRAPP interacting proteins FLJ13611 and SPATA4

Débora Teixeira Duarte

The mammalian TRAPP complex is a multi-subunit tethering factor acting in vesicular transport between the endoplasmic reticulum and the Golgi apparatus. Here we describe two novel interactors of this complex, FLJ13611 and SPATA4. FLJ13611, a previously uncharacterized protein, was shown to interact with TRAPP components by yeast two hybrid, co-immunoprecipitation and *in vitro* binding, and was shown to co-fractionate with TRAPP by size exclusion chromatography. FLJ13611 depletion by siRNA caused the Golgi apparatus to fragment, indicating its importance in maintenance of Golgi structure. Moreover, FLJ13611 was found to interact with the Golgi stacking proteins GRASP55 and GRASP65 by yeast two hybrid, co-immunoprecipitation and *in vitro* binding. We propose FLJ13611 is a new component of the mammalian TRAPP complex which should be called TRAPPC13. SPATA4, a spermatocyte-specific protein of unknown function, was identified in a yeast two hybrid screen using TRAPPC2 as a bait. It is present in both nuclear and cytosolic compartments and it interacts with the TRAPPC2 portion of the TRAPP complex. SPATA4 contains a domain of unknown function called DUF1042 domain, which is necessary but not sufficient for the interaction with TRAPPC2. We also show by *in vitro* binding that the presence of the two C-terminal helices of TRAPPC2 is required for the interaction and the interaction is stronger when TRAPPC2 is in its heterotrimeric form. Our results suggest a role for SPATA4 in membrane traffic and a specialized function for TRAPP in spermatocytes.

ACKNOWLEDGEMENTS

I would like to thank my supervisor Dr. Michael Sacher for his guidance and support during my time at Concordia University.

To everyone at the Sacher Lab, and in particular to Nassim Sharzad and Stephanie Brunet, thanks for the friendship and all the help. It was a wonderful experience sharing these days with you guys. To the previous members of the lab, Vanessa Laflamme, Adrian Moores, Baraa Noueihed and Dr. James Scrivens for the company and useful suggestions. To Dr. Ziad El-Hajj for kindly helping me in the revision process.

Thank you to my committee members, Dr. Christopher Brett, Dr. Alisa Piekny and Dr. Catherine Bachewich, for reagents, suggestions and for accepting my invitation.

For financial support I am thankful to Groupe de Recherche Axé sur la Structure des Protéines (GRASP) from McGill University and Concordia University for awards that helped me to finance my studies here in Montreal.

Special thanks to my boyfriend Daniel Foshag, with whom I shared the doubts and certainties about life and science.

Finally, I would like to thank my family in Brazil, who has unconditionally supported me: Marcia, Luiz Augusto, Livia, and Rafael.

Table of Contents

List of Tables	vii
List of Figures	viii
List of Acronyms	ix
1 Introduction.....	1
1.1 Membrane trafficking and the Golgi apparatus.....	1
1.2 Tethering and vesicle fusion	3
1.3 TRAPP Complexes	5
1.3.1 Yeast TRAPP complexes.....	7
1.3.2 Mammalian TRAPP complex.....	8
1.3.2.1 TRAPP and diseases	11
1.3.3 TRAPP complexes in other organisms.....	12
1.4 SPATA4	13
1.5 Golgi Reassembly Stacking proteins (GRASPs)	15
1.6 Project: Characterization of TRAPP interacting proteins FLJ13611 and SPATA4	17
2 Materials and Methods.....	19
2.1 Buffers and Solutions	19
2.2 Oligonucleotides, strains and plasmids	22
2.3 Plasmid construction	27
2.4 Yeast two-hybrid.....	28
2.4.1 Yeast transformation.....	28
2.5 Purification of recombinant protein	29
2.5.1 MBP tagged proteins	29
2.5.2 GST tagged proteins.....	29
2.6 In vitro Binding	30
2.7 Electrophoresis and Western Blotting.....	30
2.8 Cell Culture and knockdown.....	31
2.9 Co-immunoprecipitation	32
2.10 Size exclusion chromatography	32

2.11 Immunofluorescence and Fluorescence microscopy.....	33
2.12 Secondary structure prediction.....	33
2.13 UV spectroscopy	33
2.14 Far UV Circular Dichroism.....	34
2.15 Fluorescence Spectroscopy	34
3 Results.....	35
3.1 FLJ13611 interacts with TRAPP subunits by yeast two-hybrid	35
3.2 FLJ13611 interacts with the TRAPP complex in vivo.....	37
3.3 FLJ13611 depletion leads to Golgi fragmentation.....	39
3.4 FLJ13611 interacts with GRASP55 by yeast two-hybrid	41
3.5 FLJ13611 interacts with GRASP65	43
3.6 FLJ13611 interacts with GRASPs in vivo	45
3.7 Optimization of recombinant protein purification and removal of MBP.....	48
3.8 Acrylamide quenching reveals the position of tryptophan residues in FLJ13611 ..	53
3.9 Assessment of FLJ13611 secondary structure	58
4 Discussion	64
5 References.....	70
6 A yeast two hybrid screen identifies SPATA4 as a TRAPP interactor (Published manuscript)	80
6.1 Introduction	80
6.2 Materials and Methods.....	82
6.2.1 Oligonucleotides and plasmid constructs	82
6.2.2 Yeast two hybrid screen	84
6.2.3 Tissue culture and lysate preparation	85
6.2.4 Co-immunoprecipitation and gel filtration.....	85
6.2.5 Recombinant protein preparation	86
6.2.6 In vitro binding assay	88
6.2.7 Fluorescence microscopy	88
6.2.8 Live cell imaging.....	89
6.2.9 Cellular fractionation.....	89

6.3 Results	90
6.3.1 Identification of SPATA4 as a C2 binding partner	90
6.3.2 C2 and SPATA4 interact in vivo	93
6.3.3 SPATA4 binds to the TRAPP complex.....	95
6.3.4 Defining the regions of interaction between SPATA4 and C2	99
6.3.5 SPATA4 is found in both the cytosol and in the nucleus.....	100
6.4 Discussion	103
6.5 Supplemental material.....	106
6.6 Acknowledgements	107
6.7 References	108

List of Tables

Table 1.1 Nomenclature of mammalian and yeast TRAPP subunits.....	6
Table 2.1 Oligonucleotides used in this study	22
Table 2.2 Yeast strains used in this study	23
Table 2.3 Plasmids used for yeast two hybrid	24
Table 2.4 Plasmids used for recombinant protein production	26
Table 2.5 Plasmids used for transfection of mammalian cells.....	26
Table 3.1 Calculated secondary structure fractions for FLJ13611	62
Table 6.1 Oligonucleotides used in this study	82
Table 6.2 Plasmid constructs used in this study	83
Table 6.3 C2 interactors identified in yeast two-hybrid screen	91

List of Figures

Figure 3.1 Physical interactions of FLJ13611 with TRAPP subunits	36
Figure 3.2 FLJ13611 co-fractionates with TRAPP subunits and co-precipitates with TRAPPC2	38
Figure 3.3 FLJ13611 knockdown leads to fragmentation of the Golgi	40
Figure 3.4 Physical interaction of GRASP proteins with TRAPP subunits and FLJ13611.	42
Figure 3.5 GRASP65 interacts with FLJ13611	44
Figure 3.6 FLJ13611 interacts with GRASP55 and GRASP65 in vivo.	46
Figure 3.7 GRASP65 does not co-precipitate with the TRAPP complex	47
Figure 3.8 Purification and stability of FLJ13611-MBP	49
Figure 3.9 Digestion of FLJ13611-MBP with FactorXa	51
Figure 3.10 FLJ13611 after digestion and removal of MBP fragment	52
Figure 3.11 FLJ13611 amino-acid sequence	54
Figure 3.12 FLJ13611 fluorescence is quenched by acrylamide	56
Figure 3.13 Modified Stern-Volmer plot of FLJ13611 fluorescence quenching.	57
Figure 3.14 Predicted secondary structure of FLJ13611 by PSI-PRED	59
Figure 3.15 Far-UV CD spectrum of FLJ13611	60
Figure 3.16 Fitting of reconstructed data generated by Dichroweb to experimental data. 63	
Figure 6.1 SPATA4 interacts with C2 by yeast two-hybrid	92
Figure 6.2 SPATA4 and C2 interact in vivo.	94
Figure 6.3 SPATA4 binds to TRAPP	97
Figure 6.4 Localization of SPATA4 in HEK293T cells	102
Supplemental Figure 6.5	106

List of Acronyms

3-AT: 3-amino-1,2,4-triazole

ADP: adenosine diphosphate

AEBSF: 4-(2-aminoethyl) benzenesulfonyl fluoride hydrochloride

ARF: ADP ribosylation factor

Bet3: Blocked early in transport protein 3

BLAST: basic local alignment search tool

CD: circular dichroism

CD8 α : Cluster of differentiation 8 α receptor

CFTR: cystic fibrosis transmembrane conductance receptor

CGN: cis Golgi network

CLIC1: chloride intracellular channel protein 1

CLIC2: chloride intracellular channel protein 2

COG: conserved oligomeric Golgi

COPII: coat protein complex II

CORVET: class C core vacuole / endosome tethering complex

COS7: CV-1 origin SV40 cells 7

C-TVM: C-terminal valine motif

DDO: double drop-out medium

DMEM: Dulbecco's Modified Eagle Medium

Dsl1: Dependent on SLY1-20 protein 1

DTT: dithiothreitol

EDTA: ethylenediaminetetraacetic acid

ER: endoplasmic reticulum

ERGIC: ER-Golgi intermediate compartment

Erk: extracellular signal regulated kinase

FAPP1: four-phosphate adaptor protein 1

FAPP2: four-phosphate adaptor protein 2

FBS: fetal bovine serum

GARP: Golgi associated retrograde protein complex

GDP: guanosine diphosphate

GEF: guanine exchange factor

GFP: green fluorescent protein

GRASP55: Golgi reassembly stacking protein of 55 kDa

GRASP65: Golgi reassembly stacking protein of 65 kDa

GTP: guanosine triphosphate

HEK 293T: human embryonic kidney 293T

HEPES: 2-[4-(2-hydroxyethyl)piperazin-1-yl]ethanesulfonic acid

HOPS: homotypic fusion and vacuole protein sorting

LH β : luteinizing hormone β

MCF7: Michigan Cancer Foundation – 7 cell line

MBP-1: *c-myc* promoter-binding protein 1

MMP: matrix metalloproteinase

MT: microtubules

NF- κ B: nuclear factor kappa-light-chain-enhancer of activated B cells

NSF: N-ethylmaleimide-sensitive factor

PAM14: protein associated with MRG 14 kDa

PBS: phosphate buffered saline

PBS_t: PBS tween

PCR: polymerase chain reaction

PDZ: PSD95 Dlg1 zo-1 domain

PEG: Polyethylene glycol

PI4K β : phosphatidylinositol 4-kinase β

PMSF: phenylmethylsulfonyl fluoride

PSI-BLAST: position-specific iterative BLAST

PVDF: polyvinylidene difluoride

QDO: quadruple drop-out medium

RPE: retinal pigmented epithelium

SDS: Sodium dodecyl sulfate

SED1: spondyloepiphyseal dysplasia tarda

siRNA: small interfering ribonucleic acid

SNARE: soluble NSF attachment protein receptor

SPATA4: spermatogenesis associated protein 4

SPR: serine-proline rich domain

TAP: tandem affinity purification

TDO: triple drop-out medium

TECPR1: tectonin beta-propeller repeat 1 containing protein

TGN: trans Golgi network

TRAPP: transport protein particle

t-SNARE: target SNARE

v-SNARE: vesicle SNARE

VTC: vesicular-tubular cluster

YFP: yellow fluorescent protein

YPD: yeast peptone dextrose medium

1 Introduction

1.1 Membrane trafficking and the Golgi apparatus

Membrane trafficking is central to eukaryotic cells and describes the process of delivering proteins and lipids to various intracellular locations and to the extracellular space by using membrane-delimited carriers (vesicles). This process consists of three main steps, (i) the budding of a vesicle from the donor compartment, (ii) translocation of the vesicle to the destination compartment, and (iii) vesicle fusion with the acceptor compartment. Nearly all forms of membrane transport, including exocytosis, endocytosis and retrograde transport occur through vesicles (Bonifacino and Glick, 2004).

Most secreted proteins, after properly folding in the endoplasmic reticulum (ER), are packaged into coat protein complex II (COPII) coated vesicles that bud from ER exit-sites and are delivered to the Golgi apparatus (Hughes and Stephens, 2008). After being processed in the Golgi, they are packaged into carriers that bud from the trans-Golgi network in a process controlled by the four-phosphate adaptor proteins 1 and 2 (FAPP1 and FAPP2) and the small GTPase ADP ribosylation factor (ARF). Then, the carriers travel toward the plasma membrane, where fusion occurs, ultimately releasing the protein to the extracellular environment (Godi et al., 2004).

The Golgi apparatus is not only the central axis of the membrane trafficking system, but also a signaling platform and the site for lipid and carbohydrate biosynthesis and post-

translational modifications of proteins (glycosylation, phosphorylation and sulfation). The set of glycosyltransferases that reside in Golgi cisternae make possible glycosylation events significantly more complex than those in the ER, which are thought to be merely facilitators of protein folding. Glycosylation at the Golgi allows further functional diversification of mature proteins, adding a spectrum of novel functions especially important in adaptive and innate immune responses. In addition, the Golgi apparatus has a role in determining cell polarity in secretory cells by guiding the exocytic traffic toward a specific part of the plasma membrane as well as in migrating cells, which is accomplished by adding new membranes to the leading edge (Shorter and Warren, 2002).

Although its function is highly conserved among eukaryotes, Golgi morphology can vary substantially between different species. In mammals, the Golgi apparatus is composed of a large number of membranous flattened cisternae, organized in stacks, which are linked by tubular bridges (non compact zones), resulting in the formation of a ribbon in the perinuclear region near the centrosome (Colanzi et al., 2003; Wei and Seemann, 2009). This localization allows a close association to microtubules (MT), which are essential for membrane trafficking in higher eukaryotes. In addition, MTs help to maintain the structure of the Golgi, since depolymerisation of the MT network leads to disruption of the Golgi structure (Rios and Bornens, 2003).

In plants and *Drosophila*, the Golgi stacks are not linked, but found dispersed throughout the cytoplasm and each one is associated with an ER exit site. In *Saccharomyces cerevisiae*, the Golgi cisternae appear dispersed in the cytoplasm, while in the protozoa *Toxoplasma gondii* and *Trypanosoma brucei* only one stack is present (He, 2007).

In all the Golgi stacks three distinct functional regions have been identified, (i) cis Golgi network (CGN), where vesicles from the ER fuse to deliver their cargo, (ii) medial Golgi network, and (iii) trans Golgi network (TGN), where the content is sorted, packaged and sent to its final destination (Klumperman, 2011).

The Golgi receives and donates vesicles in both anterograde (ER to Golgi) and retrograde (Golgi to ER) directions, as well as to endosomes, lysosomes and other membrane-bound organelles (Klumperman, 2011). Such variety of interconnected routes requires control mechanisms, either to ensure that the cargo reaches the right destination or to coordinate the fission (budding) and fusion of membranes. Indeed, many factors control membrane trafficking, including Rab GTPases, SNARE (soluble NSF attachment protein receptor) proteins and vesicle tethering factors (Cai et al., 2007).

1.2 Tethering and vesicle fusion

Tethering is defined as the first contact between a vesicle and its target membrane, which is mediated by “tethering factors”. Tethering factors can be either single polypeptides or multisubunit complexes, and they are found in a variety of locations, and act recognizing and capturing specific vesicles. As such, they are believed to provide the first layer of specificity in membrane trafficking. Some known multisubunit tethering factors are: TRAPP (transport associated protein particle) complex, that participates in the transport from ER to Golgi and between Golgi cisternae; Dsl1, that acts in transport from the Golgi to the ER, COG (conserved oligomeric Golgi) complex, that acts in the retrograde transport of Golgi resident proteins,

HOPS (homotypic fusion and vacuole protein sorting), CORVET (class C core vacuole / endosome tethering complex) and GARP (Golgi associated retrograde protein) complex (Angers and Merz, 2011).

Rab proteins are usually synthesized as soluble proteins, and are inserted into membranes after the addition of geranylgeranyl groups to their C-terminus. During tethering events, inactive Rab proteins already inserted in the membrane become active by exchanging guanosine diphosphate (GDP) for guanosine triphosphate (GTP). The Rab can then recruit effectors at the membrane, which will act in events upstream of vesicle fusion. Different Rabs are found in different compartments, ensuring an additional layer of specificity (Hutagalung and Novick, 2011).

After tethering occurs, vesicles are thought to uncoat, and at some point following uncoating, vesicle SNARE (vSNARE) binds to the target SNARE (tSNARE), bringing the membranes closer, so that the leaflets can ultimately fuse. Several pairs of SNAREs have been described, and they also contribute to the specificity of membrane fusion (Bonifacino and Glick, 2004). After the external leaflets fuse, there is the formation of a pore, which expands, allowing the contents of the vesicle to be released into the lumen of the target compartment (Chernomordik et al., 2006).

In addition to physically capturing vesicles, some tethering factors can activate Rabs through guanine nucleotide exchange factor (GEF) activity, and may also play a role in the uncoating of the vesicle and in the assembly of trans-SNARE complexes (Sztul and Lupashin, 2009).

1.3 TRAPP Complexes

Transport protein particle (TRAPP) complex is a highly conserved multi-subunit tethering factor known to mediate ER-to-Golgi and intra-Golgi transport. First described in 1998 by Sacher et al. as an 800 kDa protein complex localized to the cis-Golgi, the TRAPP complex is now thought to be present in at least three different forms in *Saccharomyces cerevisiae* (TRAPP I, TRAPP II and TRAPP III) and one in mammalian cells (Lynch-Day et al., 2010; Sacher et al., 1998, 2001; Sacher and Ferro-Novick, 2001).

In yeast, TRAPP I is composed of Bet3, Bet5, Trs20, Trs23, Trs31 and Trs33 (Sacher et al., 1998). This forms a common core upon which the other two complexes are built by the addition of specific subunits for both TRAPP II (Trs65, Trs120, Trs130 and Tca17) and TRAPP III (Trs85). Although originally implicated in ER-to-Golgi transport, TRAPP I was recently suggested to be an *in vitro* artifact (Brunet et al., 2012). TRAPP II acts in the late Golgi trafficking (Sacher et al., 2001); and TRAPP III is targeted to phagophore assembly sites, where it participates in autophagy-related processes (Lynch-Day et al., 2010).

The mammalian TRAPP complex is composed of homologues of all yeast TRAPP subunits (except for Trs65, with no homolog found yet) named from TRAPPC1 to TRAPPC10, and the subunits TRAPPC11 and TRAPPC12, which have no homologues in *S. Cerevisiae* (see Table 1.1) (Scrivens et al., 2011).

Table 1.1 Nomenclature of mammalian and yeast TRAPP subunits (adapted from Scrivens et al., 2011).

Mammalian		Yeast		
Name	Size (kDa)	Name	Size (kDa)	Complex
TRAPPC1	17	Bet5	18	I, II, III
TRAPPC2	16	Trs20	20	I, II, III
TRAPPC2L	16	Tca17	16	II
TRAPPC3 / TRAPPC3L	20	Bet3	22	I, II, III
TRAPPC4	24	Trs23	23	I, II, III
TRAPPC5	21	Trs31	31	I, II, III
TRAPPC6a / TRAPPC6b	19 / 15	Trs33	33	I, II, III
-	-	Trs65	65	II
TRAPPC8	161	Trs85	85	III
TRAPPC9	140	Trs120	120	II
TRAPPC10	142	Trs130	130	II
TRAPPC11	129	-	-	-
TRAPPC12	79	-	-	-

The following subsections will discuss yeast TRAPP complexes (1.3.1), the particularities of the mammalian TRAPP complex (1.3.2) and information about TRAPP proteins in other species (1.3.3).

1.3.1 Yeast TRAPP complexes

Despite being classified as a tethering factor, there is no direct evidence that TRAPP can bridge the vesicle and the target membrane. The idea of TRAPP as a tether came from the fact that TRAPP mutants show vesicle accumulation (Rossi et al., 1995; Sacher et al., 2001). However, vesicles can accumulate for many different reasons and not only due to a defect in tethering. Any block in the trafficking process after the vesicle buds could, in theory, lead to this phenotype. Interestingly, yeast TRAPP I is a GEF for the small Rab GTPase Ypt1 (Wang et al., 2000), which controls ER-to-Golgi and intra-Golgi trafficking, and this could explain the phenotype observed in TRAPP mutants even if TRAPP is not a tether. Likewise, yeast TRAPP II is a GEF for Ypt31/32 (Jones et al., 2000; Zou et al., 2012), a GTPase that functions in Golgi-to-plasma membrane and endosome-to-Golgi transport.

Localization studies performed on yeast TRAPP subunits have been controversial. Initially, Bet3 was found only in cis-Golgi membranes (Sacher et al., 1998). Conversely, Trs33 (Tokarev et al., 2009), Trs65, Trs120, Trs130 were seen mainly in the trans-Golgi (Cai et al., 2005; Liang et al., 2007). Whereas Trs65, Trs120 and Trs130 are TRAPP II-specific subunits, Bet3 and Trs33 are part of all TRAPP complexes, therefore they are expected to have a broader localization, and a fraction of them should certainly co-localize with Trs130. These conflicting results could be attributed to the use of different tags (GFP, YFP, etc) and their position (C-terminal or N-terminal), as well as to different fixation methods. Alternatively, these data may suggest that the number of yeast TRAPP complexes is less than the three reported. Interestingly, the existence of a functional TRAPP I in yeast was recently questioned, and it is possible that functions attributed to it in ER-to-Golgi transport are actually performed by the autophagy-

related TRAPP III complex. Trs85 mutants are defective in the cytosol-to-vacuole (CVT) pathway and Trs85 does colocalize with pre-autophagosomal structures, but the role of TRAPP III in autophagy might be indirect, derivative of its role in the early secretory pathway (Choi et al., 2011). A recent study using the v-SNARE Snc1 as a marker of intracellular transport suggested that Trs85 (a TRAPP III specific subunit) acts in the ER-to-Golgi transport (Zou et al., 2012).

Corroborating this idea, biochemical studies have pointed to TRAPP I as an *in vitro* artifact, generated from TRAPP II and III in the presence of high salt concentrations. Interestingly, TRAPP I is absent in Trs23 mutants where the *Saccharomyces cerevisiae* specific domain (SMS) is deleted, but no trafficking or growth defects are observed (Brunet et al., 2012).

1.3.2 Mammalian TRAPP complex

The mammalian TRAPP complex functions are similar to the ones attributed to yeast TRAPP I, participating in the early secretory pathway (Loh et al., 2005). It is reported to have GEF activity towards Rab1, a small GTPase that regulates ER-to-Golgi and early Golgi trafficking, homolog of the yeast Rab Ypt1, although the activity does not appear to be as robust as that seen for the yeast complex on Ypt1p (Yamasaki et al., 2009).

ER-to-Golgi trafficking in mammalian cells is, however, more complex than in yeast, due to the presence of the ER-Golgi intermediate compartment (ERGIC). The ERGIC, also known as vesicular-tubular clusters (VTC) or pre-Golgi intermediates, is localized in the vicinity of ER exit sites, and is formed by homotypic fusion of COPII coated vesicles derived

from the ER (Appenzeller-Herzog and Hauri, 2006). The mammalian TRAPPC3 protein has been shown to be required for ERGIC biogenesis (Yu et al., 2006), and TRAPPC12 partially colocalizes to this compartment (Scrivens et al., 2011). Moreover, depletion of either TRAPPC11 or TRAPPC12 leads to accumulation of cargo in ERGIC53 positive structures. Therefore, mammalian TRAPP seems to be involved in ER-to-ERGIC transport (Scrivens et al., 2011).

Although only one TRAPP complex is found in mammalian cells, it might be present in numerous different subtypes that differ in the isoform of several TRAPP proteins they incorporate, including TRAPPC6 (present in at least three isoforms: two splice variants of TRAPPC6a, and TRAPPC6b), TRAPPC9 and TRAPPC3 . These isoforms could function in different places inside the cell or be expressed in different tissues, adding more complexity to vesicular transport in mammals (Kümmel et al., 2008).

The association of TRAPP with membranes was suggested to be mediated by TRAPPC3. This subunit has a hydrophobic channel that could fit a myristate or other fatty acid and attach the complex to a lipid bilayer. In addition to this lipid anchor, the crystal structure of a mouse TRAPPC3 dimer reveals a flat and positively charged surface that could participate in non-specific electrostatic interactions with the negatively charged head groups of the phospholipids in the membrane (Kim et al., 2005). The yeast homolog, Bet3, seems to function in a similar way, since charge-inversion mutations in this flat charged surface lead to mislocalization of the protein and conditional lethality (Kim et al., 2005).

Despite the fact that the mammalian cells do not have a separate “autophagy-related” TRAPP complex like yeast (TRAPP III), many mammalian TRAPP subunits are somehow involved in autophagy-related processes. A proteomic analysis of the autophagy network in human cells identified TRAPPC5, TRAPPC8 and TRAPPC11 as required for autophagosome formation and TRAPPC12 as an inhibitor of the same process. Furthermore, these subunits, as well as TRAPPC2L, TRAPPC3 and TRAPPC4 interact with the tectonin beta-propeller repeat containing 1 protein (TECPR1), a component of the autophagosome assembly machinery (Behrends et al., 2010).

TRAPPC2, in addition to its presence in the TRAPP complex, interacts with other proteins, apparently not related to secretion, such as the transcription repressor *c-myc* promoter binding protein 1 (MBP-1) (Ghosh et al., 2001). This interaction negatively regulates the transcription of the luteinizing hormone β (LH β) gene in the pituitary gland (Ghosh et al., 2003). Other TRAPPC2 binding partners are the chloride intracellular channel proteins 1 and 2 (CLIC1 and CLIC2) (Fan et al., 2003) and the nuclear protein associated with MRG 14 kDa (PAM14) (Liu et al., 2010).

Another mammalian subunit with roles outside the TRAPP complex is TRAPPC4, which is found to interact with the extracellular signal-regulated kinase 2 (ERK2), activating it and consequently regulating cell proliferation and apoptosis in colorectal cancer cells (Zhao et al., 2011).

The mammalian TRAPP has also been reported to participate in ciliogenesis in retinal pigmented epithelium (RPE) cells, by targeting Rabin8 to the centrosome upon serum

starvation (Westlake et al., 2011). Rabin 8 is a GEF for Rab8, a GTPase required for the assembly of primary cilia (Nachury et al., 2007). The transport of Rabin8 to the centrosome also requires the participation of Rab11, the human homolog of Ypt31/32. Essentially, TRAPP and Rab11 recruit Rabin8 to the centrosome, and Rabin 8 activates Rab8 (Westlake et al., 2011). Whether the GEF activity of TRAPP towards Rab proteins is relevant in this process has not been addressed.

1.3.2.1 TRAPP and diseases

Mutations in TRAPP subunits have been linked to different diseases. Point mutations in TRAPPC2 are known to cause the X-linked skeletal disorder spondyloepiphyseal dysplasia tarda (SED) which results in a defect in endochondral bone growth (Gedeon et al., 2001; MacKenzie et al., 1996). SED is characterized by the presence of flattened vertebral bodies and thick and short femoral necks, which is indicative of a defective endochondral ossification (MacKenzie et al., 1996). SED patients often develop premature osteoarthritis due to perturbations in the extracellular matrix of articular cartilage. At a cellular level, chondrocytes from SED patients have a reduced nuclear : cytoplasm ratio, abundant Golgi and dilated ER, suggesting a defect in secretion of matrix component (Tiller et al., 2001). TRAPPC2 is a broadly expressed protein; however, SED patients have no extra skeletal symptoms, which suggests the involvement of a second protein that would confer tissue specificity, or may indicate a specialized role for TRAPPC2 in chondrocytes.

Truncations in TRAPPC9 have been associated with autosomal-recessive mental retardation (Mir et al., 2009) and postnatal microcephaly (Mochida et al., 2009). Postnatal microcephaly in patients bearing TRAPPC9 mutations is characterized by diminished *corpus callosum* and cerebral white matter, indicating a role for TRAPPC9 in axon and dendrite growth (Mir et al., 2009). This role might be related to the activation of NF- κ B, which is also involved in adult neurogenesis, by TRAPPC9. In mouse brains, TRAPPC9 is found in neurons of the cortical area, hippocampus and deep gray matter, and the expression increases with time, reaching its maximum in adult animals (Mochida et al., 2009). Therefore, TRAPPC9 seems to have a role in brain development.

1.3.3 TRAPP complexes in other organisms

In *Drosophila*, TRAPP II is required for cytokinesis in meiotic cells, where it is needed for constriction of the contractile ring and for recruiting Rab11 to the cleavage furrow. The *Drosophila* ortholog of Trs120, called *brunelleschi* (*bru*) collaborates with phosphatidylinositol 4-kinase β (PI4K β) and Rab11 in order to control the membrane addition to the cleavage furrow (Robinett et al., 2009). Surprisingly, mutations in the *bru* gene do not seem to affect mitotic cytokinesis in larval neuroblasts, indicating that the gene is required only for meiotic cytokinesis (Giansanti et al., 2004; Robinett et al., 2009).

In *Arabidopsis thaliana*, TRAPP II seems to be important for the formation of the cell plate, a transient membrane compartment that appears during cytokinesis and is later converted into a cell wall. Trs120 and Trs130 mutants show severe phenotypic defects,

including multinucleate cells, cell wall stubs, floating cell walls and vesicle accumulation, indicating a failure in tethering and/or fusion (Jaber et al., 2010; Qi et al., 2011; Thellmann et al., 2010). Nevertheless, these mutants show no defects in ER-to-Golgi or biosynthetic vacuolar transport (Qi et al., 2011). Cytokinetic defects are also seen in *Arabidopsis* TRAPP I mutants (Bet5, Trs31 and Trs33), although with milder phenotypes (Thellmann et al., 2010).

In addition to a role in cytokinesis, *Arabidopsis* Trs120 and Trs130 are required for the delivery of the membrane transporter PIN2 to the plasma membrane (Qi et al., 2011), and confirming what is seen in yeast, *Arabidopsis* TRAPP II seems to be linked to Rab-A, which is a homolog of Ypt31/32, but not to Rab-D, a homolog of Ypt1 / Rab1 (Qi and Zheng, 2011).

1.4 SPATA4

Spermatogenesis associated protein 4 (SPATA4) was originally identified as a testis-specific apoptosis related gene (Liu et al., 2004a) expressed exclusively in testis in human, rat and chicken (Liu et al., 2004a; Liu et al., 2004b; Xie et al., 2007), but also found in ovaries of rainbow trout and zebrafish (Liu et al., 2005a; Liu et al., 2005b).

Human SPATA4 has been reported to localize to the nucleus in COS7 cells and to accelerate cell cycle progression in MCF7 cells by speeding up the transition from S-phase to G2-phase. Thus, it can be considered an oncogene rather than an apoptosis-promoting gene, as initially thought (Liu et al., 2004b).

In rats testis, SPATA4 expression varies according to the developmental stage, with no expression in the first month after birth and increasing levels of expression throughout the second month (Liu et al., 2004a). This expression pattern overlaps with the peak of increase in testicular volume in rats, which occurs between days 20 and 70 after birth (Gaytan et al., 1986), and also with the development of interstitial Leydig cells, which starts after day 30 (Christensen, 1975).

In mouse, SPATA4 also seems to be linked to testis development, with increasing expression levels from day 10 to day 14, and constant expression after that (Liu et al., 2005c).

More recently, SPATA4 was also found to be expressed in hypertrophic cartilage of femur growth plates and osteoblasts, where it promotes mineralization of the tissue by activating an Erk1/2 signaling cascade (Wang et al., 2011). This pattern of expression suggests that SPATA4 could have a role in endochondral ossification, which is particularly important for the formation and lengthening of long bones. In this type of ossification, cartilage is progressively replaced by bone tissue during pre-natal development and, at birth, there is still some cartilage remaining at the epiphyseal plates of the long bones, so that they can grow in length during childhood and early adulthood (Mackie et al., 2011). As it will be presented in section 6, SPATA4 interacts with the TRAPP complex and specifically with TRAPPC2, thus it could explain why mutations of a broadly expressed protein (TRAPPC2) cause a tissue specific disorder (SEDT).

1.5 Golgi Reassembly Stacking proteins (GRASPs)

In order to keep the Golgi cisternae organized in stacks, mammalian cells depend mainly on two Golgi reassembly stacking proteins of 55 and 65 kDa, named GRASP55 and GRASP65, respectively. GRASPs are peripheral membrane proteins that form trans-oligomers, bringing together two cisternae. They also are involved in Golgi fragmentation during mitosis, enabling an efficient partition of the Golgi between two daughter cells (Wang and Seemann, 2011).

Both GRASP65 and GRASP55 have a highly conserved N-terminal GRASP domain composed of two PDZ subdomains, responsible for oligomerization, and a regulatory and less conserved C-terminal serine-proline rich domain (SPR). The SPR domain contains several phosphorylation sites that are targeted by mitotic kinases, allowing for the Golgi disassembly to be synchronized with the cell cycle (Vinke et al., 2011).

The two GRASP proteins have similar structure and functions, but differ in their localization inside the cell. GRASP65 is found mainly at the cis-Golgi, whereas GRASP55 is found in medial and trans-Golgi (Vinke et al., 2011).

Aside from their roles in maintaining Golgi structure, GRASPs also participate in secretion of proteins containing a C-terminal valine motif (C-TVM) such as the receptors CD8 α and Frizzled4. GRASP65 and GRASP55 sequentially bind to the C-TVM region of these receptors, assisting in their progression throughout the Golgi (D'Angelo et al., 2009). GRASP55 has also been reported to function in the activation of matrix metalloproteinases (MT1-MMP, MT2-MMP, MT3-MMP, MT5-MMP), extracellular enzymes that are synthesized as inactive zymogens and are later activated by furin. GRASP55 physically interacts with these

enzymes through its PDZ2 subdomain and it is supposed to act like a molecular bridge, connecting furin to the metalloproteinases (Roghi et al., 2010).

Since organisms that do not possess a stacked Golgi such as *S. cerevisiae* have GRASP homologues, it is likely that their primary function is not in the formation of stacks. Indeed, GRASPs are involved in a non-canonical secretory route that bypasses the Golgi, called “unconventional secretion”. This route is thought to be associated with stress conditions and sometimes requires part of the molecular machinery used in early steps of autophagy, such as Atg1, Atg5, Atg7 and Atg8 (Manjithaya and Subramani, 2010, 2011).

In the protozoan *Dictyostellium discoideum* and in the fungi *S. cerevisiae* and *Pichia pastoris*, GRASP homologues (GrpA and Grh1, respectively) participate in the unconventional secretion of acyl-CoA binding protein (AcbA/Acb1), a sporulation factor (Duran et al., 2010; Kinseth et al., 2007; Manjithaya et al., 2010). In *Drosophila*, dGRASP is required for the unconventional secretion of integrin α to the plasma membrane during epithelium development. In this case, dGRASP is no longer a Golgi protein, and localizes to the plasma membrane (Schotman et al., 2008). In mammals, GRASPs are required for the unconventional secretion of interleukin 1 β (Dupont et al., 2011) and the cystic fibrosis transmembrane conductance receptor (CFTR), a transmembrane protein that is usually delivered to the plasma membrane through conventional exocytosis, but can use the unconventional pathway upon ER stress (Gee et al., 2011).

As it will be presented, both GRASP55 and GRASP65 were found to interact with FLJ13611, a new component of the mammalian TRAPP complex.

1.6 Project: Characterization of TRAPP interacting proteins FLJ13611 and SPATA4

Most proteins inside the cell do not perform their functions in isolation, but interact with other proteins and/or protein complexes, either in a stable or in a transient manner. As a consequence, the functions of a given protein can be inferred from its binding partners. Mapping these interactions is crucial for understanding the complexity of the cell and its functions, including how they sense the environment and respond to it. Indeed, much effort has been devoted over the last 20 years to establish the “interactome” of many model organisms such as yeast, *C. elegans* and *Drosophila*, as well as human (Vidal et al., 2011). In order to better understand the functions of the mammalian TRAPP complex, we decided to characterize two of its interactors, FLJ13611 and SPATA4

FLJ13611 was originally found to interact with TRAPPC3 by tandem affinity purification (TAP) and mass spectrometry (Gavin et al., 2002), together with AL136752.1 and CGI-87, that were later characterized as components of the mammalian TRAPP complex (TRAPPC11 and TRAPPC12, respectively (Scrivens et al., 2011)). This led us to hypothesize that FLJ13611 might also be a TRAPP component, and we addressed this by yeast two-hybrid, co-immunoprecipitation and size-exclusion chromatography.

Since the structure of FLJ13611 is unknown and it does not show significant homology to any protein already crystallized, a preliminary assessment of its structure was also conducted by using spectroscopic methods such as circular dichroism, UV spectroscopy, and fluorescence spectroscopy. These techniques are frequently used for characterization of protein structure in solution. With the advantages of being faster, simpler, cheaper, and requiring less

protein than x-ray crystallography, they are often used for preliminary characterization when a three-dimensional structure of the protein is not available, or to determine whether recombinant proteins fold similarly to their endogenous counterparts (Kelly and Price, 2000). The methodology used for characterization of FLJ13611 is detailed in section 2, and the results are presented in section 3 and discussed in section 4.

The other TRAPP interactor, SPATA4, was previously identified by our lab in a yeast two-hybrid screen performed by Sokunthea Hul using TRAPPC2 as the bait. I further characterized the TRAPPC2-SPATA4 interaction by defining the binding regions in both proteins through *in vitro* binding assays, yeast two-hybrid and co-immunoprecipitation. The results of this project were recently published and are presented as a separate manuscript in section 6, with its own introduction, material and methods, results, discussion, and references.

2 Materials and Methods

2.1 Buffers and Solutions

Circular dichroism buffer (CD buffer): 20 mM Tris-H₂SO₄ pH 7.4, 150 mM NaF.

Column Buffer A: 20 mM Tris-HCl pH 7.4, 200 mM NaCl, 1 mM EDTA, 1 mM DTT, 0.1 mM AEBSF, 0.1 mM PMSF.

Column Buffer B: 20 mM Tris-HCl pH 7.4, 200 mM NaCl, 1 mM EDTA, 1 mM DTT, 0.1 mM AEBSF, 0.1 mM PMSF, 25% glycerol.

Digestion buffer A: 20 mM Tris-HCl pH 7.4, 100 mM NaCl, 1mM CaCl₂.

Digestion buffer B: 20 mM Tris-HCl pH 7.4, 100 mM NaCl, 1mM CaCl₂, 10% glycerol.

Double drop-out medium (DDO): 0.67% yeast nitrogen base, 2% dextrose, 0.08% double dropout mix (aminoacid mixture lacking leucine and tryptophan).

Gel Filtration Buffer: 50 mM Tris-HCl pH 7.2, 150 mM NaCl, 0.5 mM EDTA, 1 mM DTT.

GST elution buffer: 50 mM Tris-HCl pH 8.0, 400 mM NaCl, 15 mM glutathione

GST lysis buffer: 50 mM Tris-HCl pH 8.0, 400 mM NaCl, 1 mM DTT, 0.1 mM AEBSF, 0.1% Triton X-100, 5% glycerol (v/v).

GST wash buffer: 50 mM Tris-HCl pH 8.0, 400 mM NaCl, 1 mM DTT, 5% glycerol (v/v).

HBS 2x: 50mM HEPES, 280mM NaCl, 1.5mM Na₂HPO₄, pH 7.1.

Immunofluorescence blocking solution: 2% BSA (w/v), 2%FBS (v/v), 0.2% fish skin gelatin

(v/v), in PBS.

***In vitro* binding buffer:** 10mM HEPES pH 7.4, 25 mM NaCl, 115 mM KCl, 2 mM MgCl₂, 0.1% Triton X-100 (v/v), 5% glycerol (v/v).

-Leu medium: 0.67% yeast nitrogen base, 2% dextrose, 0.08% -leu dropout mix (aminoacid mixture lacking leucine).

Luria Bertani broth (LB): 0.5% yeast extract (w/v), 1% tryptone (w/v), 1% NaCl (w/v).

LB glucose: 0.5% yeast extract (w/v), 1% tryptone (w/v), 1% NaCl (w/v), 0.2% dextrose (w/v).

Mammalian lysis buffer: 50 mM Tris-HCl pH 7.2, 150 mM NaCl, 0.5 mM EDTA, 1 mM DTT, 1% Triton X-100 (v/v), 1 tablet of protease inhibitor cocktail per 10 mL.

PBS: 136 mM NaCl, 2.7 mM KCl, 10.1 mM Na₂HPO₄, 1,8mM KH₂PO₄.

PBS_t: 136 mM NaCl, 2.7 mM KCl, 10.1 mM Na₂HPO₄, 1,8mM KH₂PO₄, 0.1% Tween-20 (v/v).

Quadruple dropout medium (QDO): 0.67% yeast nitrogen base, 2% dextrose, 0.08% quadruple dropout mix (aminoacid mixture lacking leucine, tryptophan, histidine and adenine).

Running Buffer: 25 mM Tris-base, 200 mM glycine, 0.1% SDS.

Sample buffer 4x: 250 mM Tris-HCl pH 6.8, 8% SDS (w/v), 30% glycerol, 0.02% bromophenol blue (w/v), 5% β-Mercaptoethanol (v/v).

Transfer Buffer: 25 mM Tris-base, 200 mM glycine, 20% methanol.

Triple drop-out medium (TDO): 0.67% yeast nitrogen base, 2% dextrose, 0.08% triple dropout mix (aminoacid mixture lacking leucine, tryptophan and histidine).

-Trp medium: 0.67% yeast nitrogen base, 2% dextrose, 0.08% -trp dropout mix (aminoacid

mixture lacking tryptophan).

Yeast peptone dextrose medium (YPD): 1% yeast extract (w/v), 2% peptone (w/v), 2% dextrose (w/v).

Yeast Transformation Mix: 33.3% PEG 3500 (w/v), 0.1 M LiAc, 14% boiled salmon sperm DNA (v/v), 0.5% plasmidial DNA of interest (v/v).

2.2 Oligonucleotides, strains and plasmids

Table 2.1 Oligonucleotides used in this study

Oligonucleotide	Sequence (5' → 3')
FLJ13611GWY-F	GGGGACAAGTTTGTACAAAAAAGCAGGCTTCAT GGAAGTGAATCCCCCTAAAC
FLJ13611GWY-R	GGGGACCACTTTGTACAAGAAAGCTGGGTTTTA GCTTCCACTTTAATGGCAGAAG
GRASP65-F-GWY	GGGGACAAGTTTGTACAAAAAAGCAGGCTTCAC CATGGGCCTGGGCGTCAGCGCTGAG
GRASP65-R-GWY	GGGGACCACTTTGTACAAGAAAGCTGGGTTTTA TTATTCTGTGGTAGAGATCTGGGC
GRASP65-C-term-F-GWY	GGGGACAAGTTTGTACAAAAAAGCAGGCTTCAC CATGAAGCCACCTGGCACCCAC
GRASP65-N-term-R-GWY	GGGGACCACTTTGTACAAGAAAGCTGGGTTTTA CTTGTGGTAGCTGGGGGGC
GRASP55-F-GWY	GGGGACAAGTTTGTACAAAAAAGCAGGCTTCAC CATGGGCTCCTCGCAAAGCGTCGAG
GRASP55-R-GWY	GGGGACCACTTTGTACAAGAAAGCTGGGTTTTA TTAAGGTGACTCAGAAGCATTGGC

pDONR201-F-seq	TCGCGTTAACGCTAGCATGGATCTC
pDONR201-R-seq	GTAACATCAGAGATTTTGAGACAC

Table 2.2 Yeast strains used in this study

Strain	Genotype	Source
AH109	<i>MATa, trp1-901, leu2-3, 112, ura3-52, his3-200, gal4Δ, gal80Δ, LYS2::GAL1_{UAS}-GAL1_{TATA}-HIS3, GAL2_{UAS}-GAL2_{TATA}-ADE2, URA3::MEL1_{UAS}-MEL1_{TATA}-lacZ</i>	Clontech
Y187	<i>MATα, ura3-52, his3-200, ade2-101, trp1-901, leu2-3, 112, met-, gal4Δ, gal80Δ, URA3::GAL1_{UAS}-GAL1_{TATA}-lacZ</i>	Clontech

Table 2.3 Plasmids used for yeast two hybrid

Bacterial Strain	Plasmid	Yeast selection marker	Bacterial selection marker	Source
MSB652	TRAPPC1-pGBKT7	TRP1	Ampicillin	M. Sacher
MSB601	TRAPPC1-pGADT7	LEU2	Ampicillin	M. Sacher
MSB429	TRAPPC2-pGBKT7	TRP1	Ampicillin	M. Sacher
MSB602	TRAPPC2-pGADT7	LEU2	Ampicillin	M. Sacher
MSB435	TRAPPC2L-pGBKT7	TRP1	Ampicillin	M. Sacher
MSB610	TRAPPC2L-pGADT7	LEU2	Ampicillin	M. Sacher
MSB653	TRAPPC3-pGBKT7	TRP1	Ampicillin	M. Sacher
MSB603	TRAPPC3-pGADT7	LEU2	Ampicillin	M. Sacher
MSB660	TRAPPC3L-pGBKT7	TRP1	Ampicillin	M. Sacher
MSB611	TRAPPC3L-pGADT7	LEU2	Ampicillin	M. Sacher
MSB654	TRAPPC4-pGBKT7	TRP1	Ampicillin	M. Sacher
MSB604	TRAPPC4-pGADT7	LEU2	Ampicillin	M. Sacher
MSB655	TRAPPC5-pGBKT7	TRP1	Ampicillin	M. Sacher
MSB605	TRAPPC5-pGADT7	LEU2	Ampicillin	M. Sacher
MSB656	TRAPPC6a-pGBKT7	TRP1	Ampicillin	M. Sacher
MSB606	TRAPPC6a-pGADT7	LEU2	Ampicillin	M. Sacher
MSB657	TRAPPC6b-pGBKT7	TRP1	Ampicillin	M. Sacher
MSB607	TRAPPC6b-pGADT7	LEU2	Ampicillin	M. Sacher

MSB663	TRAPPC8-pGBKT7	TRP1	Ampicillin	M. Sacher
MSB650	TRAPPC8-pGADT7	LEU2	Ampicillin	M. Sacher
MSB993	TRAPPC9-pGBKT7	TRP1	Ampicillin	M. Sacher
MSB994	TRAPPC9-pGADT7	LEU2	Ampicillin	M. Sacher
MSB658	TRAPPC10-pGBKT7	TRP1	Ampicillin	M. Sacher
MSB608	TRAPPC10-pGADT7	LEU2	Ampicillin	M. Sacher
MSB659	TRAPPC11-pGBKT7	TRP1	Ampicillin	M. Sacher
MSB651	TRAPPC11-pGADT7	LEU2	Ampicillin	M. Sacher
MSB681	TRAPPC12-pGBKT7	TRP1	Ampicillin	M. Sacher
MSB705	TRAPPC12-pGADT7	LEU2	Ampicillin	M. Sacher
MSB661	FLJ13611-pGBKT7	TRP1	Ampicillin	M. Sacher
MSB609	FLJ13611-pGADT7	LEU2	Ampicillin	M. Sacher
MSB986	GRASP55-pGBKT7	TRP1	Ampicillin	This study
MSB1002	GRASP55-pGADT7	LEU2	Ampicillin	This study
MSB976	GRASP65-pGBKT7	TRP1	Ampicillin	This study
MSB1003	GRASP65-pGADT7	LEU2	Ampicillin	This study
MSB1163	N-GRASP65-pGBKT7	TRP1	Ampicillin	This study
MSB1164	N-GRASP65-pGADT7	LEU2	Ampicillin	This study
MSB1182	C-GRASP65-pGBKT7	TRP1	Ampicillin	This study
MSB1183	C-GRASP65-pGADT7	LEU2	Ampicillin	This study
MSB272	pGBKT7	TRP1	Kanamycin	Clontech
MSB273	pGADT7	LEU2	Ampicillin	Clontech

Table 2.4 Plasmids used for recombinant protein production

Bacterial strain	Plasmid	Tag	Bacterial selection marker	Source
MSB593	pMAL c2X	MBP	Ampicillin	NEB
MSB596	FLJ13611-pMAL c2X	MBP (N terminal)	Ampicillin	M.Sacher
MSB171	pRL652	GST	Ampicillin	Invitrogen
MSB1074	GRASP65-pDEST15	GST (N terminal)	Ampicillin	This study

Table 2.5 Plasmids used for transfection of mammalian cells

Bacterial strain	Plasmid	Epitope	Bacterial selection marker	Source
MSB1031	FLJ13611-GFP	GFP (N terminal)	Ampicillin	This study
MSB1032	FLJ13611-V5	V5 (N terminal)	Ampicillin	This study
MSB1076	GRASP55-GFP	GFP (N terminal)	Ampicillin	This study
MSB976	GRASP65-GFP	GFP (N terminal)	Ampicillin	This study

2.3 Plasmid construction

Plasmids were constructed using the Gateway[®] system, where the gene of interest is first cloned into an entry vector and then transferred to destination vectors.

For cloning into the entry vector pDONR201, attB1 (at the 5' end) and attB2 (at the 3' end) sites flanking the gene of interest were introduced by polymerase chain reaction (PCR). The amplification was verified by electrophoresis on 1% agarose gel, and the PCR product was purified using the GeneJET[™] PCR purification kit (Fermentas), as per manufacturer's instructions. A BP recombination reaction was then carried out in 0.2 mL PCR tubes by mixing 45 ng of pDONR201 plasmid, 45 ng of the purified PCR product, 0.5 μ L of BP clonase[™] enzyme mix and TE clonase buffer up to a final volume of 2.5 μ L. The reactions were incubated at 25 °C overnight and then stored at -20 °C. Afterwards, 1 μ L of the reaction was transformed into *E. coli* DH5 α competent cells, and the colonies obtained were subjected to plasmid DNA extraction using the Plasmid DNA Miniprep kit (BioBasic), as per manufacturer's instructions. The presence of the insert was confirmed by digestion with BsrGI and sequenced to ensure no mutations were inserted during the cloning.

For transferring the gene of interest from pDONR201 to the various destination vectors (V5, GFP, GST), an LR recombination reaction was carried out in a similar manner as the BP reaction (45 ng of destination vector, 45 ng of pDONR201 containing the insert, 0.5 μ L of LR clonase[™] enzyme mix and TE clonase buffer up to a final volume of 2.5 μ L; incubated at 25 °C overnight and stored at -20 °C), and 1 μ L of the reaction was transformed into *E. coli* DH5 α competent cells. The presence of the insert was verified by digestion with either BamHI or BsrGI.

2.4 Yeast two-hybrid

Plasmids were transformed in either MSY86 (pGADT7 plasmids) or MSY87 (pGBKT7 plasmids), and after selection of transformants, strains were crossed in YPD plates and grown for 1-2 days at 30 °C. Diploids were then selected on DDO plates and used for spotting of serial dilutions or replica-plated onto TDO and QDO plates.

For spotting in serial dilutions, all the strains were normalized to the same OD, and diluted in sterile water at 1:10, 1:100 and 1:1000 and spotted onto DDO, TDO and QDO plates. Each spot contained 2 µL of yeast suspension. Plates were then incubated at 30 °C and growth was analyzed daily. Two proteins were considered to interact if growth was more intense than the growth of the negative control (plasmid with gene of interest in combination with empty vector).

2.4.1 Yeast transformation

Cells were grown in YPD to an OD₆₀₀ of 1.0, harvested by centrifugation at 3000 *g* for 5 min and washed twice in dH₂O. Cells were then incubated in transformation mix at 42°C for 40 min. The transformation mix was removed and cells were resuspended in dH₂O, and then plated in the appropriate selective medium. Plates were kept at 30 °C for 3-4 days and the colonies obtained were restreaked on selective medium.

2.5 Purification of recombinant protein

2.5.1 MBP tagged proteins

E. coli BL21 DE3 cells containing the plasmid pMAL C2X-FLJ (FLJ13611 fused to maltose binding protein (MBP) at the N-terminal portion) were grown in LB-glucose medium to an OD₆₀₀ of 0.5, and IPTG was added to a final concentration of 1mM to induce protein production. Cells were grown for 16h at 25°C, harvested by centrifugation at 4000 rpm for 20 min and resuspended in Column buffer. Cells were lysed by sonication for 2 min and the insoluble portion was removed by centrifugation at 20 000x g. The resulting supernatant was diluted 1:1 in column buffer, bound to 500uL of amylose resin for 40 min at 4°C and then poured into a 1.5 x 12cm chromatography column. Amylose resin was washed 5 times with 10mL of column buffer, and the fusion protein was eluted in 500µL aliquots of column buffer with 10mM maltose after a 5 min incubation at room temperature. Buffer was exchanged to either Circular Dichroism (CD) buffer or *in vitro* binding buffer in a 10DG desalting column (Bio-Rad), and proteins were stored at -80 °C.

2.5.2 GST tagged proteins

E. coli BL21 DE3 cells were grown in LB to an OD₆₀₀ of 0.5, and IPTG was added to a final concentration of 1mM to induce protein production. Cells were grown for 16h at 25°C, harvested by centrifugation at 4000 rpm for 20 min and resuspended in GST lysis buffer. Cells

were lysed by sonication for 2 min and the insoluble portion was removed by centrifugation at 20 000 g. The resulting supernatant was incubated with 500 μ L of glutathione sepharose beads for 1h at 4°C and then poured into a 1.5 x 12cm chromatography column. The beads were washed 5 times with 10mL of GST wash buffer, and the purified protein was eluted in 500 μ L fractions of GST elution buffer after 5 min incubation at room temperature. Buffer was exchanged to *in vitro* binding buffer in a 10DG desalting column (Bio-Rad), and proteins were stored at -80°C.

2.6 In vitro Binding

For *in vitro* binding reactions, the indicated amounts of protein were mixed in a 1.5 mL microcentrifuge tube, and the volume was completed to 250 μ L with *in vitro* binding buffer. The tubes were kept on ice for 1h to allow proteins to bind. Then, 10 μ L of glutathione beads was added to each reaction, and the tube was left to mix on a nutator for 1h hour at 4 °C. Beads were pelleted for 1 min at 1000 rpm in a refrigerated centrifuge (4°C), and the supernatant was discarded. Beads were washed three times with 250 μ L of *in vitro* binding buffer, and the proteins were eluted by boiling the beads for 2 min in 25 μ L of 1x Sample Buffer. Samples were kept at -20 °C until further procedures.

2.7 Electrophoresis and Western Blotting

Proteins were separated using SDS polyacrylamide gel electrophoresis (SDS-PAGE) and transferred to PVDF membranes for 1h at 100V in cold transfer buffer. The efficiency of

the transfer was assessed by staining the membrane with Ponceau, which was promptly removed by rinsing the membrane in distilled water. Membranes were blocked in 5% skim milk for 1h, and then incubated with primary antibody for 1h. After washing twice for 10 min with PBSt, membranes were incubated with the appropriate secondary antibody (goat anti-mouse or goat anti-rabbit, at dilution of 1: 10,000) for 1h, and then washed 3 times for 10 min. The blots were incubated with ECL for two minutes and then exposed to photographic film for 1s – 10 min.

2.8 Cell Culture and knockdown

HeLa and HEK293T cells were grown in Dulbecco's Modified Eagle medium (DMEM) supplemented with 10% fetal bovine serum (FBS) at 37°C in humidified incubator with 5% CO₂. Upon 60% confluency cells were transfected with DNA using either JetPrime (Polyplus Transfection) or CaPO₄. JetPrime was used for transfection of plasmid DNA and siRNA in HeLa cells, and CaPO₄ was used for transfection of plasmid DNA in HEK cells. For transfection with CaPO₄, the appropriate amount of DNA (5-10 µg of plasmid DNA per 10cm dish and 0.5 -1 µg per well for 6-well dishes) was diluted in 500 µL of 168 mM CaCl₂ and then poured dropwise into 500 µL of 2x HBS, so that the final mix contained 1x HBS and 84 mM CaCl₂. After adding the mix dropwise, the cells were returned to the incubator. The medium was replaced 24h after transfection, and cells were then either harvested by scraping with Lysis Buffer or fixed in 100% methanol at -20°C for 4 min for immunofluorescence. For cell lysates, protein concentration was determined using the Bradford assay (Bio-Rad Protein Assay, BioRad) and BSA as standard.

For FLJ13611 knockdown, HeLa cells were plated onto coverslips in a 6-well dish and transfected with 400ng of FLJ13611-V5 plasmid and 60 picomoles of siRNA using JetPrime. 24h after transfection cells were washed with PBS and the medium was replaced, and 48h after transfection cells were either harvested or fixed as above.

2.9 Co-immunoprecipitation

For co-immunoprecipitation reactions, 1 μ g of antibody and 0.5 mg of protein were mixed in a microcentrifuge tube, the volume was completed to 500 μ L with mammalian lysis buffer and the tubes were incubated for 16h at 4°C. Then, 10 μ L of previously blocked protein A or protein G agarose beads was added to each reaction, followed by a 2h incubation on a nutator at 4 °C. The beads were washed three times with 0.5 mL of mammalian lysis buffer and boiled in 25 μ L of 1x SB for 2 min. Samples were kept at -20 °C until further procedures.

2.10 Size exclusion chromatography

HEK293T cells were harvested 48h post-transfection by scraping in mammalian lysis buffer. The lysates were clarified at 15 000 rpm for 15 min, protein concentration was determined as described above, and 2.5 mg was loaded onto a Superdex 200 column (GE Healthcare). The sample was fractionated in gel filtration buffer at flow rate of 0.5 mL/min, and 0.5 mL fractions were collected and frozen until further analysis by Western blotting.

2.11 Immunofluorescence and Fluorescence microscopy

Fixed HeLa cells were incubated with immunofluorescence blocking solution for 30 min, and then with primary antibody diluted in blocking solution (1:500) for 1h. After washing three times with PBS, the cells were incubated with the appropriate secondary antibody (at a dilution of 1:250) and DAPI (at a dilution of 1:1000) for 45 min. After three washes in PBS, coverslips were mounted onto a slide containing one drop of anti-fade and sealed with nail polish. All incubations were performed at room temperature. Pictures were taken on a Zeiss Axioplan epifluorescence microscope and overlaid using Adobe Photoshop.

2.12 Secondary structure prediction

Secondary structure of FLJ13611 was predicted on the online server PSIPRED (www.psidred.net) using PSIPRED algorithm (v 3.0) (Buchan et al., 2010).

2.13 UV spectroscopy

Absorbance at 280nm was used to determine protein concentration of FLJ13611 and FLJ13611-MBP for circular dichroism and fluorescence spectroscopy experiments, and the extinction coefficients were predicted with ProtParam (Gasteiger et al., 1999) on the ExPASy server. Light scattering at 310-320nm was employed to monitor the presence of aggregates and follow the stability of the purified protein in different buffer systems.

2.14 Far UV Circular Dichroism

Far-UV CD spectrum was acquired on a Jasco J-815 spectrophotometer with a scan speed of 100 nm/min, data pitch of 0.2nm, sensitivity of 100, and with 5 accumulations, at room temperature. Signals were recorded from 180 to 260 nm with 0.06 mg/mL of protein in a 0.2 cm path length cell. The percentage of different secondary structure elements was determined using Dichroweb server, with CDSSTR algorithm, reference set 7 and scaling factor 0.1 (Lobley et al., 2002; Sreerama and Woody, 2000; Whitmore and Wallace, 2004).

2.15 Fluorescence Spectroscopy

Intrinsic tryptophan fluorescence of FLJ13611 was measured on a Varian Cary Eclipse Fluorescence Spectrophotometer from 300 to 400 nm using CAT MODE with scan speed set to “FAST”. Ten scans were collected and averaged. Protein concentration was 0.02 mg/mL. To analyze acrylamide quenching of tryptophan fluorescence, a stock solution of 5M acrylamide was prepared in column buffer and added to the protein solution up to a final concentration of 1.2 M. The sample was excited at 295 nm and emission spectrum was observed from 300 to 400 nm. Spectrum of buffer was also recorded and subtracted from all protein spectra. All the measurements were done using a 1cm quartz cuvette.

3 Results

3.1 FLJ13611 interacts with TRAPP subunits by yeast two-hybrid

We first checked whether FLJ13611 might be a TRAPP component by mapping its physical interactions with all known mammalian TRAPP subunits (C1, C2, C2L, C3, C3L, C4, C5, C6a, C6b, C8, C9, C10, C11 and C12) by yeast two-hybrid. FLJ13611 was crossed with TRAPP subunits in two orientations (FLJ13611 in pGAD x TRAPP in pGBK and FLJ13611 in pGBK x TRAPP in pGAD). Growth on 1mM 3-amino-1,2,4-triazole (3-AT) and quadruple drop-out (QDO) plates was considered as an interaction, and 1mM 3-AT was used to distinguish between real interactions and the false positives that arise from autoactivation of the reporter genes. 3-AT is a competitive inhibitor of the product of the *HIS3* gene, imidazoleglycerol-phosphate dehydratase, an enzyme that participates in histidine biosynthesis. The addition of 3-AT in the medium ensures that only colonies expressing high levels of *HIS3* (or true interactions) will grow. As seen in Figure 3.1, FLJ13611 interacts with C2, C2L, C6a, C6b, C11, C12 and with itself when in pGAD, but only with C12 and with itself when in pGBK.

The fact that fewer interactions were seen when FLJ13611 was in pGBK could be attributed to a possible masking of certain regions of FLJ13611 by the fusion protein (when in pGBK, the gene of interest is fused to the binding domain of GAL4). Alternatively, it might indicate that the protein is not properly folded, which could also disrupt some interactions.

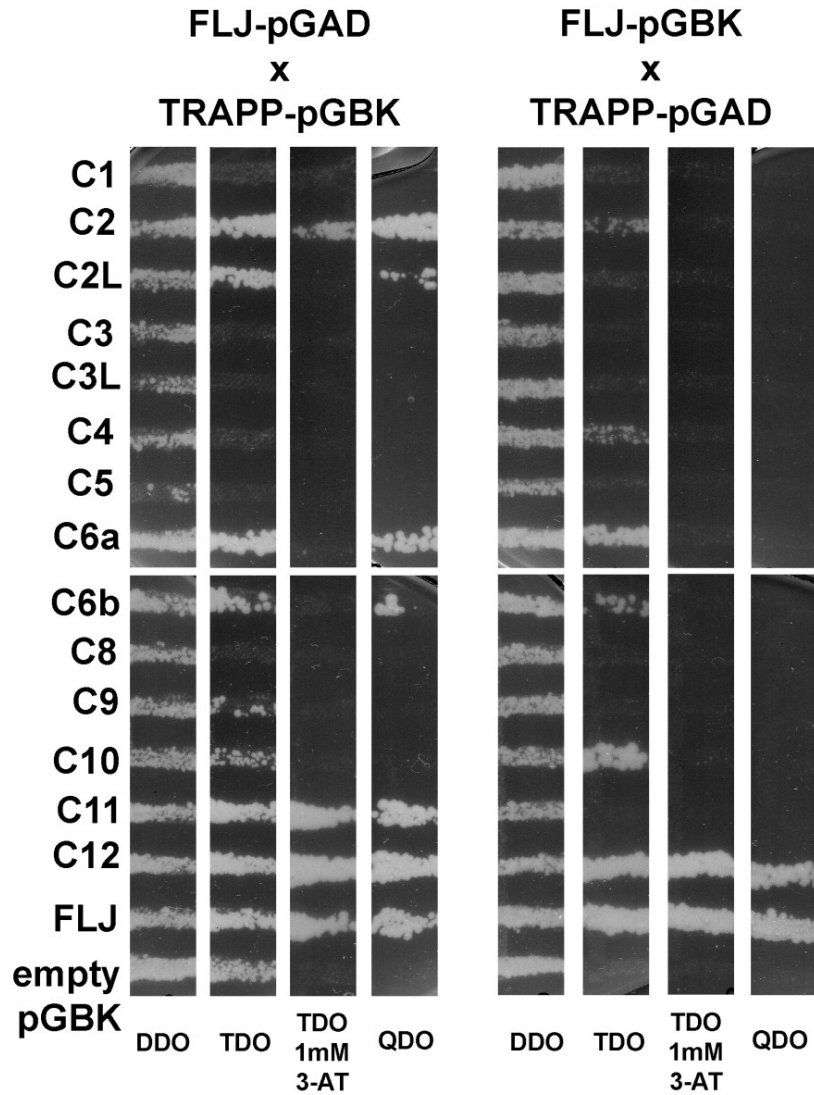


Figure 3.1 Physical interactions of FLJ13611 with TRAPP subunits. *FLJ13611 interacts with C2, C2L, C6a, C6b, C11, C12 and with itself. Growth on double drop-out (DDO) plates indicates the presence of both plasmids (pGAD and pGBK), and growth on the subsequent plates indicates the activation of the reporter genes. Plates were scanned after 7 days. DDO: double drop-out media (-leu / -trp); TDO: triple drop-out media (-leu / -trp / -his); 3-AT: 3-amino-1, 2,4-triazole; QDO: quadruple drop-out media (-leu / -trp / -his / -ade).*

3.2 FLJ13611 interacts with the TRAPP complex in vivo

To confirm that the interaction seen by yeast two-hybrid also occurs *in vivo*, human embryonic kidney (HEK293T) cells were transfected with either GFP or V5 tagged FLJ13611, and lysates were prepared and fractionated on a Superdex 200 size exclusion column. The fractions were analyzed by Western Blotting. As seen in Figure 3.2 (A), both FLJ13611-V5 and FLJ13611-GFP are found in two pools. The high molecular weight pool (left side of the panel) co-fractionates with the TRAPP complex, as demonstrated by the presence of TRAPPC2 and TRAPPC12, whereas the lower molecular weight pool (right side of the panel) corresponds to presumed monomeric protein.

Some TRAPP subunits such as TRAPPC2 and TRAPPC3 also exhibit monomeric pools, whereas others like TRAPPC12 appear to be mostly incorporated in the complex. While overexpressed FLJ13611 shows a monomeric pool, this might be an artifact of overexpression and not necessarily true for the endogenous FLJ13611. Since the other TRAPP components are not overexpressed, there is exceeding FLJ13611 that simply cannot be incorporated into complexes.

Although both forms of FLJ13611 co-fractionate with the TRAPP complex, this result *per se* does not prove that it is truly part of the TRAPP complex. To examine whether FLJ13611 is indeed interacting with the TRAPP complex, we performed a co-immunoprecipitation (Co-IP), using anti-V5 to precipitate FLJ13611-V5 and blotted for TRAPPC2. As shown in Figure 3.2 (B), TRAPPC2 is efficiently co-precipitated with FLJ13611, indicating that they are in the same complex.

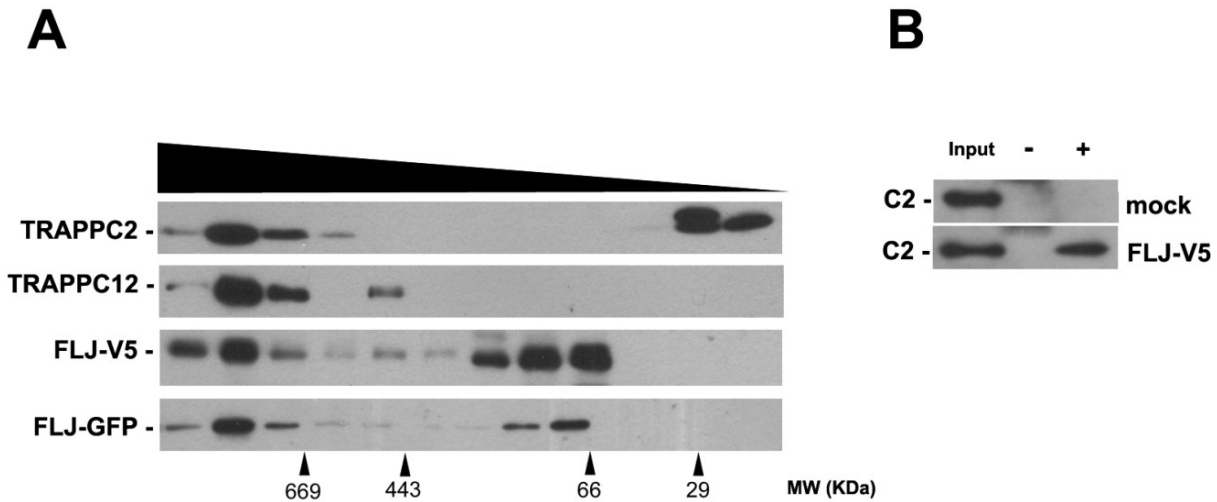


Figure 3.2 *FLJ13611 co-fractionates with TRAPP subunits and co-precipitates with TRAPPC2.* **A:** HEK293T cells transfected with either FLJ13611-V5 or FLJ13611-GFP were lysed and fractionated on a Superdex 200 column. 20 μ L of each fractions was analyzed by Western Blotting using affinity purified anti-TRAPPC2 (1:1000 dilution), anti-TRAPPC12 (1:1000 dilution), anti-V5 (1:000 dilution) or anti-GFP (1:2500 dilution). **B:** HEK293T cells were either transfected with FLJ13611-V5 or mock transfected (the usual volume of plasmid used in $CaPO_4$ transfections was replaced by dH_2O), lysed and subjected to co-immunoprecipitation with anti-V5 (+). A portion of lysate not treated with antibody was used as a negative control (-), to ensure that TRAPPC2 was not non-specifically binding to the beads used for the pull down. Input (total cell lysate, 50 μ g) represents 10% of the amount of protein used in the precipitation.

3.3 FLJ13611 depletion leads to Golgi fragmentation

In order to characterize the function of FLJ13611 we decided to perform a knockdown using small interfering RNA (siRNA). Presently, we do not have an antibody against endogenous FLJ13611, thus it was necessary to transfect the cells with FLJ13611-V5 simultaneously, in order to demonstrate the efficiency of the knockdown (Figure 3.3 A). As shown in Figure 3.3 (A), two different siRNAs were tested, and siRNA1 seemed to be the most efficient, therefore it was used in the subsequent experiments. After staining the Golgi with anti-Mannosidase II, three different morphologies were observed (compact, extended and punctate). As shown in Figure 3.3 (C), knockdown of FLJ13611 led to disruption of the Golgi in more than 50% of the cells (punctate morphology) and to a consequent decrease of the other two morphologies (compact and extended; the decrease of the extended morphology being more prominent).

Since Golgi fragmentation occurs naturally during mitosis, it is not clear whether the depletion of FLJ13611 actively causes the Golgi to fragment, whether it somehow blocks the ER-to-Golgi transport, leading to the fragmentation, or whether it prevents its reassembly after mitosis. Because only the localization of mannosidase II was verified, it is also not known whether these Golgi fragments contain other Golgi resident proteins or whether some of them are re-localized to other compartments such as the ER.

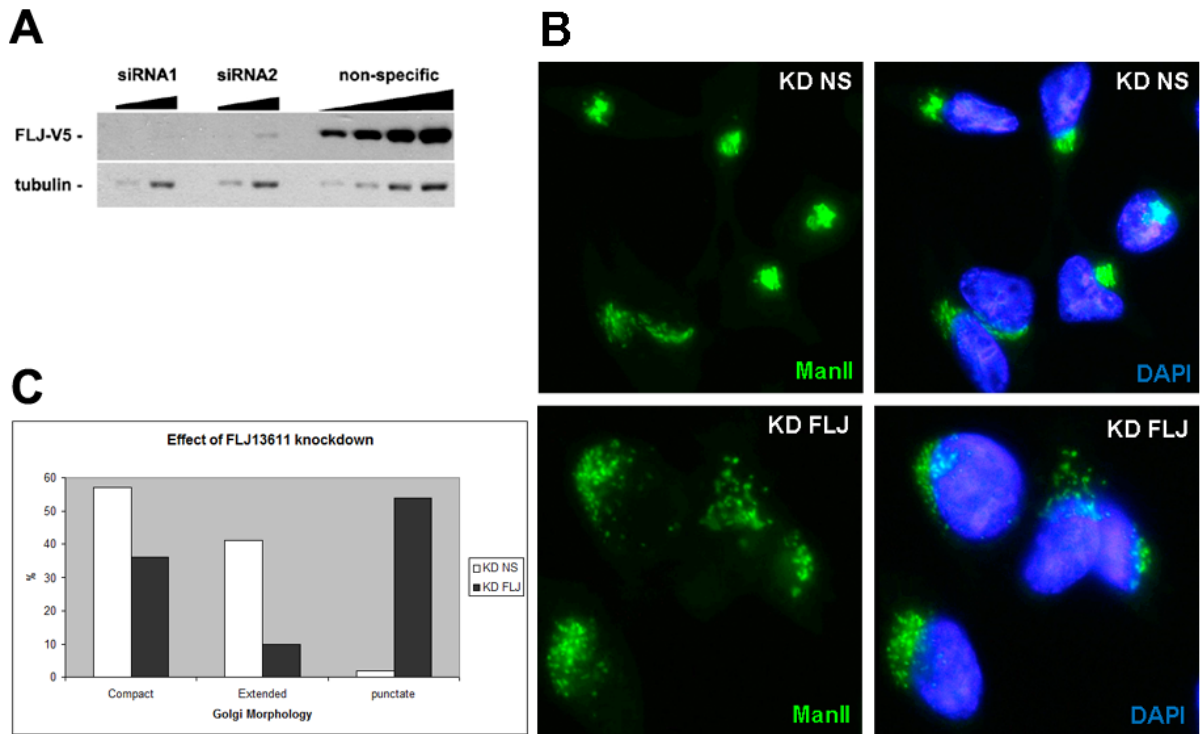


Figure 3.3 *FLJ13611* knockdown leads to fragmentation of the Golgi. **A:** Demonstration of *FLJ13611* knockdown. HeLa cells were transfected with either one of the two different siRNAs against *FLJ13611* (siRNA1 and siRNA2), or non-specific siRNA. Protein levels were analyzed by Western Blotting, and tubulin was used as a loading control. **B:** Immunofluorescence was performed after treating the cells with *FLJ13611*-directed siRNA (KD FLJ, left panel) or non specific siRNA (right panel). Anti-Mannosidase II (ManII) was used as a Golgi marker and DAPI was used to stain the nucleus. **C:** Quantification of Golgi phenotypes observed in **A**. Approximately 100 cells were counted for each condition.

3.4 FLJ13611 interacts with GRASP55 by yeast two-hybrid

One study that relied on expression patterns in *C. elegans* (Zhong and Sternberg, 2006) predicted an interaction between the *C. elegans* homologue of FLJ13611 and the protein GRASP65. The latter protein is involved in the stacking of Golgi cisternae. This led us to examine whether GRASP65 and the closely-related GRASP55 interact with FLJ13611 and with other mammalian TRAPP components by yeast two hybrid. As shown in Figure 3.4 (A), GRASP55 interacts with TRAPPC6a and to a lesser extent TRAPPC6b, and also with FLJ13611. These interactions were only seen in one orientation. For GRASP65, no interaction was seen when GRASP65 was in pGAD, and a strong autoactivation occurred when GRASP65 was in pGBK (see Figure 3.4 B). Therefore it was not possible assess the existence of interactions solely by yeast two-hybrid.

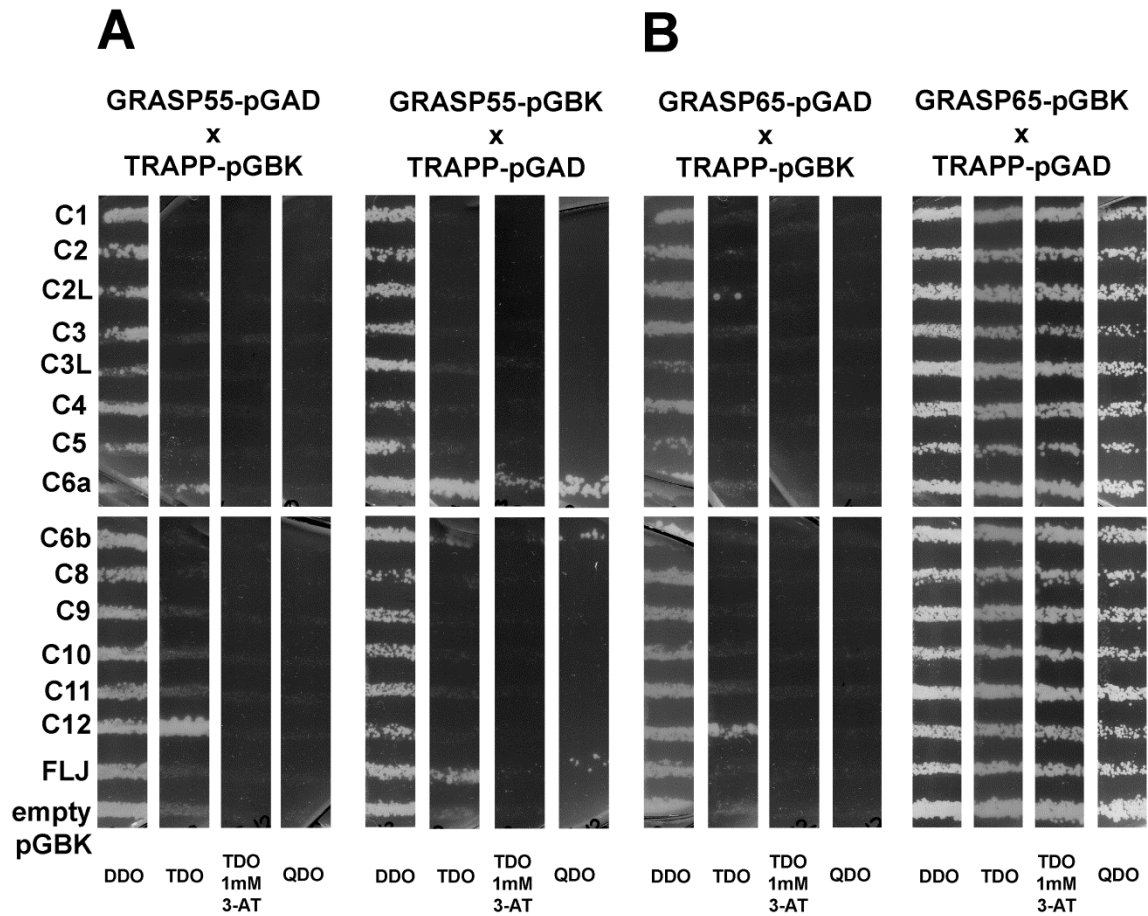


Figure 3.4 Physical interaction of GRASP proteins with TRAPP subunits and FLJ13611. A: GRASP55 interacts with C6a, C6b and FLJ13611. **B:** GRASP65 exhibits strong autoactivation when in pGBK, and no interactions are seen when in pGAD. DDO: double drop-out media (-leu / -trp); TDO: triple drop-out media (-leu / -trp / -his); 3-AT: 3-amino-1, 2,4-triazole; QDO: quadruple drop-out media (-leu / -trp / -his / -ade).

3.5 FLJ13611 interacts with GRASP65

Since yeast two-hybrid could not be used to assess interactions between FLJ13611 and full length GRASP65, we decided to truncate GRASP65 in two portions, in an attempt to overcome the autoactivation. The two fragments (N-terminal fragment from residues 1 to 211 and C-terminal fragment from residues 212 to 440) were cloned into yeast two-hybrid vectors and crossed with TRAPP subunits and FLJ13611. As shown in Figure 3.5 (A), the N-terminal fragment of GRASP65 interacts with FLJ13611. The C-terminal fragment still autoactivates (not shown).

To further support this interaction, we performed an *in vitro* binding assay with full length GRASP65. For this study we fused FLJ13611 to maltose binding protein (MBP). Increasing concentrations of purified FLJ13611-MBP were incubated with either GST or GRASP65-GST. As shown in Figure 3.5 (B), FLJ13611 binds to GRASP65 in a concentration dependent manner.

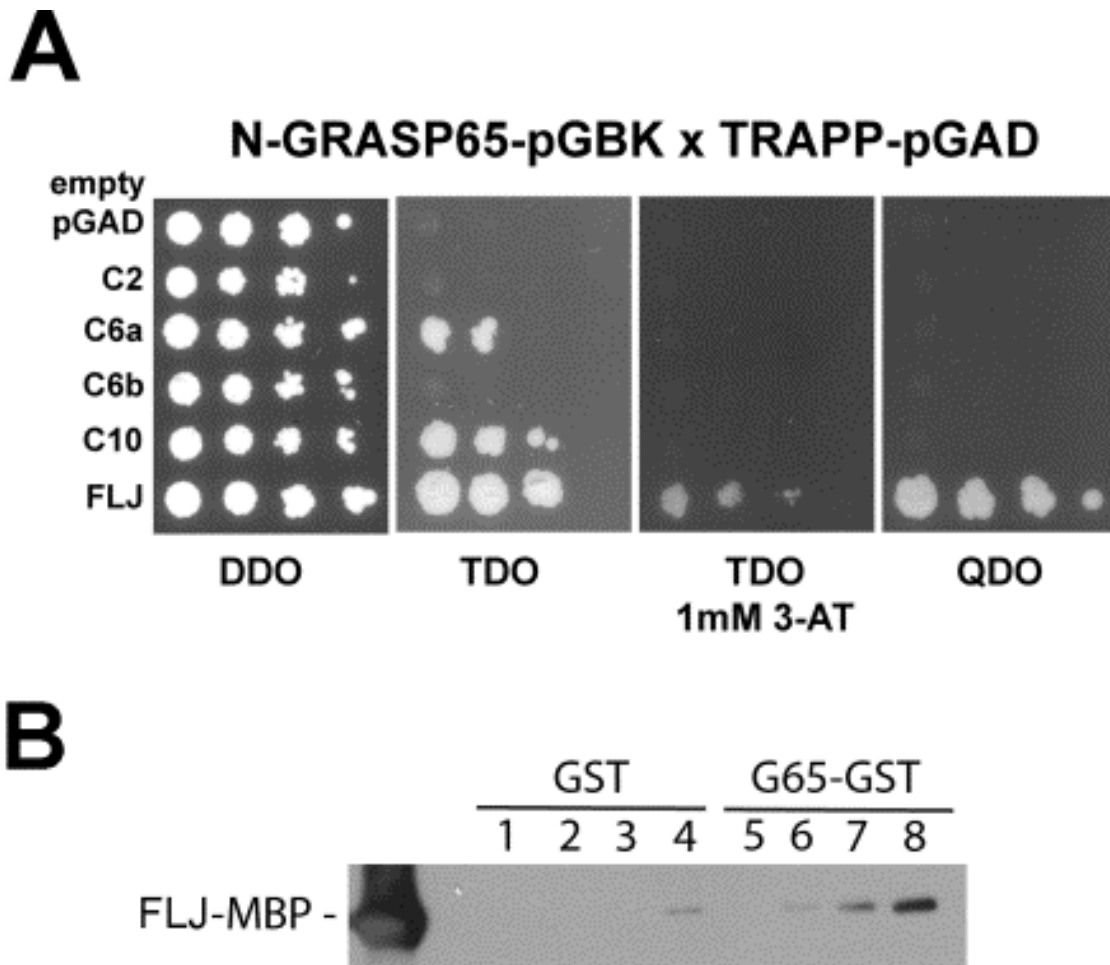


Figure 3.5 GRASP65 interacts with FLJ13611. *A:* The N-terminal portion of GRASP65 interacts with FLJ13611 by yeast two-hybrid. Serial dilutions spotted on DDO, TDO, TDO with 1mM 3-AT and QDO. Growth on 1mM 3-AT and QDO was considered an interaction. *B:* Binding reactions contained 0.5 μ M of GST (lanes 1 to 4) or GRASP65-GST (lanes 5 to 8) and increasing concentrations (0, 0.5, 1 and 2 μ M in lanes 1-4 and 5-8, respectively) of FLJ13611-MBP. Samples were analyzed by Western Blotting using rabbit anti-FLJ13611 serum (1:1000 dilution)

3.6 FLJ13611 interacts with GRASPs in vivo

To confirm that the interaction of FLJ13611 with GRASP55 and GRASP65 occurs *in vivo* in mammalian cells, HEK293T cells were transfected with either GFP-tagged GRASP55 or GRASP65 along with FLJ13611-V5, and a Co-IP was performed. Anti-V5 was used to precipitate FLJ13611-V5, and anti-GFP was used to precipitate either GRASP65 or GRASP55. As shown in Figure 3.6 (A), FLJ13611-V5 is efficiently precipitated with both GRASP55 and GRASP65, but neither GRASPs are pulled down when FLJ13611-V5 is precipitated. This may indicate that the epitope recognized by the anti-V5 antibody is obscured by the interaction with GRASP. In this case, only FLJ13611 that was not interacting with GRASP could have been precipitated. Moreover, TRAPPC2 did not co-precipitate with any of the GRASPs. TRAPPC2 did, however, coprecipitate with FLJ13611, confirming once again (as in Figure 3.2) that FLJ13611 interacts with TRAPP.

To address whether GRASP65 interacts with other TRAPP subunits, we performed other Co-IPs, precipitating TRAPPC2 and blotting for GRASP65 and precipitating GRASP65 and blotting for TRAPPC2, TRAPPC3 and TRAPPC11. As seen in Figure 3.7, no interaction was detected. Therefore, GRASPs seem to interact mainly with FLJ13611 that is not incorporated in the TRAPP complex.

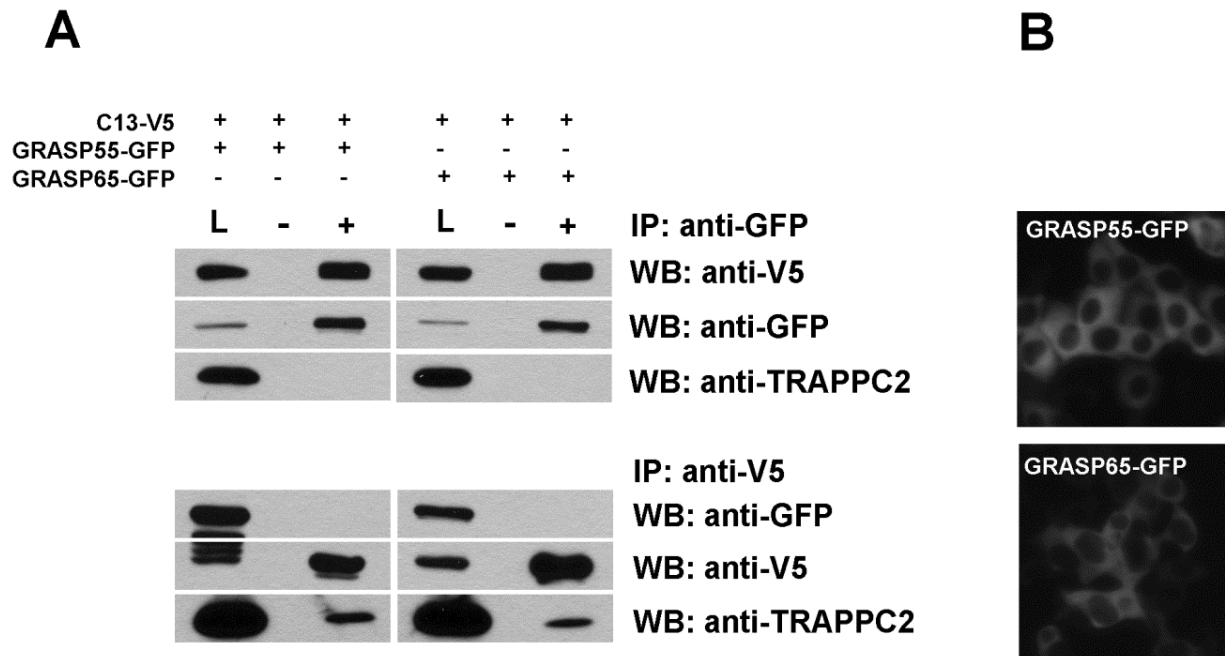


Figure 3.6 *FLJ13611* interacts with *GRASP55* and *GRASP65* in vivo. **A:** HEK293T cells were transfected as indicated and the lysates were subjected to immunoprecipitation with anti-GFP or anti-V5, and blotted with anti-V5, anti-GFP or anti-TRAPPC2. IP: immunoprecipitation; WB: western blot. L: total cell lysate (50 μ g, representing 10% of the amount of protein used in the precipitation). **B:** HEK293T cells just prior to harvesting, showing the expression of GRASP55-GFP and GRASP65-GFP in the cytosol.

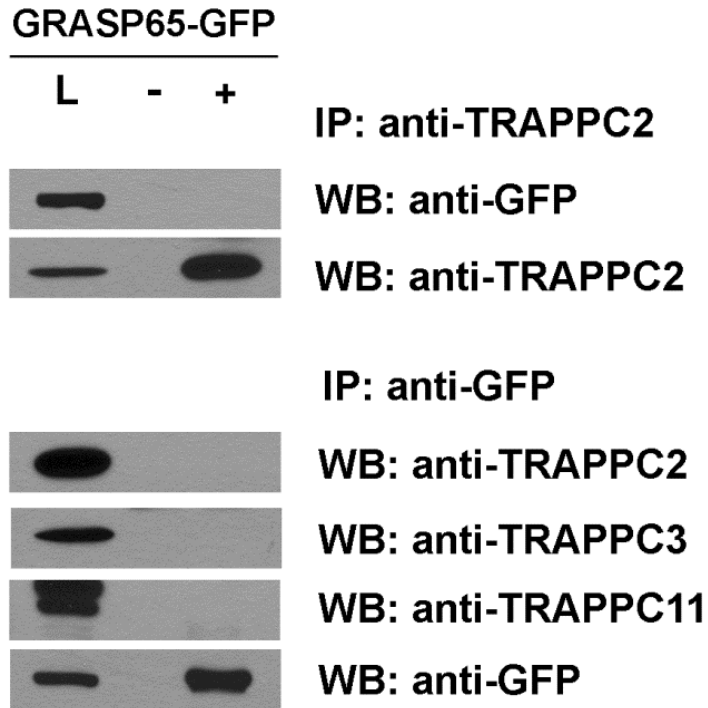


Figure 3.7 GRASP65 does not co-precipitate with the TRAPP complex. HEK293T cells were transfected with GRASP65-GFP, and the lysate was subjected to immunoprecipitation with anti-TRAPPC2 or anti-GFP (lanes +). The negative control (lane -) consisted of the same lysate not treated with any antibody. The samples were blotted with anti-GFP, anti-TRAPPC2, anti-TRAPPC3 and anti-TRAPPC11. IP: immunoprecipitation; WB: western blot; L: total cell lysate (50 μ g, representing 10% of the amount of protein used in the precipitation).

3.7 Optimization of recombinant protein purification and removal of MBP

One way to address the function of a protein is to determine its three-dimensional structure and, using this information, examine the effects of mutating certain residues. Purification of various recombinant forms of tagged FLJ13611 resulted in unstable protein. To determine the best conditions for the purification of the fusion protein FLJ13611-MBP, we performed the purification from *E. Coli* BL21 DE3 cultures using either Column buffers A or B. Column buffer B was chosen for the subsequent experiments because, although Column buffer A gave a considerably higher yield, it also enhanced the presence of undesirable lower molecular weight components (between 60 and 50 kDa, see Figure 3.8 A and B).

A UV absorption spectrum was recorded to determine the protein concentration and assess the stability of FLJ13611-MBP in column buffer B. Absorption spectra of proteins have a major component at 280 nm, which corresponds to mainly tryptophans (although other aromatic residues also contribute), and this is usually used to calculate protein concentration. In the region between 310 nm and 350 nm, no signal is seen if the protein is completely in solution (Absorbance (Abs) = 0). If the sample aggregates and the size of the particles are in the order of the wavelength, we have Abs above zero, but what is being observed is light scattering and not real absorbance. Therefore, UV absorption spectrum between 310 and 350 nm can be used to monitor the stability of a purified protein. This is particularly useful for proteins that tend to aggregate or if different buffer systems have to be used for different experiments.

As seen in Figure 3.8 (C), FLJ13611-MBP remained stable for at least 12h at room temperature, and only minor changes were seen in the spectra over this time period.

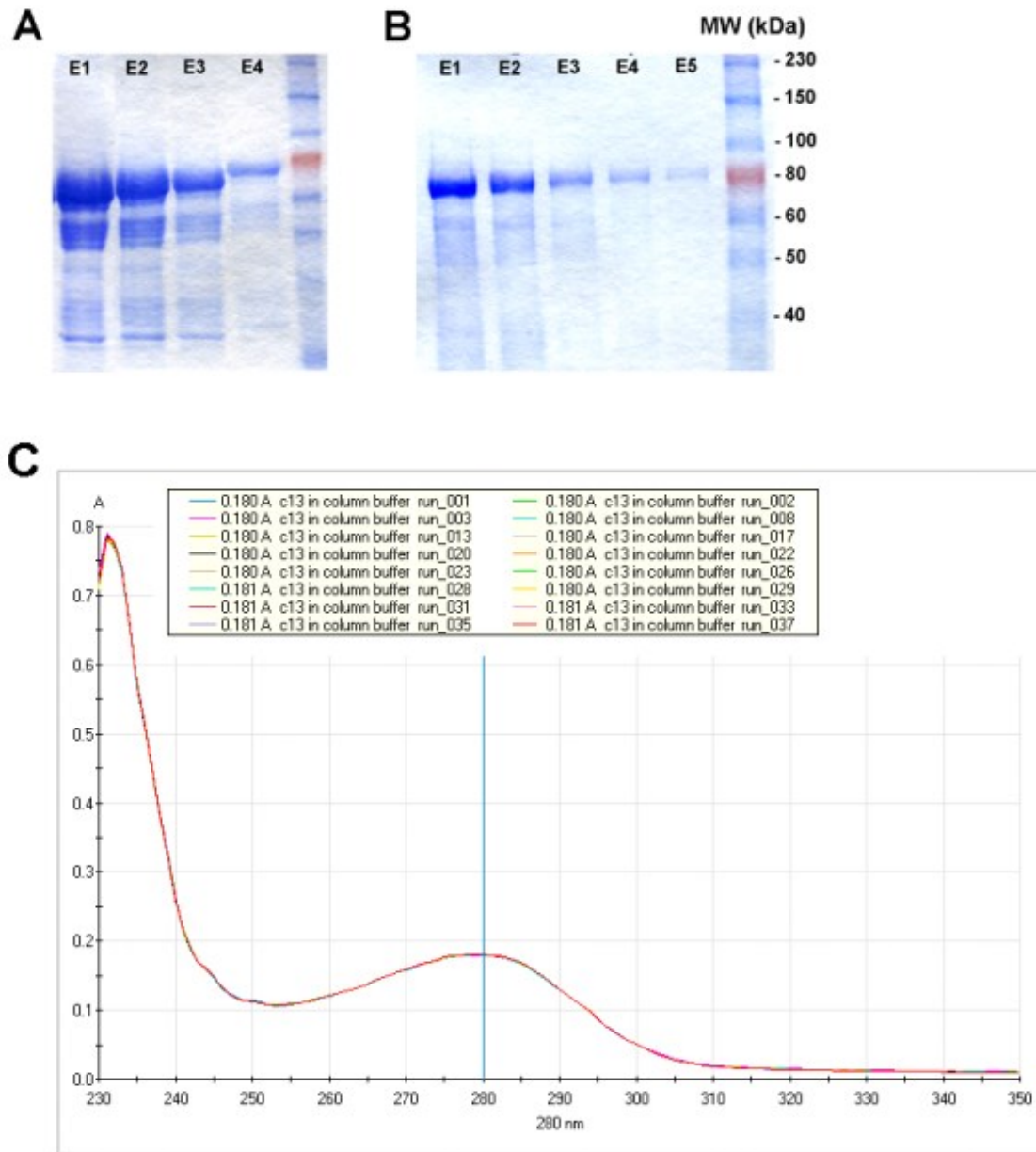


Figure 3.8 Purification and stability of FLJ13611-MBP. Recombinant FLJ13611-MBP purified in either Column buffer A (A) or Column buffer B (B). SDS-PAGE stained with Coomassie Blue. E1 – E5: elutions 1 to 5. FLJ13611-MBP has a predicted molecular weight of 86.6 kDa. C: UV spectroscopy confirms stability of FLJ13611-MBP at room temperature in Column buffer B. The graph shows some of the 37 scans recorded over a period of 16h.

Having found a buffer to keep FLJ13611-MBP stable, the next step was the cleavage of the MBP tag. FLJ13611-MBP was kept in Column buffer B and was immobilized on amylose resin and digested with FactorXa for 12h. Under these conditions, the MBP fragment would stay bound to the resin, while FLJ13611 would be released into the supernatant. As seen in Figure 3.9 (A), Column buffer B did not permit the digestion to occur, and all FLJ13611 remained fused to MBP. This was likely due to the high glycerol concentration present in Column buffer B (25%), which might have inhibited the enzymatic activity of Factor Xa.

Therefore, we decided to test digestion in two other buffers (Digestion Buffers A and B; A being an ideal buffer for FactorXa, and B a modified version, with 10% glycerol to improve protein stability). Digestion Buffer A caused immediate protein precipitation, visible to the naked eye. Digestion Buffer B still caused some protein precipitation, which was efficiently removed by a 20 min centrifugation. Digestion was successfully completed after 3h incubation at RT + 12h incubation at 4°C (see Figure 3.9 B), with all FLJ13611-MBP cleaved (note the disappearance of the band at 80 kDa, which corresponds to FLJ13611-MBP, and the appearance of a band ~ 45 kDa, which corresponds to FLJ13611 alone.)

Following digestion, MBP was removed by binding to amylose resin, and the remaining FLJ13611 was checked for aggregation. As seen in Figure 3.10, the existing aggregates were removed by a 20 min centrifugation. Subsequently, sample was exchanged back into Column buffer A for fluorescence spectroscopy, or into CD buffer for Far-UV CD measurements.

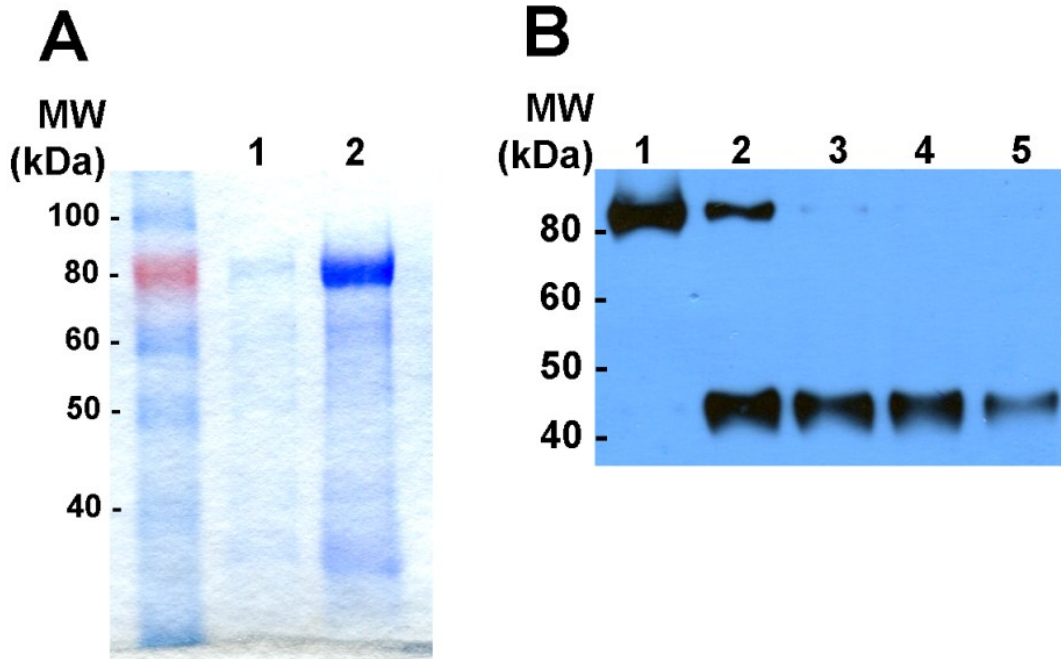


Figure 3.9 Digestion of FLJ13611-MBP with FactorXa. *A: digestion performed in Column buffer B. SDS-PAGE stained with Coomassie Blue. 1: Digested product; 2: Undigested product recovered from amylose resin. B: digestions performed in Digestion buffer B. Complete digestion of FLJ13611-MBP with FactorXa in Digestion buffer B. 1: t=0; 2: t=3h; 3: t=3h RT + 12h 4°C; 4: t=4h RT + 12h 4°C; 5: FLJ13611 after MBP removal. Samples were analysed by Western Blotting using rabbit anti-FLJ13611 serum at 1:1000 dilution.*

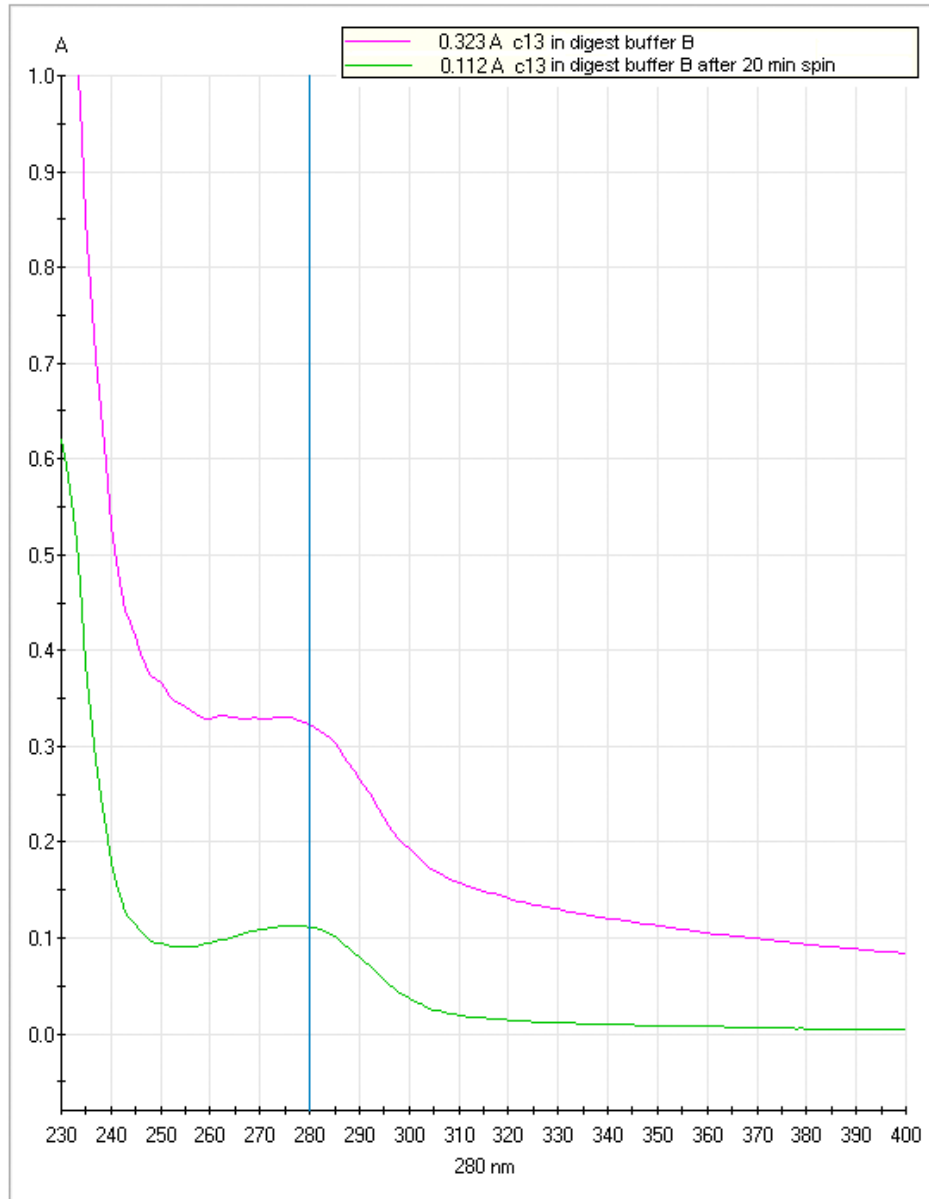


Figure 3.10 *FLJ13611 after digestion and removal of MBP fragment. Centrifugation for 20 min efficiently removes aggregates from the sample. Note light scattering at 310 nm before centrifugation (pink line), which is almost completely absent after centrifugation (green line). The peak at 280 nm is also reduced accordingly.*

3.8 Acrylamide quenching reveals the position of tryptophan residues in FLJ13611

With well-behaved, purified FLJ13611 in hand we set out to determine its structure by several biophysical methods. FLJ13611 presents some aromatic residues (two tryptophan residues at positions 281 and 352, and several tyrosine residues; Figure 3.11), which gives it intrinsic fluorescence and makes it suitable for fluorescence spectroscopy.

Since all of the fluorescence experiments were conducted in Column Buffer A, this buffer was scanned with the same instrument settings and used as a blank. As seen in Figure 3.12 (A), the buffer has no fluorescent component, and gives a nearly flat baseline of low intensity, therefore it is suitable for this type of experiment. The only peak, seen at 330 nm, is the Raman band, which is not real fluorescence, but represents light scattered by the H-O bond from the solvent water. This blank was subtracted from all spectra presented.

The excitation ($\lambda_{em} = 340$ nm) and the emission spectra ($\lambda_{ex} = 280$ nm and $\lambda_{ex} = 295$ nm) of FLJ13611 are presented in Figure 3.12 (B and C). As expected, maximum emission was reached when the sample was excited at 280 nm, since this wavelength excites both tryptophans and tyrosines. The fluorescence intensity at $\lambda_{ex} = 295$ nm is about 50% lower than the observed for $\lambda_{ex} = 280$ nm (Figure 3.12 C), since at 295 nm only tryptophan fluorescence is observed (tyrosines are excluded). Because there are eleven tyrosine residues, it is not possible to make any assumptions about their position in FLJ13611 from the fluorescence spectrum. The position of tryptophans, however, can be assessed. Therefore the subsequent experiments were performed with $\lambda_{ex} = 295$ nm, in order to exclude tyrosine fluorescence.

MEVNPPKQEHL LALKVMRLTKPTLFTNIPVTCEEKDLPGDLFNQLMRDDP
STVNGAEVLMLGEMLTLPQNFIGNIFLGETFSSYISVHNSNQVVKDILVK
ADLQTSSQRLNLSASNAVAELKPDCCIDDV IHHEVKEIGTHILVCAVSY
TTQAGEKMYFRKFFKFQVLKPLDVKTKFYNAESDLSSVTDEVFLEAQIQN
MTTSPMFMEKVSLEPSIMYNVTE LNSVSQAGECVSTFGSRAYLQPM DTRQ
YLYCLKPKNEFAEKAGI IKGVTVIGKLDIVWKTNLGERGRLQTSQLQRMA
PGYGDVRLSLEAIPDTVNLEEPFHITCKITNCSSERTMDLVLEMCNTNSI
HWCGISGRQLGKLHPSSSLCLAL TLLSSVQGLQSIGLRLTDTFLKRTYE
YDDIAQVCVVSSAIKVES

Figure 3.11 FLJ13611 amino-acid sequence. Aromatic residues are highlighted in yellow (tyrosine) or orange (tryptophan).

Tryptophan maximal emission is seen around 350 nm, and since tryptophan fluorescence is very sensitive to the polarity of the environment (varying from 350 nm for free tryptophan in solution to 308 nm for completely buried tryptophan residues; (Möller and Denicola, 2002)), it suggests that the tryptophan residues in FLJ13611 are in a hydrophilic environment. To determine tryptophan accessibility, a fluorescence quenching experiment was performed using acrylamide as a quencher. Acrylamide is known to quench the fluorescence of solvent exposed tryptophan residues, and the fraction of accessible tryptophans can be estimated by a modified Stern-Volmer plot (Möller and Denicola, 2002). As shown in Figure 3.12 D, the fluorescence was efficiently quenched with acrylamide.

The accessibility of both tryptophan residues of FLJ13611 is corroborated by the modified Stern-Volmer plot (see Figure 3.13). The intercept value (1.0156) indicates the percentage of accessible tryptophans, which in this case can be rounded to 1 (100% of the residues are accessible).

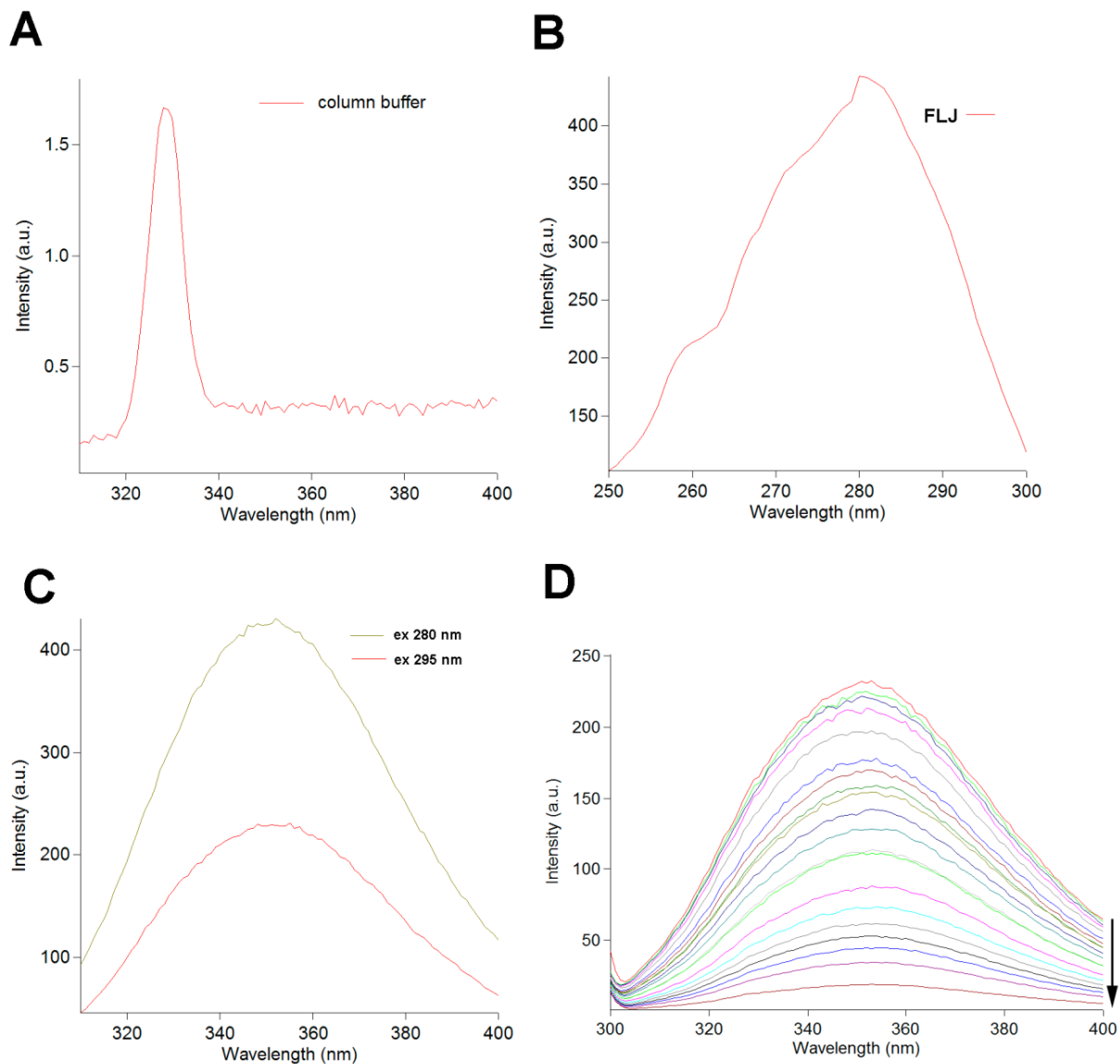


Figure 3.12 *FLJ13611 fluorescence is quenched by acrylamide. A: Emission spectrum of Column Buffer A. B: Excitation spectrum of FLJ13611. C: Emission spectra of FLJ13611 excited at 280 nm and 295 nm. D: Emission spectra of FLJ13611 excited at 280 nm upon successive additions of acrylamide. Vertical arrow indicates increasing concentrations of acrylamide (fluorescence intensity decreases as acrylamide concentration increases).*

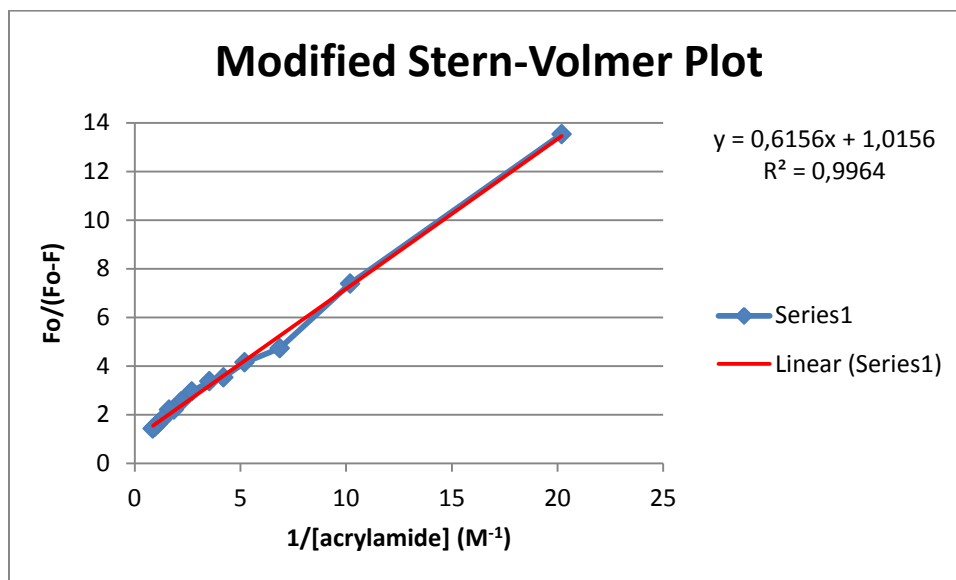


Figure 3.13 Modified Stern-Volmer plot of FLJ13611 fluorescence quenching. F_o : initial fluorescence; F : fluorescence after acrylamide addition.

3.9 Assessment of FLJ13611 secondary structure

Since all of the proteins that show homology to FLJ13611 have been poorly studied thus far, the secondary structure of FLJ13611 was predicted using the online tool PSI-PRED. PSI-PRED is currently the most accurate program for secondary structure prediction based on the amino acid sequence of a protein, and uses position-specific iterated BLAST (PSI-BLAST) results as an input (Buchan et al., 2010).

As seen in Figure 3.14, the protein was predicted to be half strand and half coil, with no helical segments. The coil segments could be either structured loops or unordered segments, because PSI-PRED uses only three classes of secondary structure (helix, strand and coil) (Jones, 1999). In this classification, turns, high curvature bends and π helices, as well as the absence of a regular secondary structure (random coils) are all grouped as “coil”.

PSI-PRED prediction was then compared with experimental data obtained by Far-UV-CD. Since any chiral molecule can give a signal in CD, the buffer used (CD buffer) was scanned prior to the protein sample, to ensure it would give an acceptable baseline at the wavelength of interest (180 to 260 nm). As seen in Figure 3.15, the spectrum obtained for FLJ13611 resembles one of an alpha-helical protein, with two minima around 208 nm and 222 nm.

In order to make a more accurate comparison, this spectrum was analyzed in Dichroweb using the algorithm CDSSTR, with data points from 190 to 240 nm. This algorithm assigns six possible classes of secondary structure: regular α -helix (helix 1), distorted α -helix (helix 2), regular β -strand (strand 1), distorted β -strand (strand 2), turns (T) and unordered (U) (Sreerama and Woody, 2000).

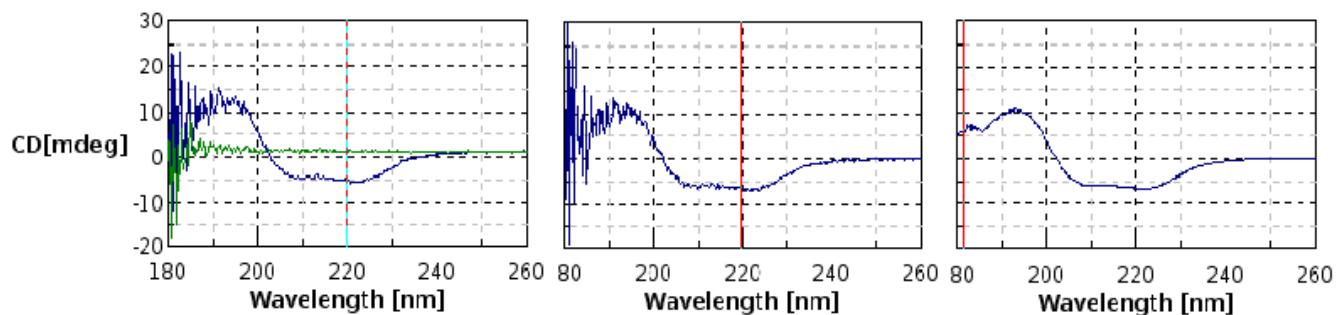


Figure 3.15 Far-UV CD spectrum of FLJ13611. Left: baseline spectrum in green and FLJ13611 spectrum in blue; middle: FLJ13611 spectrum after baseline subtraction; right: FLJ13611 spectrum smoothed. Average of five scans. The noisy region seen in the left portion of the graph is due to the high tension voltages present at lower wavelengths, and was not considered in the quantitative secondary structure assignment.

The proportions for each of these types of secondary structures were calculated from the reconstructed CD spectrum, and are summarized on Table 3.1. The fitting of the reconstructed data to the experimental data is shown graphically in Figure 3.16, and is also represented by the normalized root mean square deviation (NRMSD) value of 0.028. The NRMSD can assume any value from 0 (perfect fit) to 1 (no fit), and values lower than 0.1 indicate a reliable prediction (Kelly and Price, 2005).

Interestingly, Dichroweb analysis revealed a helix content of 17%, which is completely absent in the PSI-PRED prediction. Dichroweb also gives a lower percentage for strands (33%), and high percentage of unordered structure (30%), along with 20% of turns.

The differences in these estimations of the secondary structure of FLJ13611 can be partially explained by the different classification systems used. In PSI-PRED, everything that is not α -helix or β -strand is considered coil, whereas CDSSTR separates turns and unordered segments, and also puts single residues assigned as β -strands or α -helices in the unordered category. This does not explain, however, the complete absence of helices in the PSI-PRED prediction and it is reasonable to suspect that at least a portion of those helical segments were computed as coils. Since PSI-PRED is based solely on sequence information rather than experimental data, Dichroweb values for secondary structure elements can be considered more reliable in this case, given the good NRMSD value.

Table 3.1 Calculated secondary structure fractions for FLJ13611 using the CDSSTR algorithm (Dichroweb).

Type of secondary structure	Fraction
Helix 1	0.08
Helix 2	0.09
Strand 1	0.22
Strand 2	0.11
Turns	0.20
Unordered	0.30
Total	1.00

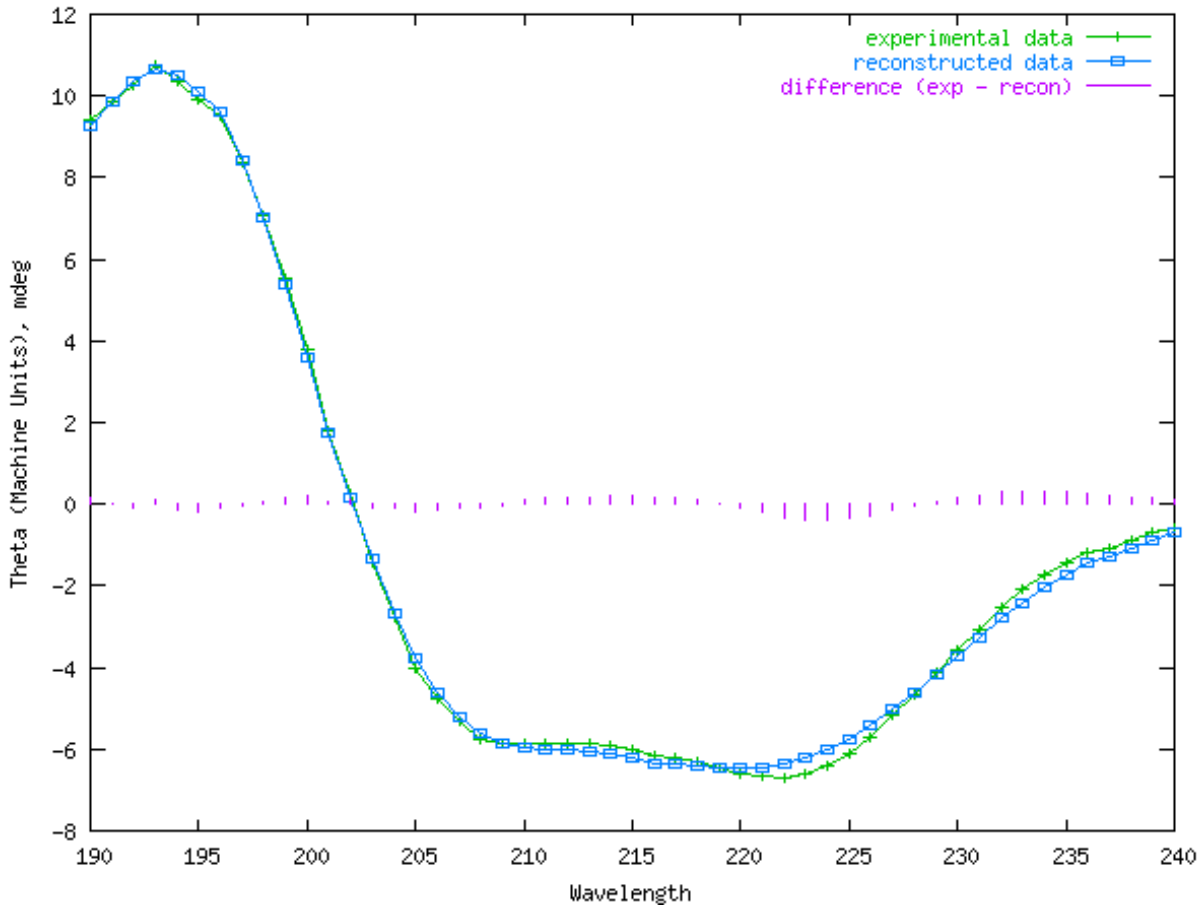


Figure 3.16 Fitting of reconstructed data generated by Dichroweb to experimental data. The short vertical lines indicate a good fit between the two groups of data. The fractions presented in Table 3.1 are calculated from the reconstructed data.

4 Discussion

Here we demonstrate that the previously uncharacterized protein FLJ13611 interacts with the mammalian TRAPP complex. The interaction was confirmed by yeast-two hybrid, size exclusion chromatography and co-immunoprecipitation. These results are in accordance with previous reports demonstrating FLJ13611 co-precipitating with TRAPPC3, TRAPPC8 and TRAPPC2L (Choi et al., 2011; Gavin et al., 2002). Moreover, our data suggest that FLJ13611 has a role in maintaining the Golgi structure, since its depletion by siRNA leads to Golgi fragmentation. A similar phenotype is seen for the knockdown of the TRAPP components TRAPPC2, TRAPPC2L, TRAPPC8, TRAPPC11 and TRAPPC12 (Scrivens et al., 2009, 2011). Taken together, these results suggest that FLJ13611 is a new component of the mammalian TRAPP complex that we propose calling TRAPPC13.

Unlike the yeast TRAPP complexes, mammalian TRAPP does not have a known architecture, and the approximate positioning of each subunit is inferred from its interactions with other subunits. Here we show that FLJ13611 interacts strongly with TRAPPC11 and TRAPPC12 by yeast two hybrid. The exact position of TRAPPC11 and TRAPPC12 in the complex is not known, but it is reasonable to hypothesize that FLJ13611 sits on the extremity, together with TRAPPC2, where it would be accessible for an interaction with non-TRAPP components such as GRASP55 and GRASP65. FLJ13611 also interacts with the Golgi t-SNARE syntaxin 5 (Shahzad, 2012, unpublished results), further supporting the idea of its localization to the extremity of the complex.

It is still not clear what the specific role of FLJ13611 within the TRAPP complex is, nor if it has any function outside of the complex. A BLAST search reveals homologues of FLJ13611 in all animals, including model organisms (*C. elegans* and *Drosophila*), but none of them have been characterized yet. The only clues about its function come from protein-protein interaction databases.

In *C. elegans*, apart from the predicted interaction with GRASP65, the FLJ13611 homolog (C56C10.7) has been shown to physically interact with pas-4 (proteasome subunit alpha 4) and sdz-38 (a zinc binding protein) (Li et al., 2004)

In *Drosophila*, the FLJ13611 homologue (FBgn0032204) has been found to interact with Tango-7 (transport and Golgi organization protein 7), snama (something that sticks like glue, an E3 ubiquitin ligase), CG7033 (a chaperone involved in spindle organization), rob1 (roadblock protein, a component of cytoplasmic dynein), nonA-1 and CG2021 (both involved in mRNA splicing via spliceosome) (Guruharsha et al., 2011).

Tango-7 has no apparent ortholog in *S. cerevisiae*, and the human ortholog, EIF3M (eukaryotic translation initiation factor 3 subunit M; also known as PCID1 (PCI domain containing protein 1)), regulates apoptosis by modulating caspase levels, a function that is conserved in *Drosophila* (Chew et al., 2009). Interestingly, this protein seems to be important for maintenance of Golgi structure since its depletion causes Golgi fragmentation (Bard et al., 2006), similar to what is seen when FLJ13611 is depleted. The PCI domain present in Tango-7 is a well conserved helical domain present in various proteins from three different complexes (26S Proteasome lid, COP9 signalosome and Initiation factor 3) (Pick et al., 2009). These complexes regulate protein life span by coupling protein synthesis and degradation in a

supercomplex called translasome, which contains initiation and elongation factors, ribosomal proteins, chaperones and other proteins involved in quality control and transport (Pick et al., 2009; Sha et al., 2009). From the interactions found in *Drosophila* and *C. elegans*, it is tempting to speculate that FLJ13611 is part of the translasome, since it interacts with an initiation factor (Tango-7), a chaperone (CG7033), a ubiquitin ligase (sname) and a proteasome subunit (pas-4). One possible strategy to verify whether these interactions are conserved in mammals is a TAP (tandem affinity purification) pull down followed by mass spectrometry. This method has been used to study many different protein complexes, including TRAPP (Gavin et al., 2002; Scrivens et al., 2011).

Despite the absence of sequence similarity, mammalian TRAPP subunits that form the core of the complex (homologs of yeast TRAPP I) have similar folds based on their three dimensional structure, and can be divided into two families: sedlin family (TRAPPC1, TRAPPC2 and TRAPPC4) and Bet3 family (TRAPPC3, TRAPPC5 and TRAPPC6) (Kim et al., 2006). The structures of the remaining subunits have not been solved yet and therefore cannot be classified. However, PSI-BLAST searches reveal that some of them share some sequence similarity. TRAPPC11 contains non-overlapping regions of homology to TRAPPC10 and to the yeast subunit Trs130p. FLJ13611 has been suggested to be the mammalian homolog of the yeast TRAPP II specific subunit Trs65p based on small regions of sequence similarity (Choi et al., 2011). However, a search in the Kyoto Encyclopedia of Genes and Genomes (KEGG) database reveals only two motifs in human FLJ13611: DUF974 (a highly conserved domain of unknown function only present in FLJ13611 and its homologs) from residues 65 to 298 and Transglut_C (transglutaminase family, C-terminal immunoglobulin-like domain) from residues

313 to 345. Interestingly, for the *C. elegans* homolog C56C10.7 three motifs are found: DUF974 from residues 67 to 288, Gryzun (one of the two conserved domains present in TRAPPC11) from residues 163 to 388 and Trs65, found in two shorter stretches (296 to 339 and 349 to 400), with a considerably lower score. Therefore, the classification of FLJ13611 as the human homolog of Trs65p does not seem to be warranted.

FLJ13611 interacts with GRASP55 and GRASP65, and these interactions were demonstrated by yeast two hybrid, co-immunoprecipitation and *in vitro* binding assays. The significance of this interaction is not clear. Since TRAPP members seem to be important for autophagy, FLJ13611 could be involved in autophagy-related unconventional secretion through its interaction with GRASPs. This hypothesis could be tested by knocking down FLJ13611 and verifying the secretion of one of the proteins that are known to be transported by this route in mammalian cells, such as IL-1 β or CFTR (Dupont et al., 2011; Gee et al., 2011).

Alternatively, GRASPs could be recruiting and / or anchoring the TRAPP complex on the Golgi membranes through FLJ13611, and this could be tested by depleting FLJ13611 and / or GRASPs, and verifying how much of the TRAPP complex is still bound to membranes. We have begun to test this hypothesis with yeast TRAPP and the GRASP homolog Grh1p, but no significant difference was seen in TRAPP solubility in a Grh1p knock-out strain (data not shown). Since yeast do not have an FLJ13611 homolog, it would be more informative to perform these experiments in a mammalian model system.

We were not able to co-precipitate GRASPs with other TRAPP subunits. Nevertheless, we cannot exclude the possibility that GRASPs interact with the TRAPP complex. Once the cells are lysed, some protein complexes do not remain stable, therefore transient or

weak interactions are less likely to be detected by this technique. In addition, the series of washing steps the samples are submitted to can also disrupt some interactions, increasing the chances of a false negative.

GRASPs are phosphorylated at several sites during mitosis, which causes the Golgi to fragment (Duran et al., 2008; Tang et al., 2010). Membrane trafficking between ER and Golgi is interrupted in mitosis, and it is possible that tethering factors are also regulated during cell division. Thus, it would be interesting to see what happens to the TRAPP complex when the Golgi fragments. Does TRAPP stay as a complex or does it disassemble either partially or completely? If it disassembles, when does it reassemble? Nothing is known about the state of mammalian TRAPP during different cell cycle stages, and it is possible that GRASPs, being a key regulator of Golgi morphology throughout the cell cycle, also regulate tethering complexes.

An MBP fusion of FLJ13611 proved to be an unstable protein, tending to aggregate, especially after cleavage of the MBP tag. MBP is known to solubilize and stabilize proteins that would normally form inclusion bodies, possibly acting as a chaperone and helping them to fold properly (Fox and Waugh, 2003). Therefore, once MBP is removed, FLJ13611 could revert to its original unstable state. The aggregation was partially inhibited by the addition of glycerol, a well-known cryoprotectant and protein stabilizer. Glycerol suppresses the conformational flexibility that is common to proteins in solution and causes them to aggregate, and also favors the assumption of more compact and rigid conformations (Sousa, 1995). We can speculate that the unordered regions and coils found abundantly in the secondary structure of FLJ13611 are probably flexible portions that were stabilized by the addition of glycerol.

FLJ13611 possesses intrinsic fluorescence due to the presence of aromatic amino acids. Among these, two tryptophan residues are exposed at the surface of FLJ13611 and were completely quenched by acrylamide. If any of these residues are involved in a protein-protein interaction, they could become buried in a more hydrophobic environment and therefore cause a shift in the emission spectra of FLJ13611. Consequently, intrinsic tryptophan fluorescence could be used to follow the binding of FLJ13611 to interacting partners.

The identification of novel interactors of mammalian TRAPP such as FLJ13611 and SPATA4 (discussed in section 6) reinforce the complexity of transport mechanisms inside the cell and the need for a better understanding of the regulation of this process. Determining the context where TRAPP is found, its structure and the proteins with which it interacts will certainly further our understanding of membrane traffic.

5 References

- Angers, C., & Merz, A. (2011). New links between vesicle coats and Rab-mediated vesicle targeting. *Seminars in cell & developmental biology*, 22(1), 18-26. doi:10.1016/j.semcdb.2010.07.003.New
- Appenzeller-Herzog, C., & Hauri, H.-P. (2006). The ER-Golgi intermediate compartment (ERGIC): in search of its identity and function. *Journal of cell science*, 119(Pt 11), 2173-83. doi:10.1242/jcs.03019
- Bard, F., Casano, L., Mallabiabarrena, A., Wallace, E., Saito, K., Kitayama, H., Guizzunti, G., et al. (2006). Functional genomics reveals genes involved in protein secretion and Golgi organization. *Nature*, 439(7076), 604-7. doi:10.1038/nature04377
- Behrends, C., Sowa, M. E., Gygi, S. P., & Harper, J. W. (2010). Network organization of the human autophagy system. *Nature*, 466(7302), 68-76. Nature Publishing Group. doi:10.1038/nature09204.Network
- Bonifacino, J. S., & Glick, B. S. (2004). The mechanisms of vesicle budding and fusion. *Cell*, 116(2), 153-66. Retrieved from <http://www.ncbi.nlm.nih.gov/pubmed/14744428>
- Brunet, S., Noueihed, B., Shahrzad, N., Saint-Dic, D., Hasaj, B., Guan, T. L., Moores, A., et al. (2012). The SMS domain of Trs23p is responsible for the in vitro appearance of the TRAPP I complex in *Saccharomyces cerevisiae*. *Cellular Logistics*, 2(1), 14-28. Landes Bioscience Inc. Retrieved from <http://www.landesbioscience.com/journals/cellularlogistics/article/19414/>
- Buchan, D. W. A., Ward, S. M., Lobley, A. E., Nugent, T. C. O., Bryson, K., & Jones, D. T. (2010). Protein annotation and modelling servers at University College London. *Nucleic Acids Research*, 38(Web Server issue), W563-W568. Oxford University Press. Retrieved from <http://discovery.ucl.ac.uk/168110/>
- Cai, H., Reinisch, K., & Ferro-Novick, S. (2007). Coats, tethers, Rabs, and SNAREs work together to mediate the intracellular destination of a transport vesicle. *Developmental cell*, 12(5), 671-82. doi:10.1016/j.devcel.2007.04.005
- Cai, H., Zhang, Y., Pypaert, M., Walker, L., & Ferro-Novick, S. (2005). Mutants in trs120 disrupt traffic from the early endosome to the late Golgi. *The Journal of cell biology*, 171(5), 823-33. doi:10.1083/jcb.200505145
- Chernomordik, L. V., Zimmerberg, J., & Kozlov, M. M. (2006). Membranes of the world unite! *The Journal of cell biology*, 175(2), 201-7. doi:10.1083/jcb.200607083

- Chew, S. K., Chen, P., Link, N., Galindo, K. a, Pogue, K., & Abrams, J. M. (2009). Genome-wide silencing in *Drosophila* captures conserved apoptotic effectors. *Nature*, *460*(7251), 123-7. Nature Publishing Group. doi:10.1038/nature08087
- Choi, C., Davey, M., Schluter, C., Pandher, P., Fang, Y., Foster, L. J., & Conibear, E. (2011). Organization and assembly of the TRAPP II complex. *Traffic (Copenhagen, Denmark)*, *12*(6), 715-25. doi:10.1111/j.1600-0854.2011.01181.x
- Christensen, A. K. (1975). Leydig cells. In D. Hamilton & R. Greep (Eds.), *Handbook of physiology: Male Reproductive System* (pp. 57-94). American Physiological Society.
- Colanzi, A., Suetterlin, C., & Malhotra, V. (2003). Cell-cycle-specific Golgi fragmentation: how and why? *Current Opinion in Cell Biology*, *15*(4), 462-467. doi:10.1016/S0955-0674(03)00067-X
- Dupont, N., Jiang, S., Pilli, M., Ornatowski, W., Bhattacharya, D., & Deretic, V. (2011). Autophagy-based unconventional secretory pathway for extracellular delivery of IL-1. *The European Molecular Biology Organization Journal*, 1-11. Nature Publishing Group. doi:10.1038/emboj.2011.398
- Duran, J., Kinseth, M., & Bossard, C. (2008). The role of GRASP55 in Golgi fragmentation and entry of cells into mitosis. (B. Glick, Ed.) *Molecular Biology of the Cell*, *19*(6), 2579-2587. The American Society for Cell Biology. Retrieved from <http://www.molbiolcell.org/content/19/6/2579.short>
- Duran, J. M., Anjard, C., Stefan, C., Loomis, W. F., & Malhotra, V. (2010). Unconventional secretion of Acb1 is mediated by autophagosomes. *The Journal of cell biology*, *188*(4), 527-36. The Rockefeller University Press. doi:10.1083/jcb.200911154
- D'Angelo, G., Prencipe, L., Iodice, L., Beznoussenko, G., Savarese, M., Marra, P., Di Tullio, G., et al. (2009). GRASP65 and GRASP55 sequentially promote the transport of C-terminal valine-bearing cargos to and through the Golgi complex. *The Journal of Biological Chemistry*, *284*(50), 34849-34860. American Society for Biochemistry and Molecular Biology. Retrieved from <http://www.pubmedcentral.nih.gov/articlerender.fcgi?artid=2787347&tool=pmcentrez&rendertype=abstract>
- Fan, L., Yu, W., & Zhu, X. (2003). Interaction of Sedlin with chloride intracellular channel proteins. *FEBS Letters*, *540*(1-3), 77-80. doi:10.1016/S0014-5793(03)00228-X
- Fox, J. D., & Waugh, D. S. (2003). Maltose-binding protein as a solubility enhancer. *Methods in molecular biology (Clifton, N.J.)*, *205*, 99-117. Retrieved from <http://www.ncbi.nlm.nih.gov/pubmed/12491882>
- Gasteiger, E., Bairoch, A., Sanchez, J. C., Williams, K. L., Appel, R. D., Hochstrasser, D. F., & Wilkins, M. R. (1999). Protein identification and analysis tools in the ExPASy server. *Methods in molecular biology (Clifton, N.J.)*, *112*, 531-52. Retrieved from <http://www.ncbi.nlm.nih.gov/pubmed/10027275>

- Gavin, A.-C., Börsche, M., Krause, R., Grandi, P., Marzioch, M., Bauer, A., Schultz, J., et al. (2002). Functional organization of the yeast proteome by systematic analysis of protein complexes. *Nature*, *415*(6868), 141-7. doi:10.1038/415141a
- Gaytan, F., Lucena, M. C., Munoz, E., & Paniagua, R. (1986). Morphometric aspects of rat testis development. *Journal of anatomy*, *145*, 155-9. Retrieved from <http://www.pubmedcentral.nih.gov/articlerender.fcgi?artid=1166501&tool=pmcentrez&rendertype=abstract>
- Gedeon, A. K., Tiller, G. E., Le Merrer, M., Heuertz, S., Tranebjaerg, L., Chitayat, D., Robertson, S., et al. (2001). The Molecular Basis of X-Linked Spondyloepiphyseal Dysplasia Tarda. *The American Journal of Human Genetics*, *68*(6), 1386-1397. The American Society of Human Genetics. Retrieved from <http://www.pubmedcentral.nih.gov/articlerender.fcgi?artid=1226125&tool=pmcentrez&rendertype=abstract>
- Gee, H. Y., Noh, S. H., Tang, B. L., Kim, K. H., & Lee, M. G. (2011). Rescue of Δ F508-CFTR trafficking via a GRASP-dependent unconventional secretion pathway. *Cell*, *146*(5), 746-60. Elsevier Inc. doi:10.1016/j.cell.2011.07.021
- Ghosh, A. K., Majumder, M., Steele, R., Robert, A., Ray, R. B., & White, R. A. (2001). A Novel 16-Kilodalton Cellular Protein Physically Interacts with and Antagonizes the Functional Activity of c-myc Promoter-Binding Protein 1. *Molecular and Cellular Biology*, *21*(2), 655-662. American Society for Microbiology. doi:10.1128/MCB.21.2.655
- Ghosh, A. K., Steele, R., & Ray, R. B. (2003). Modulation of human luteinizing hormone beta gene transcription by MIP-2A. *The Journal of Biological Chemistry*, *278*(26), 24033-24038. Retrieved from <http://www.ncbi.nlm.nih.gov/pubmed/12700240>
- Giansanti, M. G., Farkas, R. M., Bonaccorsi, S., Lindsley, D. L., Wakimoto, B. T., Fuller, M. T., Gatti, M., et al. (2004). Genetic Dissection of Meiotic Cytokinesis in Drosophila Males. *Molecular Biology of the Cell*, *15*(May), 2509-2522. doi:10.1091/mbc.E03
- Godi, A., Di Campli, A., Konstantakopoulos, A., Di Tullio, G., Alessi, D. R., Kular, G. S., Daniele, T., et al. (2004). FAPPs control Golgi-to-cell-surface membrane traffic by binding to ARF and PtdIns(4)P. *Nature Cell Biology*, *6*(5), 393-404. Nature Publishing Group. Retrieved from <http://www.ncbi.nlm.nih.gov/pubmed/15107860>
- Guruharsha, K. G., Rual, J.-F., Zhai, B., Mintseris, J., Vaidya, P., Vaidya, N., Beekman, C., et al. (2011). A protein complex network of Drosophila melanogaster. *Cell*, *147*(3), 690-703. doi:10.1016/j.cell.2011.08.047
- Hughes, H., & Stephens, D. J. (2008). Assembly, organization, and function of the COPII coat. *Histochemistry and Cell Biology*, *129*(2), 129-151. Springer-Verlag. Retrieved from <http://www.pubmedcentral.nih.gov/articlerender.fcgi?artid=2228377&tool=pmcentrez&rendertype=abstract>

- Hutagalung, A. H., & Novick, P. J. (2011). Role of Rab GTPases in Membrane Traffic and Cell Physiology. *Physiological Reviews*, 119-149. doi:10.1152/physrev.00059.2009.
- Jaber, E., Thiele, K., Kindzierski, V., Loderer, C., Rybak, K., Jürgens, G., Mayer, U., et al. (2010). A putative TRAPP II tethering factor is required for cell plate assembly during cytokinesis in Arabidopsis. *The New Phytologist*, 187(3), 751-63. doi:10.1111/j.1469-8137.2010.03331.x
- Jones, D. T. (1999). Protein secondary structure prediction based on position-specific scoring matrices. *Journal of molecular biology*, 292(2), 195-202. doi:10.1006/jmbi.1999.3091
- Jones, S., Newman, C., Liu, F., & Segev, N. (2000). The TRAPP complex is a nucleotide exchanger for Ypt1 and Ypt31/32. (C. Kaiser, Ed.) *Molecular Biology of the Cell*, 11(12), 4403-4411. The American Society for Cell Biology. Retrieved from <http://www.pubmedcentral.nih.gov/articlerender.fcgi?artid=15082&tool=pmcentrez&rendertype=abstract>
- Kelly, S M, & Price, N. C. (2000). The use of circular dichroism in the investigation of protein structure and function. *Current protein & peptide science*, 1(4), 349-84. Retrieved from <http://www.ncbi.nlm.nih.gov/pubmed/12369905>
- Kelly, Sharon M, Jess, T. J., & Price, N. C. (2005). How to study proteins by circular dichroism. *Biochimica et biophysica acta*, 1751(2), 119-39. doi:10.1016/j.bbapap.2005.06.005
- Kim, Y.-G., Raunser, S., Munger, C., Wagner, J., Song, Y.-L., Cygler, M., Walz, T., et al. (2006). The architecture of the multisubunit TRAPP I complex suggests a model for vesicle tethering. *Cell*, 127(4), 817-30. doi:10.1016/j.cell.2006.09.029
- Kim, Y.-G., Sohn, E. J., Seo, J., Lee, K.-J., Lee, H.-S., Hwang, I., Whiteway, M., et al. (2005). Crystal structure of bet3 reveals a novel mechanism for Golgi localization of tethering factor TRAPP. *Nature Structural & Molecular Biology*, 12(1), 38-45. Retrieved from <http://www.ncbi.nlm.nih.gov/pubmed/15608655>
- Kineth, M. a, Anjard, C., Fuller, D., Guizzunti, G., Loomis, W. F., & Malhotra, V. (2007). The Golgi-associated protein GRASP is required for unconventional protein secretion during development. *Cell*, 130(3), 524-34. doi:10.1016/j.cell.2007.06.029
- Klumperman, J. (2011). Architecture of the mammalian Golgi. *Cold Spring Harbor perspectives in biology*, 3(7), 1-19. doi:10.1101/cshperspect.a005181
- Kümmel, D., Oeckinghaus, A., Wang, C., Krappmann, D., & Heinemann, U. (2008). Distinct isocomplexes of the TRAPP trafficking factor coexist inside human cells. *FEBS letters*, 582(27), 3729-33. doi:10.1016/j.febslet.2008.09.056
- Li, S., Armstrong, C. M., Bertin, N., Ge, H., Milstein, S., Boxem, M., Vidalain, P.-O., et al. (2004). A map of the interactome network of the metazoan *C. elegans*. *Science (New York, N.Y.)*, 303(5657), 540-3. doi:10.1126/science.1091403

- Liang, Y., Morozova, N., Tokarev, A. A., Mulholland, J. W., & Segev, N. (2007). The role of Trs65 in the Ypt/Rab guanine nucleotide exchange factor function of the TRAPP II complex. (V. Malhotra, Ed.) *Molecular Biology of the Cell*, 18(7), 2533-2541. The American Society for Cell Biology. Retrieved from http://www.ncbi.nlm.nih.gov/entrez/query.fcgi?cmd=Retrieve&db=PubMed&dopt=Citation&list_uids=17475775
- Liu, B., Liu, S., He, S., Zhao, Y., Hu, H., & Wang, Z. (2005). Cloning and expression analysis of gonadogenesis-associated gene SPATA4 from rainbow trout (*Oncorhynchus mykiss*). *Journal of biochemistry and molecular biology*, 38(2), 206-10. Retrieved from <http://www.ncbi.nlm.nih.gov/pubmed/15826498>
- Liu, S., Liu, B., He, S., Zhao, Y., & Wang, Z. (2005). Cloning and characterization of zebra fish SPATA4 gene and analysis of its gonad specific expression. *Biochemistry Biokhimiia*, 70(6), 638-644. Retrieved from <http://www.ncbi.nlm.nih.gov/pubmed/16038605>
- Liu, S.-F., He, S., Liu, B.-W., Zhao, Y., & Wang, Z. (2004). Cloning and characterization of testis-specific spermatogenesis associated gene homologous to human SPATA4 in rat. *Biological & pharmaceutical bulletin*, 27(11), 1867-70. Retrieved from <http://www.ncbi.nlm.nih.gov/pubmed/15516739>
- Liu, S.-F., Lu, G.-X., Liu, G., Xing, X.-W., Li, L.-Y., & Wang, Z. (2004). Cloning of a full-length cDNA of human testis-specific spermatogenic cell apoptosis inhibitor TSARG2 as a candidate oncogene. *Biochemical and biophysical research communications*, 319(1), 32-40. doi:10.1016/j.bbrc.2004.04.160
- Liu, S.-feng, Ai, C., Ge, Z.-qi, Liu, H.-luo, Liu, B.-wen, He, S., & Wang, Z. (2005). Molecular cloning and bioinformatic analysis of SPATA4 gene. *Journal of biochemistry and molecular biology*, 38(6), 739-747. BIOCHEMICAL SOCIETY OF THE REPUBLIC OF KOREA. Retrieved from [http://www.jbmb.or.kr/jbmb/jbmb_files/\[38-6\]0511281050_739.pdf](http://www.jbmb.or.kr/jbmb/jbmb_files/[38-6]0511281050_739.pdf)
- Liu, X., Wang, Y., Zhu, H., Zhang, Q., Xing, X., Wu, B., Song, L., et al. (2010). Interaction of Sedlin with PAM14. *Journal of cellular biochemistry*, 109(6), 1129-33. doi:10.1002/jcb.22491
- Lobley, A., Whitmore, L., & Wallace, B. (2002). DICHROWEB: an interactive website for the analysis of protein secondary structure from circular dichroism spectra. *Bioinformatics*, 18(1), 211-212. Retrieved from <http://scholar.google.com/scholar?hl=en&btnG=Search&q=intitle:DICHROWEB:+an+interactive+website+for+the+analysis+of+protein+secondary+structure+from+circular+dichroism+spectra#0>
- Loh, E., Peter, F., Subramaniam, V. N., & Hong, W. (2005). Mammalian Bet3 functions as a cytosolic factor participating in transport from the ER to the Golgi apparatus. *Journal of Cell Science*, 118(Pt 6), 1209-1222. Retrieved from <http://www.ncbi.nlm.nih.gov/pubmed/15728249>
- Lynch-Day, M. A., Bhandari, D., Menon, S., Huang, J., Cai, H., Bartholomew, C. R., Brumell, J. H., et al. (2010). Trs85 directs a Ypt1 GEF, TRAPP III, to the phagophore to promote autophagy. *Proceedings of the National Academy of Sciences of the United States of America*, 107(17), 7811-

7816. National Academy of Sciences. Retrieved from
<http://www.ncbi.nlm.nih.gov/pubmed/20375281>

MacKenzie, J. J., Fitzpatrick, J., Babyn, P., Ferrero, G. B., Ballabio, A., Billingsley, G., Bulman, D. E., et al. (1996). X linked spondyloepiphyseal dysplasia: a clinical, radiological, and molecular study of a large kindred. *Journal of Medical Genetics*, 33(10), 823-828.

Mackie, E. J., Tatarczuch, L., & Mirams, M. (2011). The skeleton: a multi-functional complex organ: the growth plate chondrocyte and endochondral ossification. *The Journal of endocrinology*, 211(2), 109-21. doi:10.1530/JOE-11-0048

Manjithaya, R., Anjard, C., Loomis, W. F., & Subramani, S. (2010). Unconventional secretion of *Pichia pastoris* Acb1 is dependent on GRASP protein, peroxisomal functions, and autophagosome formation. *The Journal of cell biology*, 188(4), 537-46. doi:10.1083/jcb.200911149

Manjithaya, R., & Subramani, S. (2010). Role of autophagy in unconventional protein secretion. *Autophagy*, 6(5), 650-651. doi:10.1083/jcb.200911154.n

Manjithaya, R., & Subramani, S. (2011). Autophagy: a broad role in unconventional protein secretion? *Trends in cell biology*, 21(2), 67-73. Elsevier Ltd. doi:10.1016/j.tcb.2010.09.009

Mir, A., Kaufman, L., Noor, A., Motazacker, M. M., Jamil, T., Azam, M., Kahrizi, K., et al. (2009). Identification of mutations in TRAPPC9, which encodes the NIK- and IKK-beta-binding protein, in nonsyndromic autosomal-recessive mental retardation. *American journal of human genetics*, 85(6), 909-15. The American Society of Human Genetics. doi:10.1016/j.ajhg.2009.11.009

Mochida, G. H., Mahajnah, M., Hill, A. D., Basel-Vanagaite, L., Gleason, D., Hill, R. S., Bodell, A., et al. (2009). A truncating mutation of TRAPPC9 is associated with autosomal-recessive intellectual disability and postnatal microcephaly. *American journal of human genetics*, 85(6), 897-902. The American Society of Human Genetics. doi:10.1016/j.ajhg.2009.10.027

Möller, M., & Denicola, A. (2002). Protein tryptophan accessibility studied by fluorescence quenching. *Biochemistry and Molecular Biology Education*, 30(3), 175-178. doi:10.1002/bmb.2002.494030030035

Nachury, M. V., Loktev, A. V., Zhang, Q., Westlake, C. J., Peränen, J., Merdes, A., Slusarski, D. C., et al. (2007). A core complex of BBS proteins cooperates with the GTPase Rab8 to promote ciliary membrane biogenesis. *Cell*, 129(6), 1201-1213. Elsevier Ltd. Retrieved from <http://www.ncbi.nlm.nih.gov/pubmed/17574030>

Pick, E., Hofmann, K., & Glickman, M. H. (2009). PCI complexes: Beyond the proteasome, CSN, and eIF3 Troika. *Molecular cell*, 35(3), 260-4. Elsevier Inc. doi:10.1016/j.molcel.2009.07.009

Qi, X., Kaneda, M., Chen, J., Geitmann, A., & Zheng, H. (2011). A specific role for Arabidopsis TRAPP II in post-Golgi trafficking that is crucial for cytokinesis and cell polarity. *The Plant journal : for cell and molecular biology*, 68(2), 234-248. doi:10.1111/j.1365-3113X.2011.04681.x

- Qi, X., & Zheng, H. (2011). Arabidopsis TRAPP II is functionally linked to Rab-A, but not Rab-D in polar protein trafficking in trans-Golgi network. *Plant signaling & behavior*, 6(11), 1679-83. doi:10.4161/psb.6.11.17915
- Rios, R. M., & Bornens, M. (2003). The Golgi apparatus at the cell centre. *Current Opinion in Cell Biology*, 15(1), 60-66. Elsevier. Retrieved from <http://linkinghub.elsevier.com/retrieve/pii/S09555067402000133>
- Robinet, C. C., Giansanti, M. G., Gatti, M., & Fuller, M. T. (2009). TRAPP II is required for cleavage furrow ingression and localization of Rab11 in dividing male meiotic cells of *Drosophila*. *Journal of Cell Science*, 122(Pt 24), 4526-4534. Retrieved from <http://www.pubmedcentral.nih.gov/articlerender.fcgi?artid=2787463&tool=pmcentrez&rendertype=abstract>
- Roghi, C., Jones, L., Gratian, M., English, W. R., & Murphy, G. (2010). Golgi reassembly stacking protein 55 interacts with membrane-type (MT) 1-matrix metalloprotease (MMP) and furin and plays a role in the activation of the MT1-MMP zymogen. *The FEBS journal*, 277(15), 3158-3175. Retrieved from <http://www.ncbi.nlm.nih.gov/pubmed/20608975>
- Rossi, G., Kolstad, K., Stone, S., Palluault, F., & Ferro-Novick, S. (1995). BET3 encodes a novel hydrophilic protein that acts in conjunction with yeast SNAREs. *Molecular biology of the cell*, 6(12), 1769-80. Retrieved from <http://www.pubmedcentral.nih.gov/articlerender.fcgi?artid=301331&tool=pmcentrez&rendertype=abstract>
- Sacher, M., Barrowman, J., Wang, W., Horecka, J., Zhang, Y., Pypaert, M., & Ferro-Novick, S. (2001). TRAPP I implicated in the specificity of tethering in ER-to-Golgi transport. *Molecular Cell*, 7(2), 433-442. Elsevier. Retrieved from <http://www.ncbi.nlm.nih.gov/pubmed/11239471>
- Sacher, M., Jiang, Y., Barrowman, J., Scarpa, A., Burston, J., Zhang, L., Schieltz, D., et al. (1998). TRAPP, a highly conserved novel complex on the cis-Golgi that mediates vesicle docking and fusion. *The European Molecular Biology Organization Journal*, 17(9), 2494-2503. Retrieved from <http://www.pubmedcentral.nih.gov/articlerender.fcgi?artid=1170591&tool=pmcentrez&rendertype=abstract>
- Sacher, Michael, & Ferro-Novick, S. (2001). Purification of TRAPP from *Saccharomyces cerevisiae* and identification of its mammalian counterpart. *Methods in Enzymology*, 329(1998), 234-241. Retrieved from http://www.ncbi.nlm.nih.gov/entrez/query.fcgi?cmd=Retrieve&db=PubMed&dopt=Citation&list_uids=11210539
- Schotman, H., Karhinen, L., & Rabouille, C. (2008). dGRASP-mediated noncanonical integrin secretion is required for *Drosophila* epithelial remodeling. *Developmental cell*, 14(2), 171-82. doi:10.1016/j.devcel.2007.12.006

- Scrivens, P. J., Noueihed, B., Shahrzad, N., Hul, S., Brunet, S., & Sacher, M. (2011). C4orf41 and TTC-15 are mammalian TRAPP components with a role at an early stage in ER-to-Golgi trafficking. *Molecular biology of the cell*, 22(12), 2083-93. doi:10.1091/mbc.E10-11-0873
- Scrivens, P. J., Shahrzad, N., Moores, A., Morin, A., Brunet, S., & Sacher, M. (2009). TRAPPC2L is a novel, highly conserved TRAPP-interacting protein. *Traffic Copenhagen Denmark*, 10(6), 724-736. Retrieved from <http://www.ncbi.nlm.nih.gov/pubmed/19416478>
- Sha, Z., Brill, L. M., Cabrera, R., Kleinfeld, O., Scheliga, J. S., Glickman, M. H., Chang, E. C., et al. (2009). The eIF3 interactome reveals the translasome, a supercomplex linking protein synthesis and degradation machineries. *Molecular cell*, 36(1), 141-52. Elsevier Ltd. doi:10.1016/j.molcel.2009.09.026
- Shorter, J., & Warren, G. (2002). Golgi architecture and inheritance. *Annual review of cell and developmental biology*, 18, 379-420. doi:10.1146/annurev.cellbio.18.030602.133733
- Sousa, R. (1995). Use of glycerol, polyols and other protein structure stabilizing agents in protein crystallization. *Acta Crystallographica Section D Biological Crystallography*, 51(Pt 3), 271-7. International Union of Crystallography. doi:10.1107/S0907444994014009
- Sreerama, N., & Woody, R. W. (2000). Estimation of protein secondary structure from circular dichroism spectra: comparison of CONTIN, SELCON, and CDSSTR methods with an expanded reference set. *Analytical Biochemistry*, 287(2), 252-260. Elsevier. Retrieved from <http://www.ncbi.nlm.nih.gov/pubmed/11112271>
- Sztul, E., & Lupashin, V. (2009). Role of vesicle tethering factors in the ER-Golgi membrane traffic. *FEBS Letters*, 583(23), 3770-3783. Federation of European Biochemical Societies. Retrieved from <http://www.pubmedcentral.nih.gov/articlerender.fcgi?artid=2788073&tool=pmcentrez&rendertype=abstract>
- Tang, D., Yuan, H., & Wang, Y. (2010). The role of GRASP65 in Golgi cisternal stacking and cell cycle progression. *Traffic (Copenhagen, Denmark)*, 11(6), 827-42. doi:10.1111/j.1600-0854.2010.01055.x
- Thellmann, M., Rybak, K., Thiele, K., Wanner, G., & Assaad, F. F. (2010). Tethering factors required for cytokinesis in Arabidopsis. *Plant physiology*, 154(2), 720-32. doi:10.1104/pp.110.154286
- Tiller, G. E., Hannig, V. L., Dozier, D., Carrel, L., Trevarthen, K. C., Wilcox, W. R., Mundlos, S., et al. (2001). A recurrent RNA-splicing mutation in the SEDL gene causes X-linked spondyloepiphyseal dysplasia tarda. *American journal of human genetics*, 68(6), 1398-407. doi:10.1086/320594
- Tokarev, A. A., Taussig, D., Sundaram, G., Lipatova, Z., Liang, Y., Mulholland, J. W., & Segev, N. (2009). TRAPP II complex assembly requires Trs33 or Trs65. *Traffic Copenhagen Denmark*, 10(12), 1831-1844.
- Vidal, M., Cusick, M. E., & Barabási, A.-L. (2011). Interactome networks and human disease. *Cell*, 144(6), 986-98. doi:10.1016/j.cell.2011.02.016

- Vinke, F. P., Grieve, A. G., & Rabouille, C. (2011). The multiple facets of the Golgi reassembly stacking proteins. *The Biochemical journal*, 433(3), 575-576. Retrieved from <http://www.ncbi.nlm.nih.gov/pubmed/21235525>
- Wang, W., Sacher, M., & Ferro-Novick, S. (2000). Trapp Stimulates Guanine Nucleotide Exchange on Ypt1p. *The Journal of Cell Biology*, 151(2), 289-296. The Rockefeller University Press. Retrieved from <http://www.pubmedcentral.nih.gov/articlerender.fcgi?artid=2192651&tool=pmcentrez&rendertype=abstract>
- Wang, X., Harimoto, K., Liu, J., Guo, J., Hinshaw, S., Chang, Z., & Wang, Z. (2011). Spata4 promotes osteoblast differentiation through Erk-activated Runx2 pathway. *Journal of bone and mineral research the official journal of the American Society for Bone and Mineral Research*, 26(8), 1964-1973. doi:10.1002/jbmr.394
- Wang, Y., & Seemann, J. (2011). Golgi Biogenesis. *Cold Spring Harbor perspectives in biology*. doi:10.1101/cshperspect.a005330
- Wei, J.-H., & Seemann, J. (2009). Mitotic division of the mammalian Golgi apparatus. *Seminars in cell & developmental biology*, 20(7), 810-6. doi:10.1016/j.semcdb.2009.03.010
- Westlake, C. J., Baye, L. M., Nachury, M. V., Wright, K. J., Ervin, K. E., Phu, L., Chalouni, C., et al. (2011). Primary cilia membrane assembly is initiated by Rab11 and transport protein particle II (TRAPP II) complex-dependent trafficking of Rabin8 to the centrosome. *Proceedings of the National Academy of Sciences of the United States of America*, 108(7), 2759-2764. National Academy of Sciences. Retrieved from <http://www.pubmedcentral.nih.gov/articlerender.fcgi?artid=3041065&tool=pmcentrez&rendertype=abstract>
- Whitmore, L., & Wallace, B. a. (2004). DICHROWEB, an online server for protein secondary structure analyses from circular dichroism spectroscopic data. *Nucleic acids research*, 32(Web Server issue), W668-73. doi:10.1093/nar/gkh371
- Xie, M.-C., Ai, C., Jin, X.-M., Liu, S.-F., Tao, S.-X., Li, Z.-D., & Wang, Z. (2007). Cloning and characterization of chicken SPATA4 gene and analysis of its specific expression. *Molecular and cellular biochemistry*, 306(1-2), 79-85. doi:10.1007/s11010-007-9556-9
- Yamasaki, A., Menon, S., Yu, S., Barrowman, J., Meerloo, T., Oorschot, V., Klumperman, J., et al. (2009). mTrs130 Is a Component of a Mammalian TRAPP II Complex, a Rab1 GEF That Binds to COPI-coated Vesicles. *Molecular Biology of the Cell*, 20, 4205-4215. doi:10.1091/mbc.E09
- Yu, S., Satoh, A., Pypaert, M., Mullen, K., Hay, J. C., & Ferro-Novick, S. (2006). mBet3p is required for homotypic COPII vesicle tethering in mammalian cells. *The Journal of cell biology*, 174(3), 359-68. doi:10.1083/jcb.200603044

- Zhao, S.-L., Hong, J., Xie, Z.-Q., Tang, J.-T., Su, W.-Y., Du, W., Chen, Y.-X., et al. (2011). TRAPPC4-ERK2 interaction activates ERK1/2, modulates its nuclear localization and regulates proliferation and apoptosis of colorectal cancer cells. *PLoS one*, 6(8), e23262. doi:10.1371/journal.pone.0023262
- Zhong, W., & Sternberg, P. W. (2006). Genome-wide prediction of *C. elegans* genetic interactions. *Science (New York, N.Y.)*, 311(5766), 1481-4. doi:10.1126/science.1123287
- Zou, S., Liu, Y., Zhang, X. Q., Chen, Y., Ye, M., Zhu, X., Yang, S., et al. (2012). Modular TRAPP Complexes Regulate Intracellular Protein Trafficking Through Multiple Ypt/Rab GTPases in *Saccharomyces cerevisiae*. *Genetics*. doi:10.1534/genetics.112.139378

6 A yeast two hybrid screen identifies SPATA4 as a TRAPP interactor (Published manuscript)

The following manuscript was published in the journal FEBS Letters (FEBS Letters 585 (2011) 2676–2681), with myself and Sokunthear Hul as first authors. The following figures were my contribution: Figure 6.3 panels C, E, F, G, H; Figure 6.4, Supplemental Figure 6.5.

6.1 Introduction

The process of vesicle-mediated delivery of both membranes and proteins to their proper intracellular location requires many factors acting in a coordinated manner. Many unanswered questions remain with respect to the molecular mechanisms regulating these processes.

The complexes that tether these vesicles to the acceptor compartment have been well-studied at the structural level [1]. One such complex called TRAPP functions in the early portion of the secretory pathway leading to transport to the Golgi [2]. TRAPP or subunits within the complex have been proposed to carry out numerous functions including vesicle tethering [3, 4], nucleotide exchange for several small GTPases [5-8], regulation of gene expression [9, 10] and to contribute to Golgi morphology [8, 11]. To fulfill all of these functions, the complex interacts with specific vesicle coat proteins, GTPases, transcription factors and likely other proteins. Curiously, a mutation in one

subunit called TRAPPC2 (henceforth called C2) has been tied to a skeletal defect called spondyloepiphyseal dysplasia tarda (SED) [12]. Interestingly, while most SED patients have mutations that lead to a truncated C2 protein, one patient with a D47Y missense mutation was identified. Since this mutation is in a region of the protein that to date has not been shown to interact with any other TRAPP protein, it was suggested that it may interfere with an interaction between TRAPP and an as yet unidentified binding partner [13].

To better understand the regulation of TRAPP, we decided to look for proteins that interact with C2. Using a yeast two-hybrid screen, we show that a spermatocyte-specific protein of unknown function called SPATA4 binds specifically to this subunit. SPATA4 binds to the C2 portion of a TRAPP and co-fractionates with the high molecular weight pool of C2. Ectopically expressed SPATA4 displays a cytosolic and nuclear localization. Our data suggest a role for SPATA4 in membrane traffic in spermatocytes and imply a specialized function for the TRAPP complex in these cells.

6.2 Materials and Methods

Materials and methods are described here as in the section “Supplemental Information” of the published manuscript.

6.2.1 Oligonucleotides and plasmid constructs

Table 6.1 Oligonucleotides used in this study

Oligonucleotides	Sequence
C2-F-EcoRI	AGGAATTCATGTCTGGGAGCTTCTACTTC
C2-R-EcoRI	AGGAATCTTAGCTTAAAAGGTGTTTCTTC
SPATA4-F-BamHI	CGCGGATCCATGGCTGCCGCCGGCCAGG
SPATA4-R-XhoI	TCAGCTCGAGTCACAGGTTTTTCAGTGTTCTC
SPATA4-F-HindIII	CCCAAGCTTATGGCTGCCGCCGGCCAGG
SPATA4-R-BamHI	CGCGGATCCTCACAGGTTTTTCAGTGTTCTC
pGAD-F-ID	CTATTCGATGATGAAGATACCCACCAAACCC
pGAD-R-ID	GTGAACTTGCGGGGTTTTTCAGTATCTACGATT

Table 6.2 Plasmid constructs used in this study

Plasmid Constructs	Sources
pGBKT7	Clontech
pGBKT7-C2	This study
pGBKT7-C2L	This study
pGADT7RecAB	Clontech
pGADT7RecAB- SPATA4	Clontech
pGADT7RecAB- C3	Clontech
pFLAGCMV6a	Sigma
pFLAGCMV6a- SPATA4	This study
pRK5MYC	Clontech
pRK5MYC-C2	This study
pMALc2X	New England Biolabs
pMALc2X - SPATA4	This study
pET15b-C2	Byung-Ha Oh
pPROEXTHa-C3	Byung-Ha Oh
pACYCDuet1-C5 and C2	This study
pDEST15	Invitrogen
pCMV-(myc)3-ECT2	Alisa Piekny
pGFP-SPATA4	This study

6.2.2 Yeast two hybrid screen

The yeast two hybrid screen was performed as described in the Matchmaker™ Pretransformed Libraries User Manual (Clontech). Briefly, a 50 ml culture of the bait strain (AH109 containing pGBKT7-C2) was grown to an OD600 of 0.8-0.9 in -Trp medium, centrifuged and resuspended in 5 ml of -Trp medium. 1 ml of the prey strain (Pretransformed Normalized Matchmaker™ Human Universal cDNA Library in Y187 (Clontech)) was added and the total volume of the culture was brought to 50 ml using 2x YPDA (0.1% yeast extract, 0.2% peptone, 0.2% dextrose, 0.3% L-adenine hemisulphate). The cells were mated for 24-28 hours at 30°C with shaking at 50 rpm. Cells were subsequently plated on -Trp/-Leu/-His/-Ade medium (0.67% yeast nitrogen base, 2% dextrose, 0.08% -Trp/-Leu/-His/-Ade dropout mix) containing X- α -Gal and left at 30°C for 3-8 days.

Positive clones were tested for multiple prey plasmids by streaking on -Trp/-Leu medium (0.67% yeast nitrogen base, 2% dextrose, 0.08% -Trp/-Leu dropout mix) containing X- α -Gal. One clone from the latter plate was then picked and streaked onto -Trp/-Leu/-His medium (0.67% yeast nitrogen base, 2% dextrose, 0.08% -Trp/-Leu/-His dropout mix) containing X- α -Gal and 0.5 mM 3-amino-1,2,4-triazol (to prevent autoactivation) to verify that the phenotype was maintained. If a clone contained more than one prey plasmid then a mixture of blue and white colonies would result after streaking.

Inserts were identified by polymerase chain reaction (PCR) amplification using the oligonucleotides pGAD-F-ID and pGAD-R-ID (Table 5.1) followed by

sequence analysis. Plasmids used in this study are listed in Table 5.2.

6.2.3 Tissue culture and lysate preparation

Human embryonic kidney 293T (HEK293T) cells were grown in Dulbecco's modified Eagle Medium (DMEM) supplemented with 10% fetal bovine serum (Wisent) and 1% penicillin/streptomycin. Transfections were carried out with 10-20 μ g of DNA using the calcium phosphate method. Cells were harvested 48 hours post-transfection by scraping with lysis buffer (150 mM NaCl, 50 mM Tris pH 7.5, 1 mM EDTA, 1% Triton X-100) with 1 mM sodium orthovanadate and protease inhibitors (Roche). For gel filtration, cells were collected as above using gel filtration lysis buffer (150 mM NaCl, 50 mM Tris pH 7.2, 0.5 mM EDTA, 1 mM DTT, 1% Triton X-100) with protease inhibitor.

6.2.4 Co-immunoprecipitation and gel filtration

Samples for co-immunoprecipitation (CoIP) contained 1 mg of lysate made up to a total volume of 1 mL with 1x phosphate buffered saline (PBS; 8% NaCl, 0.2% KCl, 1.44% Na_2HPO_4 , 0.24% KH_2PO_4). Immunoprecipitation was performed with 2 μ g of rabbit anti-myc IgG (Abcam) on ice, at 4°C for 16 hours, followed by incubation with 10 μ L of Protein A-agarose, on a nutator at 4°C for 2 hours. Samples were washed 3x with 1 mL PBS and eluted by heating to 95°C for 2 minutes with 1x SDS-PAGE sample buffer (SB). For Western analysis of the CoIP samples, primary antibodies used were monoclonal mouse anti-myc (Upstate) and monoclonal mouse anti-FLAG (Sigma) both

at 1:5,000 dilution. Secondary antibody used was peroxidase-labelled goat anti-mouse IgG (Kirkegaard & Perry Laboratories) at 1:10,000 dilution.

For gel filtration analysis, samples (5 mg) were loaded on a SuperdexTM 200 column (GE Healthcare) with a flow rate of 0.5 mL/min and 0.5 mL fractions were collected. Following fractionation, 25 μ L of each sample was loaded on a SDS-PAGE gel for Western analysis.

6.2.5 Recombinant protein preparation

Cells were grown to an OD₆₀₀ of 0.5-1.0 at 37 °C and protein production was induced by the addition of 1 mM IPTG with shaking at 250 rpm at 25 °C overnight. Cells were then pelleted at 4,000 rpm for 20 minutes and resuspended in 25 mL of column buffer (20 mM Tris-HCl, 200 mM NaCl, 1 mM EDTA, 1 mM DTT) for maltose binding protein (MBP) fusion proteins, 30 mL lysis buffer (50 mM Tris-HCl pH 8.0; 400 mM NaCl; 1mM dithiothreitol (DTT), 5 mM ethylenediaminetetraacetic acid (EDTA), 5% glycerol, protease inhibitors) for glutathione-S-transferase (GST) fusion proteins or 35 ml of lysis buffer (300 mM NaCl, 50 mM Tris-HCl pH 8.5, 9.7 mM β -mercaptoethanol, 0.5% glycerol, 0.1% Triton X-100, 1 mM AEBSF) for polyhistidine (His)-tagged proteins. Triton X-100 was added to a final concentration of 1% for GST fusion proteins and the cell suspensions were sonicated for 2 minutes. The resulting lysates were clarified at 20,000 g for 20 minutes.

For MBP fusion protein purification, the crude extract was diluted 1:6 with column buffer and passed through a 500 μ L bed volume of amylose resin (New England Biolabs). Retained proteins were washed with 5 column volumes of column buffer and eluted with maltose elution buffer (20 mM Tris-HCl, 200 mM NaCl, 1 mM EDTA, 1 mM DTT, 10 mM maltose) in 1 mL fractions.

For GST fusion protein purification, the crude extract was incubated with glutathione sepharose beads (GE Healthcare) for 1h at 4°C, poured into a column and washed twice with 10mL of wash buffer (50mM Tris-HCl pH 8.0; 400mM NaCl, 5% glycerol, 1mM DTT). GST tagged proteins were eluted in 1mL fractions of elution buffer (50mM Tris-HCl pH 8.0; 400mM NaCl, 15mM glutathione) after a 5 minute incubation at room temperature.

For His-tagged proteins, the crude extract was incubated at 4°C on a nutator with 1 ml of Ni-NTA Agarose (Qiagen). The retained proteins were washed twice with 10 mL wash buffer (50 mM Tris-HCl pH 8.5, 300 mM NaCl, 10 mM β -mercaptanol) and eluted with 3 mL of imidazole elution buffer (50 mM Tris pH 8.8, 200 mM NaCl, 200 mM imidazole) in 1 mL fractions. In all cases, protein concentration was assayed using the BioRad Protein Assay dye-reagent as per the manufacturer's instructions. MBP and GST fusion proteins were passed through a 10 DG column (BioRad) in binding buffer (10 mM HEPES pH 7.4, 25 mM NaCl, 115 mM KCl, 2 mM MgCl₂, 0.1% Triton X-100) to remove excess maltose or glutathione, respectively.

6.2.6 In vitro binding assay

In vitro binding assays contained 0.1 μM of either MBP or MBP-SPATA4 with increasing amounts (0, 0.05, 0.1, 0.25 μM) of either a heterotrimeric complex composed of C2/His-C3/C5 or a peptide comprising the two C-terminal helices of C2 (H2/H3 C2), or 0.5 μM of either MBP or MBP-SPATA4 with increasing amounts (0, 0.1, 0.2, 0.5 μM) of His-C2. Samples were made up to a total volume of 250 μl with 1x binding buffer and left on ice at 4°C for 1 hour to allow binding. Pulldown employed 10 μl amylose resin on a nutator for 1 hour. Samples were washed 3x with 250 μl of 1x binding buffer and the protein was eluted from the beads by heating to 95°C in 25 μl of 1x SB for 2 minutes. Western analysis used affinity purified polyclonal antibody recognizing C2 at a dilution of 1:10,000 or anti-GST (Sigma) at 1:10,000.

6.2.7 Fluorescence microscopy

HEK293 cells were plated on coverslips in six-well dishes and transfected 24 hours later by the calcium phosphate method using 1.67 μg of plasmid per well. Cells were fixed 48 hours after transfection in 100% ice cold methanol for 4 minutes at -20°C or with pre-warmed (37 °C) 4% paraformaldehyde for 20 minutes at room temperature, rinsed with PBS and then incubated for 30 minutes with 0.01mg/mL 4',6-diamidino-2-phenylindole (DAPI). The cells were then washed two more times with PBS before mounting using Antifade Gold (Invitrogen) and visualized on a Zeiss Axioplan Fluorescence microscope using a 63x oil EC Plan-Neofluar objective. Images were

overlaid using Adobe Photoshop.

6.2.8 Live cell imaging

HEK293T cells were plated on 35mm dishes and transfected 24 hours later by the calcium phosphate method using 1 μ g of plasmid and visualized either 24 or 48 hours post-transfection. Images were captured on a Leica DMI6000 B inverted microscope coupled with a Hamamatsu C10600 ORCA-R2 digital camera.

6.2.9 Cellular fractionation

HEK293T cells were plated on 10 cm dishes, transfected 24 hours later by the calcium phosphate method with 10 μ g of pGFP-SPATA4 and harvested in 1mL of PBS 48 hours post-transfection. Cells were pelleted for 10 min at 1500 rpm at 4°C and the supernatant was discarded. The cell pellet was resuspended in 1 mL of cold hypotonic Buffer N (10 mM HEPES pH 7.5, 2 mM MgCl₂, 25 mM KCl, 1 mM DTT, 1 mM PMSF and protease inhibitor cocktail) and incubated on ice for 10 min. Cells were then disrupted by 30 strokes with a glass Dounce homogenizer using pestle "B", and sucrose was added to the lysate to a final concentration of 0.22 M. Nuclei were pelleted by centrifugation at 1500 rpm for 10 min. and the supernatant was taken as the cytoplasmic fraction. Nuclei were washed twice with 400 μ L of cold Buffer N containing sucrose at a final concentration of 250mM and resuspended in 400 μ L of 1x SDS sample buffer. For western blot analysis, equal volumes of all fractions were analyzed.

6.3 Results

6.3.1 Identification of SPATA4 as a C2 binding partner

To begin to understand the regulation of the function of TRAPP, we undertook a yeast two-hybrid (Y2H) screen using C2 as the bait. A normalized, human cDNA library in prey plasmids, produced from multiple tissues, was used in the screen. After the initial screen, >180 potential interactors were identified. Potential interactors were narrowed down by all of the following methods: (i) duplicates were identified by colony PCR and AluI restriction analysis; (ii) plasmids were rescued and tested for autoactivation; (iii) plasmids were re-tested to remove false-positives. This process left 6 potential interactors (Table 6.3) including the C3 subunit of TRAPP which was previously shown to directly interact with C2 [13].

The six interactors were tested for specificity by checking their ability to interact with the TRAPP subunit C2L which is closely related to C2 [11]. Only SPATA4 discriminated in its ability to bind to C2 and C2L while the remaining interactors bound to both proteins (Figure 6.1). For this reason, we chose to focus the remainder of this study on SPATA4.

Table 6.3 C2 interactors identified in yeast two-hybrid screen

Interactor	cDNA accession number
LAP3 - leucine aminopeptidase 3	NM_015907.2
REPS2 - RALBP1 associated Eps domain containing 2	NM_001980975.1
POSTN - periostin, osteoblast specific factor	NM_006475.1
SPATA22 - spermatogenesis associated 22	NM_032598.3
SPATA4 - spermatogenesis associated 4	NM_144644.2
TRAPPC3 - trafficking protein particle complex 3	NM_014408.3

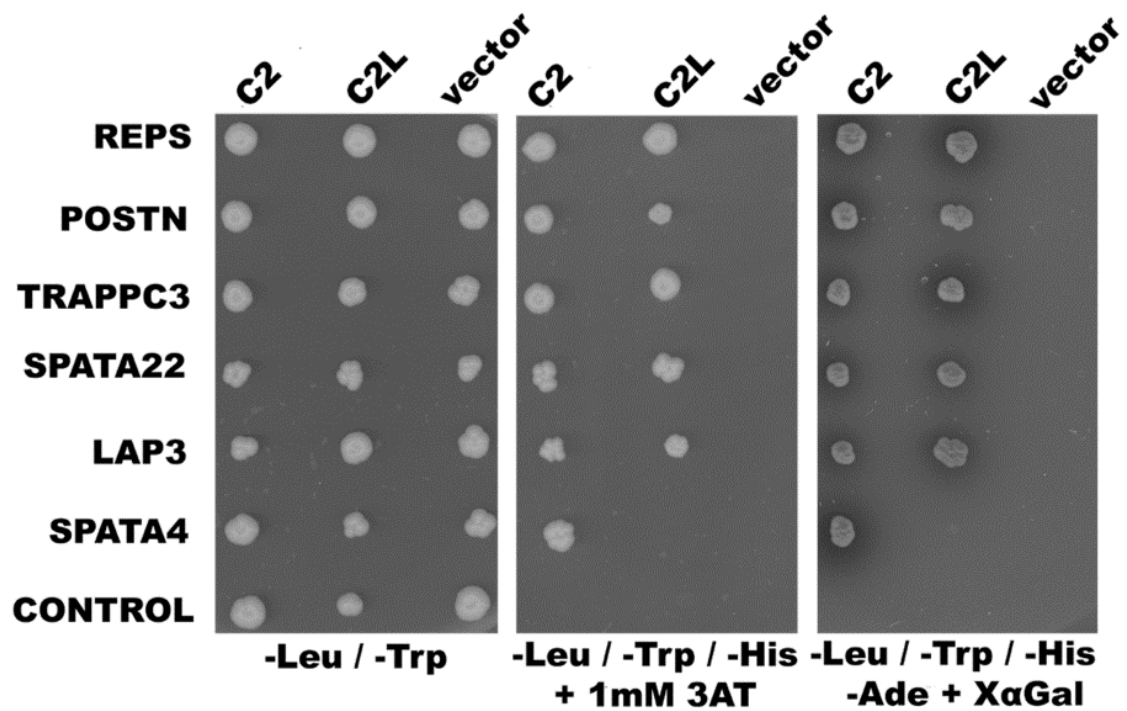


Figure 6.1 SPATA4 interacts with C2 by yeast two-hybrid. Yeast cells harboring C2 or C2L in the bait plasmid pGBKT7, or an empty bait plasmid (vector) and the prey plasmid pGADT7 with the inserts indicated (see Table 6.3) were grown on medium lacking tryptophan and leucine, lacking tryptophan, leucine and histidine with 1mM 3-amino-1,2,4-triazol (3-AT), or lacking tryptophan, leucine, histidine and adenine with X-α-Gal. SPATA4 interacted specifically with C2 and not C2L under the two experimental conditions tested.

SPATA4 is a highly conserved protein that has been found in numerous species [15-19]. Human SPATA4 is 305 residues in length and contains a DUF1042 domain of unknown function. Sequence analysis of the cDNA clone isolated in our screen revealed a frameshift that resulted in a 38 amino acid truncation of the protein from the carboxy-terminus suggesting that this region is not important for its interaction with C2 (see below).

6.3.2 C2 and SPATA4 interact in vivo

To confirm the Y2H results, we examined the ability of C2 and SPATA4 to interact in vivo. As shown in Figure 6.2 A, FLAG-SPATA4 co-precipitated with myc-C2 (lane 4). We noted that the levels of FLAG-SPATA4 were considerably higher when the protein was co-expressed with myc-C2 compared to when it was expressed in its absence (compare lanes 1 and 2). This result was seen numerous times, however the basis for it remains unclear. Although an interaction between SPATA4 and C2L was not detected by Y2H (see above), we found that myc-C2L could also precipitate FLAG-SPATA4 (Figure 6.2 B, lane 3). This is likely due to the fact that C2L is precipitating TRAPP which contains C2 [11]. FLAG-SPATA4 did not co-precipitate with myc-ECT2, a protein unrelated to C2 used as a negative control. Identical results were obtained when anti-FLAG was used as the precipitating antibody. These results confirm the Y2H interaction and suggest that SPATA4 interacts with TRAPP.

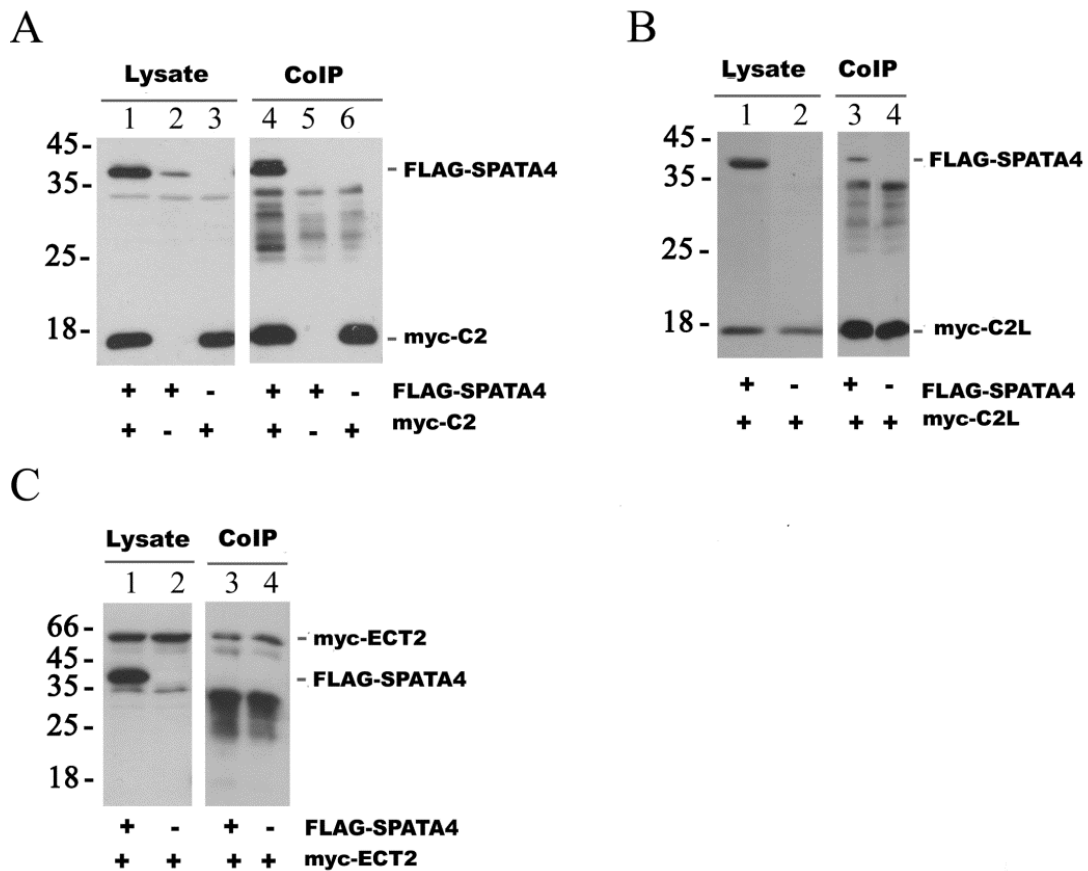


Figure 6.2 SPATA4 and C2 interact in vivo. Lysates were prepared from HEK293T cells co-transfected with plasmids expressing: (A) lanes 1 and 4: FLAG-SPATA4 with myc-C2; lanes 2 and 5: FLAG-SPATA4 with pRK5MYC; lanes 3 and 6: pFLAGCMV6a with myc-C2; (B) lanes 1 and 3: FLAG-SPATA4 with myc-C2L; lanes 2 and 4: pFLAGCMV6a with myc-C2L; (C) lanes 1 and 3: FLAG-SPATA4 with myc-ECT2 (amino acids 421-883); lanes 2 and 4: pFLAGCMV6a with myc-ECT2 (amino acids 421-883). Samples were immunoprecipitated (co-IP) with rabbit anti-C2 (A) or rabbit anti-myc (B, C). Precipitates were analyzed by western blotting using mouse anti-myc and mouse anti-FLAG IgG.

6.3.3 SPATA4 binds to the TRAPP complex

To further confirm the interaction between SPATA4 and C2 we performed an *in vitro* binding assay using MBP-SPATA4 and His6-C2. As shown in Figure 6.3 A, we were unable to detect binding between these proteins above background levels in this system. When the binding assay was performed using a heterotrimeric form of C2 bound to its neighboring subunits (C2/His-C3/C5 heterotrimer) efficient binding was readily seen (Figure 6.3 B). It is noteworthy that the binding to the heterotrimeric complex was sufficiently strong that the levels of MBP-SPATA4 were reduced 5 fold and the levels of the C2/His-C3/C5 were reduced two fold in the assay compared to monomeric C2. An interaction between glutathione-S-transferase (GST)-tagged C2L and MBP-SPATA4 could not be detected (not shown). Interestingly, when just a heterodimer of His-C3/C5 was used, binding of MBP- SPATA4 could be readily detected (Figure 6.3 C). These results suggest that SPATA4 preferentially interacts with the C2-localized portion of TRAPP and also recognizes a region on the C3/C5 dimer.

Consistent with the above notion, lysates fractionated by size exclusion chromatography showed that FLAG-SPATA4 was found in a high molecular weight fraction that also contained TRAPP-associated C2 (Figure 6.3 D). Significantly, there was no pool of SPATA4 even in fractions that contained non-TRAPP-associated C2. This fractionation was not affected by co-expression of myc-C2 (not shown) except that the levels of SPATA4 were greater when the two proteins were co-expressed as stated above.

This high molecular weight pool of FLAG-SPATA4 coimmunoprecipitated with several TRAPP proteins (Figure 6.3 E). Collectively, our results suggest that SPATA4 binds to the TRAPP complex through the C2-containing end.

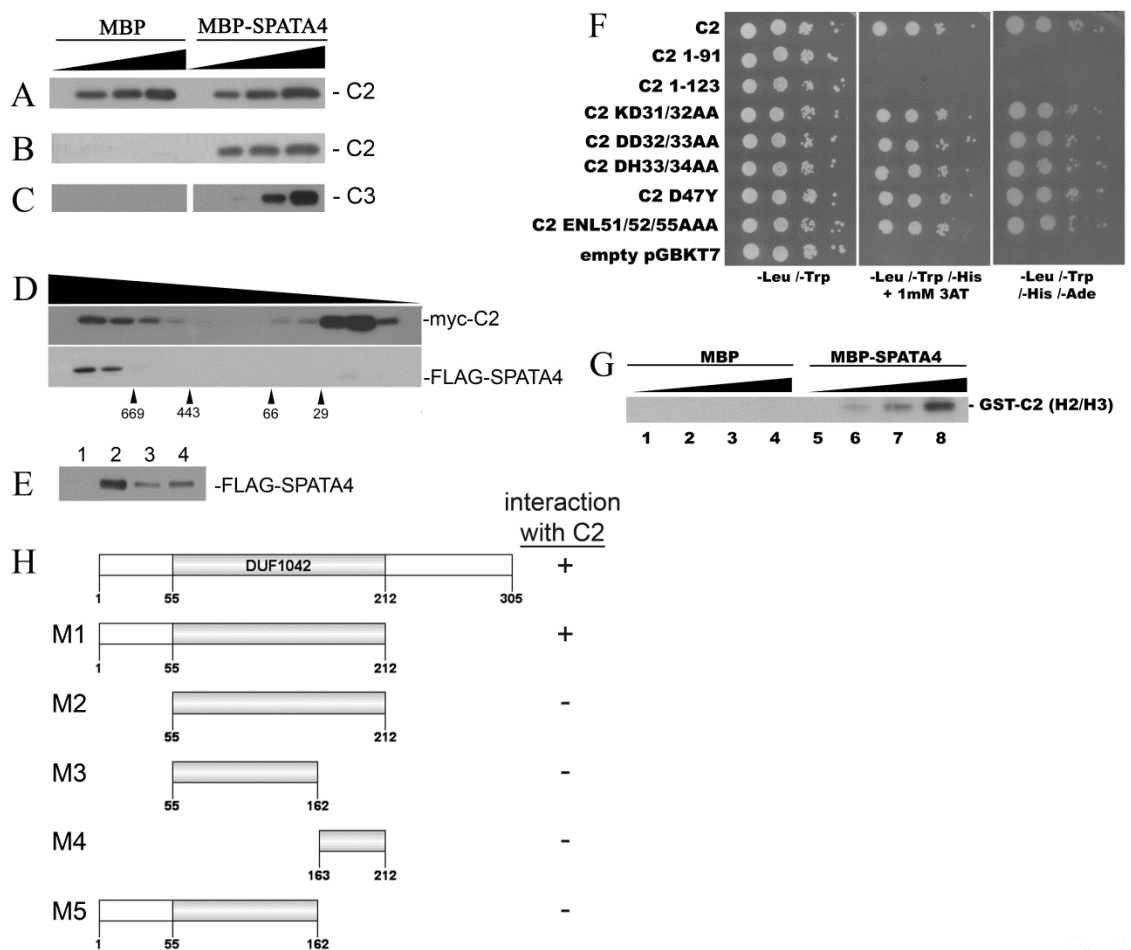


Figure 6.3 *SPATA4 binds to TRAPP.* MBP or MBP-SPATA4 were subjected to an *in vitro* binding assay as described in materials and methods using amylose resin to pull down MBP and MBP-SPATA4 with increasing amounts of either His-C2 (**A**), C2/His-C3/C5 (**B**) or His-C3/C5 (**C**). Samples were probed by western blotting using anti-C2 (**A,B**) or anti-C3 (**C**) IgG. (**D**) Lysates were prepared from HEK293T cells transfected with a plasmid expressing FLAG-SPATA4 or myc-C2. Lysates were fractionated on a SuperdexTM 200 column and fractions were analyzed by western blotting using anti-myc

and anti-FLAG antibodies. **(E)** FLAG-SPATA4 fractions from **(D)** were untreated (lane 1) or immunoprecipitated with anti-C2 (lane 2), anti-C3 (lane 3) or anti-C11 (lane 4) IgG and probed with anti-FLAG IgG. **(F)** Full length C2 or the indicated fragments and mutants were tested for an interaction with SPATA4 by yeast two hybrid. Serial dilutions were spotted on medium lacking either leucine and tryptophan, leucine, tryptophan and histidine with 3-AT, or leucine, tryptophan, histidine and adenine. **(G)** MBP or MBP-SPATA4 were subjected to an *in vitro* binding assay as in **(A)** with increasing amounts of GST fused to residues 91-140 of C2 (helices 2 and 3; GST-C2(H2/H3)). Samples were probed by western blotting using anti-GST IgG. **(H)** SPATA4 constructs were tested for interaction with C2 by yeast two hybrid (see Supplemental Figure 6.5). The SPATA4 fragments generated are (human numbering): M1 (1-212), M2 (55-212), M3 (55-162), M4 (163-212) and M5 (1-162).

6.3.4 Defining the regions of interaction between SPATA4 and C2

Since SPATA4 was identified through its interaction with C2, we sought to determine which regions of SPATA4 and C2 mediate the interaction between the proteins. Although largely similar, the three-dimensional crystal structure of C2 as part of the heterotrimeric complex differs slightly from uncomplexed C2 [13, 20]. Specifically, helix 1 is extended in the heterotrimeric complex by incorporating additional residues on both the amino- and carboxy-terminal sides. We used several C2 mutants to determine whether SPATA4 interacts with this helix. First, the amino-terminal 91 residues of C2 containing helix 1 (spanning residues 31-54 in C2 in the heterotrimeric complex) was cloned into the bait vector and tested for an interaction with SPATA4. As demonstrated in Figure 6.3 F, an interaction was not detected. We then mutated the highly conserved additional residues (31-34 and 51-55) that are incorporated into helix 1 in the heterotrimeric form of C2 into alanines. All of these mutant forms of C2 retained their ability to interact with SPATA4 (Figure 6.3 F). Finally, we found that the pathogenic D47Y SEDT mutation in helix 1 of C2 had no effect on binding to SPATA4 (Figure 6.3 F). These results argue against a role for the involvement of helix 1 of C2 with SPATA4. We then focused our attention to the carboxy-terminal portion of C2 which contains two antiparallel helices called helix 2 and helix 3 (H2/H3) which were deleted in the amino-terminal construct described above. As shown in Figure 6.3 G, GST-tagged recombinant H2/H3 (residues 91-140) was indeed able to bind MBP-SPATA4. Consistent with these results, a construct lacking the final 17 residues of C2 that represent H3 failed to interact with SPATA4 (Figure 6.3 F). These results suggest that the carboxy-terminal helix of C2

is necessary for interaction with SPATA4.

To define the portion of SPATA4 that interacts with C2 we cloned portions of the protein into the prey vector and tested their ability to bind to C2 by Y2H. As shown in Figure 6.3 H and Supplemental Figure 6.5, deletion of the entire carboxy-terminal portion of the protein until the DUF1042 domain did not affect its interaction with C2. Further truncations into the DUF1042 domain ablated the interaction suggesting that this domain is required for the interaction with C2. However, the DUF1042 domain (amino acids 55-212) alone was unable to bind to C2. When SPEF1, one of two other DUF1042-containing proteins, was tested for binding to C2, no interaction was detected (not shown). These results suggest that the DUF1042 domain of SPATA4 is necessary but not sufficient for its interaction with C2.

6.3.5 SPATA4 is found in both the cytosol and in the nucleus

The binding of SPATA4 to TRAPP suggests that SPATA4 should be found in the cytosol. We tested this notion by cell fractionation and fluorescence microscopy using green fluorescent protein (GFP)-tagged SPATA4. Upon fractionation, a portion of GFP-SPATA4 was indeed found in the cytosol (Figure 6.4 A). A significant portion was also found in the nuclear-enriched fraction consistent with an earlier study [18]. The latter result was not due to cross-contamination between the nuclear and cytosolic fractions since the cytosolic marker (β -COP) and two TRAPP subunits, C2 and C3, were only detected in the cytosolic fraction (Figure 6.4 A). This result further supports the

interaction between C2 and SPATA4 taking place in the cytosol.

We then sought to confirm the biochemical fractionation by fluorescence microscopic localization of GFP-SPATA4. When cells were visualized after fixing with 4% paraformaldehyde, GFP-SPATA4 displayed a nuclear localization in 89.4% of the cells (n=47) (Figure 6.4 B). Curiously, when cells were fixed with methanol, the localization of GFP-SPATA4 was cytosolic in 89.4% of the cells (n=104) with some cells displaying punctae (Figure 6.4 B). As neither of these results were consistent with the biochemical fractionation we visualized GFP-SPATA4 in live cells where no fixation method is used. In this case, all of the transfected cells showed the GFP-SPATA4 signal in both the nucleus and the cytosol (Figure 6.4 B). Although some cells showed a stronger signal in one of these compartments, the GFP-SPATA4 signal in those cells could also be seen in the other compartment. Although it remains to be shown whether GFP-SPATA4 is functional, the localization seen in live cells suggests that GFP-SPATA4 localization is dynamic.

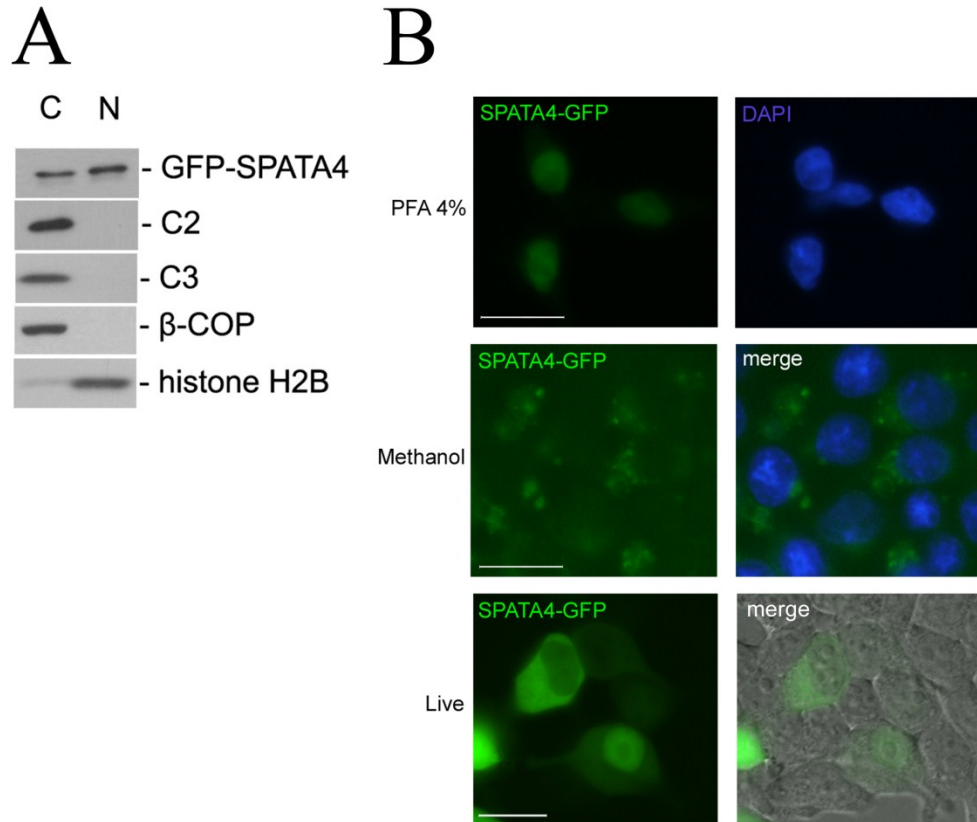


Figure 6.4 Localization of SPATA4 in HEK293T cells. (A) HEK293T cells were transfected with pGFP-SPATA4 and harvested 48 hours later. The cells were lysed and separated into cytosolic (C) and nuclear fractions (N). Aliquots were analyzed by western blotting using anti-GFP, anti-C2, anti-C3, anti-histone B (nuclear marker) and anti- β -COP (cytosolic marker). (B) HEK293T cells were transfected with pGFP-SPATA4 and visualized after fixation with either paraformaldehyde (top row) or methanol (middle row). The bottom panel shows a representative image of unfixed, live cells. Cytosolic localization is not due to background fluorescence since there are a number of untransfected, non-fluorescent cells in the fields as demonstrated by the DAPI merge for the methanol fixed samples and the DIC merge of the live cells. Scale bars: 20 μ m.

6.4 Discussion

We present evidence that SPATA4, a protein of unknown function, interacts specifically with a protein involved in membrane traffic. Collectively, our data implicate SPATA4 in a role in membrane traffic by virtue of its association with the TRAPP complex. It is noteworthy that a low molecular weight pool of SPATA4, similar to that of C2 with which it interacts, was not detected. Rather, all of the ectopically expressed, cytosolic SPATA4 co-fractionated with TRAPP. The fact that SPATA4 is expressed almost exclusively in spermatocytes, suggests that TRAPP may perform a function specific to these cells. Although subcellular fractionation suggested that a portion of SPATA4 was found in the nucleus, this pool of SPATA4 would not be seen in our gel filtration fractions since the protocol removes nuclei and DNA from the sample prior to size-exclusion chromatography. Given a previous report that C2 is found in the nucleus [21], we cannot rule out a SPATA4-C2 interaction taking place in this compartment. It should be noted, however, that the previous report was based on the fractionation of overexpressed C2 while our fractionation focused on the endogenous protein. In addition, our *in vitro* binding assay argues against a SPATA4 interaction with non-TRAPP-associated C2. Although SPATA4 was identified in a yeast two hybrid screen using C2 as the bait, SPATA4 bound more efficiently *in vitro* to His-C3/C5 compared to His-C2. It is possible that the yeast two hybrid interaction may have been mediated by a mixed TRAPP complex composed of human C2 with yeast TRAPP proteins. Such a complex is likely produced in yeast since the human protein complements its yeast ortholog [11, 22]. Alternatively, the interaction *in vivo* is more stable than that *in vitro*.

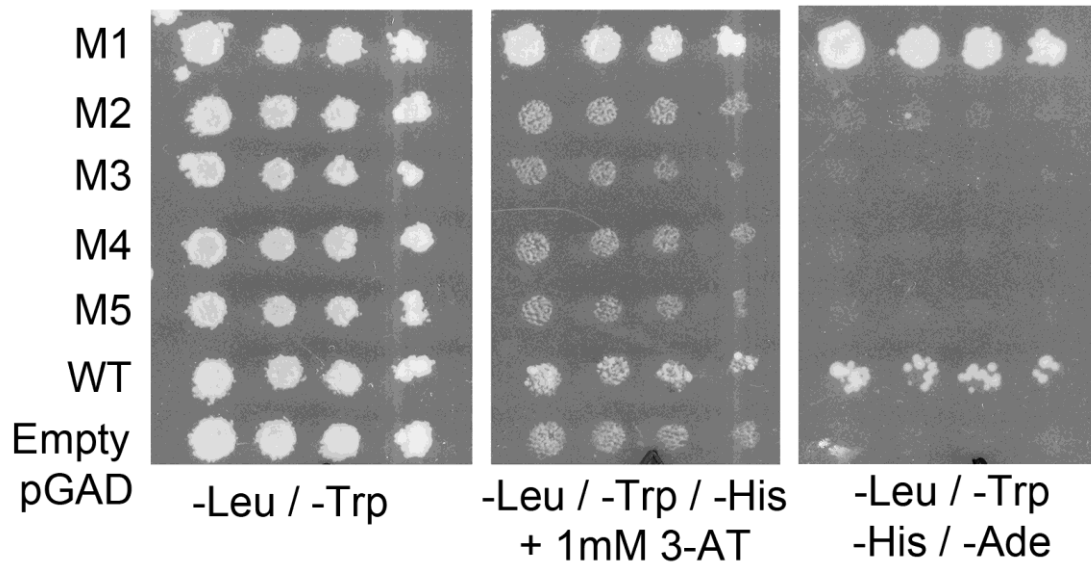
A recent study suggests that SPATA4 is localized to the cytosol in the osteoblast cell line MC3T3-E1 where it interacts with and promotes the phosphorylation of the kinase ERK1 [23]. An earlier study reported the localization of GFP-SPATA4 to the nucleus [18]. Our present work shows GFP-SPATA4 localizing to and fractionating with both the cytosol and nucleus in live cells. Clearly, this is a dynamic protein with perhaps several functions. Interestingly, mutations in C2 that lead to the skeletal defect SEDT include carboxy-terminal truncations [24], a region we have defined as important for the interaction with SPATA4. The position of C2 within TRAPP and its interactions with neighbouring subunits leave available this carboxy-terminal helix for interactions with non-stably-associated members of the complex [13]. It remains to be seen whether ablation of the SPATA4-C2 interaction in the cytosol is a contributing factor to SEDT.

A previous study on ectopically expressed SPATA4 in MCF7 cells showed that it increased their growth rate by allowing the cells to progress through S phase more rapidly [17]. While the mechanism for the increased growth rate of these cells is unclear, our present study suggests it may be due to a more active secretory pathway.

The involvement of the DUF1042 domain in binding to C2 is interesting in light of the fact that this domain has been implicated in microtubule interactions [25]. Given that ER-derived carriers migrate along microtubule tracks [26], it is tempting to speculate that SPATA4 may link TRAPP to the microtubule network to facilitate membrane traffic in spermatocytes. Alternatively, profound changes to the cytoskeletal microtubule network accompany division of spermatocytes and development of spermatids [27]. Such changes may present special needs for membrane traffic and

SPATA4 would be well positioned to allow this vesicle tether to adapt to the changing cytoskeletal landscape. In addition, given the link between SPATA4 and ERK1, it is tempting to speculate that this protein of unknown function serves to link TRAPP to ERK1 and thus allow membrane traffic to respond to signaling events as previously suggested [28]. Clearly, further studies on the SPATA4 protein in an appropriate spermatocyte model system are needed to further elucidate the function of this TRAPP-interacting protein.

6.5 Supplemental material



Supplemental Figure 6.5 Yeast cells harboring C2 in the bait plasmid pGBKT7 were transformed with the prey plasmid pGADT7 containing full-length, wild type SPATA4 (WT) or fragments of SPATA4. Cells were grown on medium lacking tryptophan and leucine, lacking tryptophan, leucine and histidine with 1mM 3-AT, or lacking tryptophan, leucine, histidine and adenine. The SPATA4 fragments were: M1 (1-212), M2 (55-212), M3 (55-162), M4 (163-212) and M5 (1-162). Only full-length and 1-212 interacted with C2.

6.6 Acknowledgements

We are grateful to Dr. James Scrivens, Nassim Shahrzad and Adrian Moores for advice, helpful discussions and constructs used in this study, and to Drs. Alisa Piekny and Gerard Dougherty for reagents. D.T.D. is supported in part by a Groupe de Recherche Axé sur la Structure des Protéines graduate recruitment award. This work was funded by grants from the Canadian Institutes of Health Research, the Canada Foundation for Innovation and the Natural Sciences and Engineering Research Council of Canada to M.S.

6.7 References

- [1] Hughson, F.M. and Reinisch, K.M. (2010). Structure and mechanism in membrane trafficking. *Curr. Opin. Cell Biol.* 22, 454-460.
- [2] Sacher, M. et al. (2008). The TRAPP complex: insights into its architecture and function. *Traffic.* 9, 2032-2042.
- [3] Sacher, M. et al. (1998). TRAPP, a highly conserved novel complex on the cis-Golgi that mediates vesicle docking and fusion. *EMBO J.* 17, 2494-2503.
- [4] Sacher, M. et al. (2001). TRAPP I implicated in the specificity of tethering in ER-to-Golgi transport. *Mol. Cell* 7, 433-442.
- [5] Jones, S. et al. (2000). The TRAPP complex is a nucleotide exchanger for Ypt1 and Ypt31/32. *Mol. Biol. Cell* 11, 4403-4411.
- [6] Morozova, N. et al. (2006). TRAPP II subunits are required for the specificity switch of a Ypt-Rab GEF. *Nat. Cell Biol.* 8, 1263-1269.
- [7] Wang, W. et al. (2000). TRAPP stimulates guanine nucleotide exchange on Ypt1p. *J. Cell Biol.* 151, 289-296.
- [8] Yamasaki, A. et al. (2009). mTrs130 is a component of a mammalian TRAPP II complex, a Rab1 GEF that binds to COPI-coated vesicles. *Mol. Biol. Cell* 20, 4205-4215.
- [9] Ghosh, A.K. et al. (2001). A novel 16-kilodalton cellular protein physically interacts with and antagonizes the functional activity of c-myc promoter-binding protein 1. *Mol.*

Cell Biol. 21, 655-662.

[10] Ghosh, A.K. et al. (2003). Modulation of human luteinizing hormone beta gene transcription by MIP-2A. *J. Biol. Chem.* 278, 24033-24038.

[11] Scrivens, P.J. et al. (2009). TRAPPC2L is a novel, highly conserved TRAPP-interacting protein. *Traffic.* 10, 724-736.

[12] Gedeon, A.K. et al. (1999). Identification of the gene (SEDL) causing X-linked spondyloepiphyseal dysplasia tarda. *Nat. Genet.* 22, 400-404.

[13] Kim, Y.G. et al. (2006). The architecture of the multisubunit TRAPP I complex suggests a model for vesicle tethering. *Cell* 127, 817-830.

[14] Collas, P. et al. (1999). The A-kinase-anchoring protein AKAP95 is a multivalent protein with a key role in chromatin condensation at mitosis. *J. Cell Biol.* 147, 1167-1180.

[15] Liu, B. et al. (2005). Cloning and expression analysis of gonadogenesis-associated gene SPATA4 from rainbow trout (*Oncorhynchus mykiss*). *J. Biochem. Mol. Biol.* 38, 206-210.

[16] Liu, S. et al. (2005). Cloning and characterization of zebra fish SPATA4 gene and analysis of its gonad specific expression. *Biochemistry (Mosc.)* 70, 638-644.

[17] Liu, S.F. et al. (2004). Cloning and characterization of testis-specific spermatogenesis associated gene homologous to human SPATA4 in rat. *Biol. Pharm. Bull.* 27, 1867-1870.

- [18] Liu, S.F. et al. (2004). Cloning of a full-length cDNA of human testis-specific spermatogenic cell apoptosis inhibitor TSARG2 as a candidate oncogene. *Biochem. Biophys. Res. Commun.* 319, 32-40.
- [19] Liu, S.F. et al. (2005). Molecular cloning and bioinformatic analysis of SPATA4 gene. *J. Biochem. Mol. Biol.* 38, 739-747.
- [20] Jang, S.B. et al. (2002). Crystal structure of SEDL and its implications for a genetic disease spondyloepiphyseal dysplasia tarda. *J. Biol. Chem.* 277, 49863-49869.
- [21] Jeyabalan, J. et al. (2010). SEDLIN forms homodimers: characterisation of SEDLIN mutations and their interactions with transcription factors MBP1, PITX1 and SF1. *PLoS One.* 5, e10646.
- [22] Gecz, J. et al. (2003). Human wild-type SEDL protein functionally complements yeast Trs20p but some naturally occurring SEDL mutants do not. *Gene.* 320, 137-144.
- [23] Wang, X. et al. (2011). Spata4 promotes osteoblast differentiation through Erk-activated Runx2 pathway. *J. Bone Miner. Res.*, doi: 10.1002/jbmr.394.
- [24] Shaw, M.A. et al. (2003). Identification of three novel SEDL mutations, including mutation in the rare, non-canonical splice site of exon 4. *Clin. Genet.* 64, 235-242.
- [25] Dougherty, G.W. et al. (2005). CLAMP, a novel microtubule-associated protein with EB-type calponin homology. *Cell Motil. Cytoskeleton* 62, 141-156.
- [26] Presley, J.F. et al. (1997). ER-to-Golgi transport visualized in living cells. *Nature* 389, 81-85.

[27] Lie, P.P. et al. (2010). Cytoskeletal dynamics and spermatogenesis. *Philos. Trans. R. Soc. Lond B Biol. Sci.* 365, 1581-1592.

[28] Sacher, M. (2003). Membrane traffic fuses with cartilage development. *FEBS Lett.* 550, 1-4.